Virulence and NLRP3 inflammasome activation of the common surface protein in oral spirochetes associated with periodontitis

치주염과 관련된 구강나선균의 공통 표면단백질의

병독력과 NLRP3 인플라마좀 활성

2013 년 02 월

서울대학교 대학원

치의학과 면역 및 분자미생물 전공

전 혜 경

ABSTRACT

Virulence and NLRP3 inflammasome activation of the common surface protein in oral spirochetes associated with periodontitis

Hye-Kyoung Jun

Department of Dental Science, Major of Immunology and Molecular Microbiology in Dentistry, Graduate school, Seoul National University

(Directed by Professor **Bong-Kyu Choi**, Ph.D.)

Objectives

Oral spirochetes are composed of an enormously heterogeneous group of *Treponema* species, and some have been implicated in the etiology of periodontitis. Multiple species or phylotypes of *Treponema* have often been found in a single patient or a single periodontal pocket. Some outer membrane proteins (OMPs) of oral spirochetes are important in immune modulation, which has been demonstrated in molecular pathogenesis studies. Tp92 of *T. pallidum*, a surface protein, has been reported to have opsonic potential and to induce a protective immune response against syphilis, *T. pallidum* infection. It has been reported that

the Tp92 homologs are a family of highly conserved OMPs in gram-negative bacteria that may have conserved functions. It is therefore important to find common virulence determinants that are localized on the surface of oral spirochetes and to characterize them in order to elucidate their role in periodontal pathogenesis. The pro-inflammatory and bone-resorptive characteristics of IL-1β are associated with the immunopathology of periodontitis, leading to periodontal tissue destruction. IL-1β secretion is required for caspase-1 activation, which is associated with the inflammasome, which contributes to innate immunity. In this study, Tp92 homologs of four representative oral spirochetes (*T. denticola*, *T. lecithinolyticum*, *T. maltophilum*, and *T. socranskii* subsp. *socranskii*), which are strongly associated with periodontitis, were identified and characterized for their virulence.

Methods

Tp92 homologs from oral spirochetes were expressed in *Escherichia coli*, and the recombinant proteins were purified. To assess the binding ability of the Tp92 homologs to KB cells (ATCC CCL-17), a carcinoma epithelial cell line was incubated with the FITC-labeled Tp92 homologs or carboxyfluorescein diacetate succinimidyl ester (CFSE)-labeled bacteria. The cross-reactivity of the Tp92 homologs was detected with antiserum (IgG fraction) against Td92, a Tp92 homolog from *T. denticola*. The biological activities of the Tp92 homologs were analyzed by assessing the expression of various factors regarding inflammation and

tissue destruction in a human monocytic cell line (THP-1) and periodontal ligament cells (PDL cells).

To identify the molecular mechanisms of *T. denticola* Td92-induced IL-1β secretion, PMA-differentiated THP-1 cells were stimulated with Td92 in the presence or absence of KCl, oxATP, and K^+ channel blockers, and then, caspase-1 activation, proIL-1β expression, and IL-1β secretion were determined. The components of the inflammasome involved in Td92-induced caspase-1 activation were examined using siRNA against NLRP3, ASC, and NLRC4. To determine whether Td92 internalization is a prerequisite for NLRP3 activation, Td92 was internalized into the cells using protein transfection reagents or in the presence or absence of cytochalasin D. A cellular receptor that binds to Td92 and results in inflammasome activation was identified using an affinity ligand-binding assay. To determine which signaling pathway contributes to the Td92-induced pro-IL-1β expression following Td92 binding to the cellular receptor, MAPK pathway activation and NF-κB translocation were determined by immunoblotting and confocal microscopy in the presence or absence of various inhibitors or neutralizing Abs.

Results

The Tp92 homologs of the four oral spirochetes had signal peptides (20-31 amino acids) and molecular masses of 88-92-kDa for the mature proteins. The *tp92* gene homologs were successfully expressed in *E. coli*, and the recombinant proteins were capable of binding to KB cells. Furthermore, the binding of the

bacteria to the cells was inhibited by the addition of *T. denticola* Td92. An antiserum (IgG fraction) raised against *T. denticola* Td92 cross-reacted with the Tp92 homologs from the three other species of treponemes, including *T. lecithinolyticum*, *T. maltophilum*, and *T. socranskii* subsp. *socranskii*. The Tp92 homologs stimulated various factors involved in inflammation and osteoclastogenesis, such as IL-1β, IL-6, IL-8, TNF-α, COX-2, PGE_2, and MMP-9, in host cells, including monocytes and fibroblasts.

T. denticola Td92 could activate caspase-1, pro-IL-1β, and IL-1β secretion, which resulted from ATP release and K^+ efflux. Td92-induced caspase-1 activation was markedly decreased by the knockdown of NLRP3 or ASC, while the knockdown of NLRC4 did not affect Td92-induced caspase-1 activation. The rapid uptake of Td92 by a protein transfection reagent into the cells decreased Td92-induced caspase-1 activation, and blocking Td92 internalization by treatment with cytochalasin D did not affect caspase-1 activation or proIL-1β expression. Integrin α5β1 played a critical role in NLRP3 inflammasome activation because integrin α5β1 is a receptor for *T. denticola* Td92. Although Td92 was able to bind integrin α5β1 and fibronectin, Td92-induced NLRP3 inflammasome activation was mediated via direct binding to integrin α5β1, independent of fibronectin binding. The integrin α5β1 priming by Td92 led to the induction of pro-IL-1β expression, NLRP3 expression, and caspase-1 activation, which were mediated via NF-κB activation.

Conclusion

Td92 directly interacts with integrin α5β1 to activate the NLRP3 inflammasome and upregulate proIL-1β synthesis, which could lead to uncontrolled IL-1β secretion. Therefore, integrin α5β1 could be regarded as a principal cell membrane receptor for both NLRP3 inflammasome activation and IL-1β transcription by Td92. Understanding of the interaction between Td92 and integrin α5β1 may contribute to the development of a new therapeutic target for periodontitis treatment.

Keywords: Oral spirochetes, Tp92 homologs, Inflammation, NLRP3 inflammasome, Integrin α5β1, Periodontitis.

Student number: 2004-22655

CONTENTS

1. Introduction

Numerous studies examining epidemiology and virulence factors have revealed strong evidence for the role of oral spirochetes in the etiology of periodontitis, and the presence of spirochetes in the subgingival plaque is associated with an increased severity of periodontitis [1-3]. Oral spirochetes are composed of highly heterogeneous *Treponema* species and are found in high numbers in periodontitis patients. Due to their distinctive morphotypes and the virulence of *Treponema* species, oral spirochetes have been used as indicators of the active progress of periodontitis using microscopic analysis of subgingival plaques. However, only 10 species of *Treponema* can be cultivated, whereas more than 50 phylotypes of oral treponemes have been identified by culture-independent methods [4]. Some species, such as *T. denticola*, *T. lecithinolyticum*, and *T. socranskii*, are more prevalently associated with periodontitis and are resistant to periodontal therapy [2]. Multiple species or phylotypes of *Treponema* have often been found in a single patient or in a single site. The molecular pathogenesis of oral treponemes demonstrates that some surface proteins are important immune modulators [5-9].

The bacterial outer membrane provides a crucial contact barrier to host cells, and outer membrane proteins (OMPs) belong to the primary class of molecules involved in host-bacteria interactions. They are involved in the adhesion to and the induction of cytopathic effects on host cells and in inflammatory and immunological responses. OMPs are valuable candidates for the study of host-

pathogen interactions and for identify appropriate targets for therapy and prophylaxis. It is therefore important to identify and characterize common virulence determinants that are localized on the surface of oral spirochetes to elucidate their role in periodontal pathogenesis. OMPs of oral spirochetes have been reported to participate in the colonization, cytopathogenesis, and inflammatory responses of the host in periodontitis [6, 10, 11]. Most of the OMPs identified in oral spirochetes are species-specific [6, 11-17].

Tp92 (837 aa residues), one of the surface antigens of *Treponema pallidum*, with a molecular mass of 92-kDa, has been reported to have opsonic potential and to induce a protective immune response to syphilis, a *T. pallidum* infection [18]. This protein has been suggested for use as a syphilis serodiagnostic marker, and it has shown a 98% sensitivity and 97% specificity when tested for this capacity [19]. Tp92-related proteins are also found in other genera of spirochetes, such as *Borrelia burgdorferi* and *Leptospira interrogans*, and they are distributed in a wide range of gram-negative bacteria, such as *Chlamydia trachomatis* (OMP85 analog), *Neisseria* spp. (Omp85), *Pasteurella multocida* (Oma87), *Haemophilus* spp. (D15), and *Helicobacter pylori* (D15)[20]. Based on functional analysis, Omp85 of *Neisseria* spp. appears to be essential for the viability of the bacteria and to be involved in the assembly of outer membrane proteins, such as the porines PorA and PorB, secretin PilQ, and the siderophore receptors FrpB and RmpM [21], as well as in lipid transport to the outer membrane [22]. Immunization with D15 *Haemophilus* spp. was shown to be protective against infection with this bacterium in animal models and has been considered as a potential vaccine candidate [23], as

shown in *T. pallidum* with Tp92 [18]. Antiserum against Oma87 of *P. multocida* and D15 of *H. influenzae* has been found to be immunoprotective in animal models [24, 25]. Tp92/Omp85 homologs are therefore a family of highly conserved outer membrane proteins in gram-negative bacteria with possibly conserved functions.

Periodontitis is characterized by bone resorption leading to tooth loss. Osteoclasts and osteoblasts play important roles in bone resorption, and osteoblastic cells regulate the differentiation, fusion and activation of osteoclasts. Osteoclasts are activated by the receptor activator of nuclear factor-κB ligand (RANKL), which is stimulated from osteoblasts/stromal cells by osteoclastogenic factors, such as parathyroid hormone, $1,25(OH)_2$ vitaminD_3, interleukins (IL-1, IL-6, IL-11), tumor necrosis factor-α (TNF-α) and prostaglandin E_2 (PGE_2) [26, 27]. The pro-inflammatory and bone-resorptive characteristics of IL-1β are associated with the immunopathology of periodontitis, leading to periodontal tissue destruction. The IL-1β level is increased in the gingival crevicular fluid of periodontitis patients and correlates with the presence of major periodontopathogens, such as *Porphyromonas gingivalis*, *Tannerella forsythia*, and *Treponema denticola*, which are known collectively as red complex according to the classification by Socranskii et al. [3, 28], and with disease severity as assessed by bleeding upon probing, probing depth, and gingival attachment loss [29, 30]. Significantly elevated IL-1β secretion was observed in a coculture composed of epithelial cells and macrophages that was infected with the red complex [31]. An IL-1β polymorphism (3954, CT or TT) has been demonstrated to be related to significantly higher IL-1β mRNA expression in gingival tissues comprising the

junctional epithelium, gingival crevicular epithelium, and connective gingival tissue when compared to the wild type (CC) [30]. Gingival tissues with the IL-1β polymorphism have been shown to have increased inflammation in response to plaque bacteria, leading to an increase in the gingival crevicular fluid flow, which supplies rich nutrients for peptidolytic periodontopathogens. Socransky et al. [28] found that periodontopathogens, primarily of the red and orange complexes, were detected at significantly higher levels in IL-1 genotype-positive subjects than in genotype-negative subjects.

IL-1β secretion is regulated in two separate steps. Upon the binding of pathogen recognition receptors with ligands, the transcription of the IL-1β gene is increased, and proIL-1β (31 kDa) is synthesized in the cell. The processing of the "pro" form into the mature form (17 kDa) requires the assembly and activation of a caspase-1-activating complex, the inflammasome. The inflammasome is a component of innate immunity and a multiprotein complex that contains nucleotide-binding oligomerization domain-like receptors (NLRs), which sense pathogens or their components. NLRs are pathogen recognition receptors that are intracellularly localized and that detect pathogen-associated molecular patterns, pathogen-specific factors, or host danger signals induced by pathogens. Recently, the signals and mechanisms leading to inflammasome activation have been intensively studied, and NLRs, such as NALP, NLRC4/IPAF, and NAIP, have been reported to be involved in caspase-1 activation [32]. Of those NLRs, NLRP3 (also known as Nalp3 and cryopyrin) has been the most intensively studied, and there are a broad range of NLRP3-activating stimuli: pathogen-associated

molecules, such as bacterial muramyl dipeptide (MDP), nucleic acids, and bacterial pore-forming toxins; danger-associated molecular patterns, such as ATP, hyaluronan, glucose, and monosodium urate crystals from the host as a result of cellular stress or damage; calcium pyrophosphate dehydrate; and environmental irritants, such as silica, asbestos, aluminum hydroxide, and imidazoquinoline [33-39]. Although IL-1β is required for host defense against pathogens, exaggerated expression and secretion of this molecule can lead to tissue damage. Dysregulated inflammasome activation is associated with the pathogenesis of a variety of inflammatory diseases [40].

Integrins are heterodimeric glycoprotein receptors composed of alpha and beta subunits. In mammals, 24 integrins, with 18 alpha and 8 beta subunits, have been identified to date [41]. Integrins mediate cell-cell or cell-extracellular matrix interactions, and the binding of integrin to ligands has pivotal roles in normal cellular functions, such as cell proliferation, differentiation, and migration, as well as in the pathogenesis of chronic inflammation and cancer. A variety of microorganisms, including bacteria, viruses, and fungi, use integrins to bind to and invade host cells either directly or indirectly.

The aim of this study is to identify and characterize the Tp92 homologs of four representative oral spirochetes that are strongly associated with periodontitis and to examine the function in pathogenesis of the common surface proteins of oral treponemes in the progression of chronic periodontitis. First, the *tp92* gene homologs were identified either from the genome sequence (in the case of *T.*

denticola) or by PCR amplification and sequencing, and the activities of the Tp92 homologs were assessed after cloning the *tp92* gene homologs into *Escherichia coli* and purifying the recombinant proteins. The amino acid sequences of the Tp92 homologs from the oral treponemes were highly homogenous. The immune cross-reactivity and the surface exposure of the Tp92 homologs in oral treponemes were demonstrated with a polyclonal antibody raised against the Tp92 homolog of *T. denticola*. The Tp92 homologs were then shown to bind to epithelial cells and induce the expression of proinflammatory and osteoclastogenic factors in host cells, including monocytes and fibroblasts. Second, a novel function of integrin α5β1 in the activation of innate immune components by Td92, a Tp92 homolog of *T. denticola*, was investigated in PMA-differentiated THP-1 cells, in a human monocytic cell line, and in human PBMC-derived macrophages. Td92 directly interacts with integrin α5β1 to activate the NLRP3 inflammasome and to upregulate proIL-1β synthesis, which could lead to uncontrolled IL-1β secretion. Td92 internalization into the cells is not required for this activity, and ATP release and K^+ efflux induced by Td92 are key functional factors. The involvement of integrin α5β1 in NLRP3 inflammation is strengthened by the fact that fibronectin and the arginine-glycine-aspartate (RGD) peptide induce caspase-1 activation via interaction with integrin α5β1.

2. Materials and Methods

2.1. Chemicals and antibodies

Chemicals and antibodies were purchased from the sources listed below. Phorbol 12-mystristate 13-acetate (PMA), muramyldipeptide (MDP), ATP, oxATP, trichloroacetate (TCA), glybenclamide, tolbutamide, human plasma fibronectin, propidium iodide, cytochalasin D, N-*p*-Tosyl-L-phenylalanine chloromethyl ketone (TPCK), BAY-117082, tunicamycin from *Streptomyces* sp., N-glycosidase F from *Elizabethlingia miricola,* Fluorescent probe 2,7-dichlorofluorescein diacetate. (DCF-DA), N-acetyl-L-cysteine (NAC), Pyrrolidine dithiocarbamate (PDTC), Apocynin, Diphenylene iodonium (DPI), and the monoclonal anti-human fibronectin Ab (IST-3) used for immunoblotting were from Sigma (St. Louis, MO, USA). *S. typhimurium* flagellin and ultra pure LPS were from InvivoGen (San Diego, CA, USA). Ac-YVAD-cho, SB202190, SB203580, SP600125, PD98059, GRGDSP peptide, and GRADSP peptide were from Calbiochem (San Diego, CA, USA). Profect P1 was from Targeting Systems (El Cajon, CA, USA). The anti-human NLRP3 Ab and anti-human TLR4 Ab were from Santa Cruz (Santa Cruz, CA, USA). The anti-human ASC Ab was from MBL (Nagoya, Japan). The anti-human NLRC4 Ab was from ProSci (Poway, CA, USA). Z-YVAD-fmk and the LDH-cytotoxicity assay Kit were from BioVision (Palo Alto, CA, USA). The anti-human integrin α5β1 Ab (monoclonal, JBS5), the anti-human fibronectin blocking Ab (monoclonal, 3E3), the anti-human integrin αvβ3 Ab (monoclonal, LM609), and Protein G agarose were from Chemicon (Temecula, CA, USA). The anti-$(his)_5$

Ab and Ni-NTA agarose were from QIAGEN (Valencia, CA, USA). The affinity purified mouse IgG_1 isotype control was from eBioscience (San Diego, CA, USA). The anti-human caspase-1 Ab (recognizing pro-caspase-1 p45 and caspase-1 p20), the anti-human IL-1β Ab (recognizing p17 and p31), antibodies against human integrin α5 (polyclonal, cat. no. 4705), integrin β1 (polyclonal, cat. no. 4706), integrin αv (polyclonal, cat. no. 4711), integrin β3 (polyclonal, cat. no. 4702), IκBα, phospho-p38 (Thr180/Tyr182), phospho-SAPK/JNK (Thr183/Tyr185), phospho-p44/42 MAP kinase (Thr202/Thr204), TRIF Ab, and MyD88 Ab were from Cell Signaling Technology (Beverly, MA,USA). The NF-κB p65 Ab was from Abcam (Cambridge, MA, USA). Ficoll-Paque PLUS™ was from Amersham Biosciences (Piscataway, NJ, USA). Human AB serum was from Bio Whittaker (Walkersville, MD, USA). Recombinant human integrin α5β1, Recombinant human αvβ3, recombinant TNF-α, and the human IL-1β ELISA Kit were from R&D Systems (Minneapolis, MN, USA). The ATP bioluminescence assay kit and protease inhibitor cocktail were from Roche (Mannheim, Germany). Hoechst 33277, Carboxyfluorescein diacetate, succinimidyl ester (5(6)-CFSE), Stealth siRNA (for NLRP3, NLRC4, ASC, TLR4, integrin α5, MyD88 and TRIF), the Stealth siRNA negative control duplex and Lipofectamine RNAiMAX were from Invitrogen (Carlsbad, CA, USA). DyLight 488 NHS Ester and the bicinchoninic acid (BCA) protein assay Kit were from Pierce (Rockford, IL, USA). The LAL endochrome Kit was from Charles River Endosafe (Wilmington, MA, USA). Biotinylated Phaseolus vulgaris leucoagglutinin (PHA-L) was from Vector Laboratory (Burlinggame, CA).

2.2. Bacterial strains and growth conditions

Oral treponemes (*T. denticola* ATCC 33521, *T. lecithinolyticum* ATCC 700332, *T. maltophilum* ATCC 51939, and *T. socranskii* subsp. *socranskii* ATCC 35536) were cultured in an anaerobic atmosphere (10% CO_2, 5% H_2, and 85% N_2) using OMIZ-Pat medium as described previously [42]. *E. coli* DH5α-T1 (Invitrogen, Carlsbad, CA, USA) was used for TA cloning and *E. coli* M15 (Qiagen, Valencia, CA, USA) was used for the expression of the treponeme Tp92 homologs. *E. coli* containing the plasmids was cultured aerobically in Luria-Bertani (LB) broth supplemented with 50 μg/ml of ampicillin for the DH5α-T1 or with 100 μg/ml of ampicillin and 25 μg/ml of kanamycin for the M15 strain.

2.3. Cell culture and treatment

To identify the expression of proinflammatory cytokines by Tp92 homologs, THP-1 cells (ATCC TIB-202), a human monocytic cell line and primary cultured periodontal ligament (PDL) cells were prepared as described previously [43]. THP-1 and PDL cells were cultured in RPMI 1640 and α-minimal essential medium (α-MEM) supplemented with 10% fetal bovine serum (FBS), respectively, and used for stimulation with the recombinant Tp92 homologs. KB cells (ATCC CCL-17), a carcinoma epithelial cell line, were cultured in RPMI 1640 medium supplemented with 10% FBS and used for a bacterial binding assay. Human monocytic THP-1 cells (1 x 10^6 cells/ml) and primary cultured PDL cells (5 x 10^5 cells/ml) were

cultured as described above and plated in 35-mm culture dishes in the absence of serum. The cells were then treated with 10 μg/ml of each of the recombinant Tp92 homologs for 8-24 h. The cells were harvested and used for RNA isolation, and the conditioned supernatants were collected and stored at -70°C for the gelatin zymography and ELISA. An NF-κB reporter cell line, CHO/CD14/TLR4, which expresses CD14 and TLR4 and has the CD25 reporter gene with the human E-selectin promoter, was kindly provided by Dr. Han (School of Dentistry, Seoul National University, Seoul) and cultured as described previously [44]. The CHO/CD14/TLR4 cells were cultured in Hams-F12 medium (Hyclone Laboratories, Loan, UT, USA) supplemented with 10% FBS and were used to verify that prepared recombinant proteins were endotoxin free by flow cytometry analysis after treatment with the recombinant protein of the Tp92 homologs.

To study stimulation of Td92 in the system for the inflammasome activation, THP-1 cells and human PBMC-derived monocytes that were differentiated into macrophages were used. For the experiments, THP-1 cells (2 x 10^6/well in 6-well plates) were differentiated into macrophage-like cells with 0.5 μM PMA for 3 h. Human monocytes were purified using Ficoll-Paque PLUS™ and were differentiated for 6 days in RPMI 1640 with 10% FBS. The cells were detached using 0.25% trypsin/EDTA and were seeded at 2 x 10^6/well in 6-well plates in RPMI 1640 with 10% human AB serum. The differentiated cells were treated with Tp92 homologs, live whole *T. denticola* cells, truncated Td92 polypeptides (Td-G and Td-B), MDP, fibronectin, GRGDSP peptide, GRADSP peptide, PP4, or LPS in serum-free medium for 1-6 h. In some experiments, the cells were pretreated with

NAC, PDTC, Apocynin, DPI, cytochalasin D, oxATP, Ac-YVAD-cho, Z-YVAD-fmk, KCl, glybenclamide, tolbutamide, SB202190, SB203580, TPCK, BAY-117082, SP600125, PD98059, an anti-human integrin α5β1 Ab, an anti-human fibronectin Ab, or an anti-human integrin αvβ3 Ab at the indicated concentrations for 30 min or 1 h before stimulation with the various stimuli for 6 h. MDP- or LPS-stimulated cells were further incubated with 2.5 mM ATP for 30 min. Procaspase-1 and proIL-1β in the cell extracts and the active forms secreted in the culture supernatant precipitated by 10% TCA were analyzed by immunoblotting. For the detection of NLRP3 expression, the cell lysates and culture supernatants were combined and used for immunoblotting.

2.4. Sequencing of *tp92* homologs

The *tp92* homolog of *T. denticola* (ATCC 35405, TDE2601 ORF, 46) was identified in the genome sequence of the bacterium using the NCBI BLAST program with the *T. pallidum* subsp. *pallidum tp92* sequence. Nucleotide sequences of the *tp92* gene and the *T. denticola tp92* homolog were aligned using the program Align from EMBL-EBI, and several degenerate primers were designed for the initial amplification of the *tp92* homologs of *T. maltophilum* and *T. socranskii* by PCR. In the case of *T. lecithinolyticum*, a portion of the *tp92* homolog (400 bp) was originally identified by screening an expression library of this organism with antibodies directed against the *T. lecithinolyticum* outer membrane fraction. The full sequences of the *tp92* homologs of *T. lecithinolyticum*, *T. maltophilum* and *T.*

socranskii were obtained by PCR amplification using the degenerate primers described above or by inverse PCR with specific primers designed from the partial sequence, followed by sequencing using a DNA sequencer (ABI, Applied Biosystems, CA, USA).

Primary structure analysis of translated proteins was performed by using ProtParam from ExPASy. Pairwise sequence comparisons were performed using Align from EMBL-EBI to analyze sequence homology. Prediction of protein subcellular localizations and signal peptides were analyzed using PSORTb (version 2.0, 20) and SignalP (version 3.0, 6), respectively.

2.5. Cloning and expression of *tp92* homologs, Td-G, and Td-B domain

The *tp92* gene homologs of *T. denticola*, *T. lecithinolyticum*, *T. maltophilum*, and *T. socranskii* were amplified from the genomic DNA by PCR and cloned without the sequences encoding their leader peptides. The sequences of the PCR primers were as follows: 5'-AAC TGA GCT CGG ATG GTA TAA TGG AAA ACC TG-3' (SacI-tagged) and 5'-AAC TCT GCA GCT ATA AAT TGG GTA TAT TGA ATG AA-3' (PstI tagged) for *T. denticola*; AAC TGA GCT CGA AAG CGA TTG GTA TTA CGG A (SacI-tagged) and AAC TCT GC A GTT ATT GAT TGG TAA GGT TAA AAG (Pst1-tagged) for *T. lecithinolyticum*; AAC TGG ATC CCA AAG CGA CAA TAA CTG GTA (BamH1-tagged) and AAC TGA GCT CTT ATT GAT TGA CCA AAT TG (Sac1-tagged) for *T. maltophilum*; AAC TGG

ATC CGA AGA AAG CGA AGA CGA AGG (BamH1-tagged) and AAC TAA GCT TTT ATC AGC GGT TCG TTA TGT TGA (HindIII-tagged) for *T. socranskii*. Tp92 homologs of oral spirochetes had predicted signal peptides (20-31 amino acids) and molecular masses of 88-92-kDa for mature proteins. The Tp92 homologs were named Td92 for *T. denticola*, Tl88 for *T. lecithinolyticum*, Tm88 for *T. maltophilum*, and Tss88 for *T. socrnaskii* subsp. *socranskii* according to their molecular weights.

To produce truncated Td92 polypeptides, Td92 gene fragments were divided into two fragments (the G-domain, which corresponded to the amino acid positions 1-400 and the B-domain, which corresponded to the amino acid positions 401-798) according to the structural protein analysis using MODELLER. The fragments were amplified from the genomic DNA of *T. denticola* by PCR and cloned in *E. coli* using the expression vector pQE-30 for recombinant Td92 preparation. The primers used for PCR to amplify the G- and B-domain gene fragments were as follows: for the G-domain: 5'-AAC TGA GCT CGG ATG GTA TAA TGG AAA ACC TG-3'(SacI-tagged) and 5'- AAC TCT GCA GAT CAG GTT CCG AAC CCT GT-3'(Pst1-tagged); for the B domain: 5'-AAC T GA GCT CCT TGT GGA TAT TGT CAT CAA TG-3'(SacI-tagged) and 5'-AAC TCT GCA G CT ATA AAT TGG GTA TAT TGA ATG AA-3'(Pst1-tagged). The underlined sequences are the introduced recognition sites. Four nucleotides were added to the 5' ends of these restriction sites. The molecular masses of the recombinant G-domain (Td-G) and B-domain (Td-B) proteins were 46- and 45.5-kDa, respectively. PCR was performed in a total volume of 50 μl containing 15 pmol of each primer, 1.25 U of

Ex*Taq* polymerase (Takara Bio, Otsu, Japan), and 100 pmol of dNTPs in a thermal cycler (MJ Research, Walham, MA, USA). The thermal cycle chosen included an initial denaturation step at 94°C for 4 min, 30 cycles of a denaturation step at 94°C for 1 min, an annealing step at 62°C for 1 min, and an extension step at 72°C for 1 min, with a final incubation at 72°C for 5 min. The PCR products were cloned in *E. coli* using the TA cloning vector pCR2.1-TOPO and TA cloning kit (Invitrogen, Carlsbad, CA, USA). The plasmid DNA was isolated and digested with each of the above restriction enzymes. The fragments of each gene were cut out from agarose gel after electrophoresis and purified with a gel extraction kit (QIAGEN, Valencia, CA, USA). The purified gene was then ligated into the predigested pQE30 expression vector using T4 DNA ligase (Boeringer Mannhein, Germany) at 16°C for 16 h as described previously [15]. *E. coli* M15 was transformed with the recombinant plasmids, plated on LB agar plates containing 100 μg/ml of ampicillin and 25 μg/ml of kanamycin, and grown overnight. Single recombinant colonies were grown in LB broth containing antibiotics until optical density (O.D) at 600 nm is 0.60, the expression of recombinant proteins were induced with 1 mM isopropyl-β-D-thiogalactopyranoside (IPTG) for 4 h. The proteins were detected by immunoblotting by using polyclonal antibodies directed against penta-histidine (QIAGEN, Valencia, CA, USA). After confirmation of each protein expression, 50 ml overnight cultures of *E. coli* transformed with each genes construct were inoculated into 500 ml of fresh LB broth and cultured until the optical density (O.D) at 600 nm is 0.60. After 1 mM IPTG was added, the cultures were incubated for an additional 4 h. The recombinant proteins formed in the inclusion bodies were

purified as follows. The bacteria harvested by centrifugation at 6,500 x g for 15 min at 4°C and resuspended in 50 ml of IB washing buffer (20 mM Tris-HCl pH 7.5, 10 mM EDTA, and 1% Triton X-100). The cells were lysed by incubating them with 100 μg/ml of lysozyme at 4°C for 15 min and subsequently sonicating them with an ultrasonic processor (10 sec bursts at output 20 W with a 10 sec cooling period between burst; Sonics&Materials, Inc. Newtown, Conn., USA). In order to minimize protein degradation, phenylmethylsulfonyl fluoride (PMSF; 1 mM) was added to the bacterial lysates, and the inclusion bodies obtained by centrifugation at 10,000 x g for 10 min. The pellets were resuspended in 50 ml of the IB washing buffer and then centrifuged. This procedure was repeated 5 times. The inclusion bodies were resuspended in solubilization buffer (50 mM 3-cyclohexylamino-1-propansulfonic acid (CHAPS pH 11.0), 1 mM DTT and 0.3% N-laurylsarcosine) and incubated at RT for 15 min. The suspension was then centrifuged at 10,000 x g for 10 min, and the supernatants containing the solubilized proteins were collected and dialyzed against 100 volumes of 20 mM Tris-HCl (pH 8.5) for 24 h with three times changes. The recombinant proteins were purified by using nickel-nitrilotriacetic acid agarose (Ni-NTA agarose; QIAGEN, Valencia, CA), which bound to the histidine-tagged recombinant proteins, according to the manufacturer's protocol with a few modification. Briefly, the recombinant proteins binding to Ni-NTA agarose was washed 5 times with 10 ml of wash buffer (50 mM NaH_2PO_4, 300 mM NaCl, 250 mM imidazole, pH 8.0). Endotoxins present in *E. coli*, which could potentially contaminate the recombinant proteins, were removed using polymyxin B-agarose, according to the

manufacturer's instructions (Sigma Chemical Co., St. Louis, MO, USA). The purified recombinant proteins were dialyzed against 200 volumes of PBS with three buffer changes for 24 h. The recombinant proteins were concentrated using Centricon YM-30 (Millipore, Bedford, MA), then were filtrated through polyvinylidene fluoride (PVDF; Millipore, Bedford, MA) membrane with 0.22 μm pore-size. The identities of purified proteins were confirmed by SDS-PAGE and immunoblotting. For the mock control, an irrelevant recombinant peptide, PP4, was also prepared using the same procedures. PP4 is a C-terminal partial peptide (187 amino acid residues, molecular mass of 20.2 kDa) of the *Treponema lecithinolyticum* surface protein MspTL (570 amino acid residues) and does not have cell-stimulating activity [45].

2.6. Verification of endotoxin decontamination in the recombinant proteins

The most critical point in this study was to minimize endotoxin contamination of recombinant Tp92 homologs. To confirm that its activity was not a result of *E. coli* endotoxin contamination, the procedures were re-examined as follows: First, TLR4-dependent NF-κB activation was analyzed to verify endotoxin decontamination in the recombinant Tp92 homologs by flow cytometric analysis. CHO/CD14/TLR4 cells were cultured to 70% confluency in Hams-F12 media and stimulated with the recombinant Tp92 homologs (10 μg/ml) or LPS (1 μg/ml) for

16 h in the presence of 2% FBS. The cells were subjected to flow cytometric analysis using fluorescein isothiocyanate (FITC)-labeled mouse anti-human CD25 (Becton Dickinson, San Diego, CA) as described previously [44]. FITC-labeled mouse IgG_1 (Becton Dickinson) was used as an isotype matched control. Second, the actual endotoxin activity of recombinant Tp92 homologs was measured by the Limulus amoebocyte lysate (LAL) assay using an LAL Endochrome Kit (Charles River Endosafe, Wilmington, MA, USA) according to the manufacturer's protocol. In principle, endotoxin activated a proenzyme in LAL. In the presence of a colorless substrate, the activated enzyme rapidly catalyzed the cleavage of the chromophore p-nitroaniline, which produced a yellow color and the color was measured at 405 nm. A standard curve was run with *E. coli* control standard endotoxin from the kit. The final preparation of recombinant Td92, Tl88, Tm88, Tss88, Td-G, and Td-B contained 0.37, 0.23, 0.21, 0.10, 0.21, and 0.20 endotoxin Unit (EU)/μg of the protein, respectively. Third, recombinant Td92 after 1% Triton X-114 extraction was evaluated. The Triton X-114 two-phase extraction method is an efficient method to dissociate endotoxin from biomolecules including recombinant proteins [46]. After phase separation, endotoxin is found in the detergent phase, and the desired biomolecule is found in the upper aqueous phase. Td92 and *E. coli* LPS were re-extracted three times with Triton X-114 (at a final concentration of 1%), and the resulting upper aqueous phase was used for cell treatment. Lastly, to exclude the possibility that proIL-1β mRNA upregulation by Td92 is the result of contaminants LPS signaling, experiments were performed with siRNA against TLR4, MyD88 and TRIF.

2.7. Production of antiserum against the Tp92 homolog of *T. denticola*

Polyclonal antibodies against *T. denticola* Tp92 homolog were raised in New Zealand White rabbits by intradermal administration of 500 μg of the purified proteins with Complete Freund's Adjuvant (500 μg, F5881, Sigma) followed by three subsequent boosts of 200 μg of the protein with Incomplete Freund's Adjuvant (500 μg, F5506, Sigma) in two-week intervals. Antiserum was collected one week after the final boost. The antiserum was shown to contain high titers of specific antibodies against the recombinant *T. denticola* Td92, as judged by ELISA and immunoblot using horseradish peroxidase (HRP)-labeled mouse anti-rabbit IgG (R&D Systems, Minneapolis, MN, USA). Antibodies which cross-reacted with *E. coli* proteins and the histidine-tag, were removed by using affinity chromatography with activated Cyanogen-bromide (CNBr)-activated Sepharose 4B (Amersham Pharmacia Biotech, Piscataway, NJ, USA) according to standard protocols. For this purpose, *E. coli* M15 sonicates or an irrelevant histidine tagged protein, PP4 [45] were coupled to CNBr-activated Sepharose 4B. The antiserum was applied to the Sepharose and the unbound fraction of the antiserum containing the specific Ab was collected. IgG antibodies (designated as a Td92 Ab) were purified using an ImmunoPure (A Plus) IgG purification kit according to the manufacturer's instructions (Pierce, Rockford, IL, USA). Finally, endotoxin contamination in the IgG fraction was removed using polymyxin-B agarose (Sigma Chemical Co., St. Louis, MO, USA).

2.8. Preparation of outer membrane of *T. denticola*

To evaluate the actual surface location of *T. denticola* Td92, the outer membrane (OM) of *T. denticola* was isolated by a combined protocol of freeze-thaw procedures and sucrose density gradient centrifugation with a slight modification [47, 48]. Briefly, *T. denticola* cells (80 ml culture) were harvested and washed with PBS by centrifugation at 8,000 x g for 10 min. The cell pellet was resuspended in 1 ml of 50 mM Tris-HCl buffer (pH 7.2) containing 20 mM $MgCl_2$, 2 mM PMSF and DNase1 (4 U/ml). After the cells were subjected to 40 freeze-thaw cycles, the disrupted cell suspension was centrifuged at 8,000 x g for 10 min. The supernatant containing the OM was transferred to a new tube and centrifuged at 25,000 x g for 30 min. The pellet was washed twice with 50 mM Tris-HCl (pH 7.2), resuspended in 1 ml of 0.1 M sodium acetate buffer (pH 3.0), and mixed gently for 2 h to remove contaminating flagella followed by centrifugation at 25,000 x g for 30 min. The pellet was washed with and resuspended in 0.8 ml of 50 mM Tris-HCl buffer and subjected to sucrose gradient centrifugation consisting of 25, 42 and 56% sucrose at 100,000 x g for 16 h at 4℃ by an ultracentrifuge (Beckman TLA110 rotor, Beckman Instruments Inc., Fullerton, CA). The upper fraction containing the OM was removed and precipitated with methanol and chloroform. The OM precipitated was resuspended in 50 μl of PBS and used to detect Td92 by SDS-PAGE and immunoblot analysis.

To test whether the native protein functions similarly to the recombinant protein, native Td92 was isolated from *T. denticola* as follows. The protein was

kindly provided by Dr. Lee (School of Dentistry, Dankook University, Cheonan). Protein G-coated agarose beads (2 ml, 1 mg/ml) were incubated with 5 ml of rabbit anti-Td92 IgG (4 mg/ml) at 4°C for 12 h. The beads were washed three times with binding buffer (0.1 M phosphate, 0.15 M NaCl, pH 7.2) and were incubated with 0.5 mM disuccinimidyl suberate on a rotator for 1 h at room temperature. The beads were washed three times with 0.2 M glycine (pH 2.5) and were placed in PBS (pH 7.2) for 4 h at 4°C. Anti-Td92 IgG-bound beads were then incubated with the whole lysates of *T. denticola* from which proteins smaller than 50 kDa were removed using an Amicon Ultra centrifugal filter (Millipore, Bedford, MA). The beads were washed three times with PBS including 0.02% Tween 20. Native Td92 was eluted with 0.2 M glycine (pH 2.5) and was immediately neutralized with phosphate buffer (1 M phosphate, 0.15 M NaCl, pH 7.5). Finally, native Td92 was dialyzed three times at 4°C for 12 h in PBS, and the protein was confirmed by immunoblotting using the Td92 Ab along with recombinant Td92. Endotoxin contamination of native Td92 was undetectable by the LAL assay.

2.9. Immunoblotting

To verify the expression of the Tp92 homologs in *E. coli*, *E. coli* M15 cells transformed with the recombinant plasmids were cultured in LB broth containing antibiotics and induced with IPTG. The *E. coli* lysates (50 μg of protein) were subjected to SDS-PAGE and subsequently transferred to nitrocellulose membranes. The membranes were blocked with 2% BSA for 1 h and reacted with anti-mouse

histidine Ab for 1 h. After washing with PBS-0.2% Tween 20, the membranes were reacted with alkaline phosphatase (AP)-labeled anti-mouse IgG for 1 h. After washing with PBS-0.2% Tween 20, the membranes were developed with 5-bromo-4-chloro-3-indolylphosphate (165 μg/ml) and nitroblue tetrazolium (330 μg/ml).

To test the reactivity of the Td92 Ab in the lysates of *T. denticola* whole cells, the OM fraction, and the recombinant Td92, whole cell lysates of *T. denticola*, the OM, and Td92 were separated by SDS-PAGE and transferred to nitrocellulose membranes. The membranes were blocked with PBS-2% BSA, reacted with a Td92 Ab for 1 h, followed by HRP-labeled mouse anti-rabbit IgG for 1 h. After washing with PBS-0.2% Tween 20, the membranes were developed with 3, 3′, 5, 5′-tetramethylbenzidine (TMB, Sigma). To verify the purity of the OM preparation, the immunoblot was performed using a FlaA (1:5000 dilution, a kind gift from Dr. Christopher Fenno (School of Dentistry, University of Michigan, USA) which detects the periplasmic protein FlaA of *T. denticola*.

To detect various host factors, the cells were treated with the different stimuli. After washing with chilled PBS, the cells were lysed in 50 μl of RIPA buffer (10 mM Tris-HCl, pH 7.5, 150 mM NaCl, 1% Triton X-100, 50 mM NaF, 1 mM EDTA, 5 μM Na_3VO_4, and 1 mM PMSF). The lysates were clarified by centrifugation at 13,000 x g for 45 min at 4°C. The protein concentration was determined using a bicinchoninic acid (BCA) protein assay Kit. Cell lysates and TCA-precipitated supernatants were separated by SDS-PAGE (using a 12% gel) and were transferred onto PVDF membranes. The membranes were incubated with

a specific antibody followed by a horseradish peroxidase-conjugated secondary antibody. Immunoreactive proteins were developed using a standard ECL reaction (Amersham/Pharmacia Biotech, Piscataway, NJ) according to the manufacturer's instructions. β-Actin was used as a loading control. The band intensities were quantified using the NIH Image J software, and the specific band intensity was normalized to β-Actin.

2.10. Immunodot blotting

The cross-reactivity of Tp92 homologs with a Td92 Ab was analyzed by immunodot blotting. The recombinant Tp92 homologs (250 ng in 1 μl) were applied onto a nitrocellulose membrane and air dried. The membranes were blocked with PBS-2% BSA, reacted with a Td92 Ab for 1 h, followed by HRP-labeled mouse anti-rabbit IgG for 1 h. After washing with PBS-0.2% Tween 20, the membranes were developed with 3, 3′, 5, 5′-tetramethylbenzidine (TMB, Sigma). An irrelevant histidine-tagged recombinant protein, MspTL [45] and *E. coli* lysates were used as negative controls.

2.11. Indirect immunofluorescence microscopy

Treponema species grown to an early stationary phase were harvested, resuspended in PBS, and applied to glass slides coated with silane (Sigma). Some

of the slides were used directly and the others were used after fixation with cold acetone for 15 min and subsequent permeabilization of the outer membrane with 0.1% Triton X-100 in PBS for 5 min. The bacteria were incubated in PBS containing 1% BSA in for 1 h and then reacted with a Td92 Ab or a FlaA Ab (1:1000 dilution) for 1 h. After washing three times with PBS, the bacteria were subsequently reacted with FITC-labeled goat anti-rabbit IgG (1:50 dilution in PBS containing 1% BSA) and washed three times with PBS. To see all the bacteria applied, the slides were further stained with a fluorescent nucleic acid stain, Hoechst dye 33342 (2 μg/ml in PBS, Invitrogen), for 30 min. The cells were washed three times with PBS and observed with a fluorescence microscope (Carl ZEISS, Axioskop, Germany) at 1000 x magnification. The FlaA Ab (1:500 dilution) was used as a control to verify that the outer membrane of the bacteria was intact during immunofluorescence assay. As a control for nonspecific binding, isotype-matched Ab (rabbit IgG) was used instead of the Td92 Ab.

To analyze ability of intact bacteria to react with the Td92 Ab, *T. denticola* cells (5×10^7) were fixed with acetone and permeabilized as described above. Non-fixed and acetone-fixed bacteria were reacted with the Td92 Ab or the FlaA Ab (1: 500 dilution) in 100 μl of PBS containing 1% BSA at room temperature for 1 h. The bacteria were washed twice with PBS containing 0.02% BSA and reacted with FITC-labeled goat anti-rabbit IgG (1:50 dilution in 1% BSA in PBS) at room temperature for 1 h. After washing twice with PBS, the bacteria were analyzed using a fluorescence-activated cell sorter (FACSCalibur; Becton Dickinson, San Jose, CA). The data were obtained by using 40,000 cells. The number of bacteria

was enumerated as described previously [49]. Isotype matched Ab (rabbit IgG) was used as a negative control.

2.12. Immunogold staining of *T. denticola*

T. denticola cells (OD 600 = 0.2; corresponded to 5 × 10^9cells/ml) were incubated with 200 µl of blocking solution (PBS containing 1% BSA) for 1 h. The bacteria were then incubated with 100 µl of the Td92 Ab (1: 50 dilution in PBS containing 1% BSA) or isotype-matched Ab (rabbit IgG) for 1 h. After washing three times with PBS, the bacteria were reacted with anti-rabbit IgG conjugated with 10-nm colloidal gold particles (1:50 dilution in PBS containing 1% BSA; Sigma) for 1 h. After washing three times with PBS, the bacteria were resuspended in PBS and absorbed onto formvar/carbon-coated 400-mesh copper grids. After washing with PBS and air drying, the bacteria were negative stained with 1% uranyl acetate for 15 s. After washing with PBS and air drying, the bacteria were observed with a transmission electron microscopy (JEOL, JEM-1200EX, Japan) at 80 kV acceleration voltage. Isotype matched Ab (rabbit IgG) was used as a negative control.

2.13. Fluorescence labeling of protein and bacteria

In order to analyze the binding and the internalization of the Tp92 homologs into the host cells and immobilized fibronectin, Tp92 homologs and fibronectin were fluorescence labeled using DyLight 488 NHS Ester according to the manufacturer's protocol (Pierce, Rockford). Calculated amount (mg) of DyLight NHS Ester fluor was added to Tp92 homologs (1 mg/ml) solution and incubated at room temperature for 1 h. To remove non-reacted reagent from the proteins, the proteins were dialyzed against 200 volumes of labeling buffer (0.05 M sodium borate buffer, pH 8.5) with three buffer changes at 4°C for 24 h.

To label bacteria, *T. denticola* was grown to an early stationary phase, harvested, resuspended in PBS, and adjusted to have an OD_{600} = 1.0. Aliquots (1 ml) of bacteria were centrifuged and resuspended in 1 ml PBS. The bacteria were stained with 10 μM carboxyfluorescein diacetate, succinimidyl ester (CFSE, Molecular Probes, Eugene, OR) for 10 min at room temperature and washed three times with PBS, followed by storage at -20°C for 24 h to induce fluorescence stabilization. CFSE-labeled bacteria were diluted with PBS to an OD_{600}=0.2 (5 x 10^9 bacteria/ml).

2.14. Cell binding and internalization assay

To determine whether the Tp92 homologs were able to bind to host cells, the binding assay was performed using KB cells, a carcinoma epithelial cell line, and

FITC-labeled Tp92 homologs. KB cells (1 x 10^5 cells/500 µl) were cultured in 24-well culture plates to confluence. After changing to serum-free medium, the FITC-labeled Tp92 homologs were added to the cells (at 2.5 µg per well) and incubated at 37°C under 5% CO_2 for 1 h. The cells were detached from the cell culture plates using 200 µl of 1 x trypsin-EDTA, and washed with serum containing medium and subsequently with PBS three times by centrifuging at 100 x g. The fluorescence of the cells was then measured by a fluorometer (FLUOStar$^+$ OPTIMA, BMG Labtechnologies Inc., Durham, NC). Protein binding was expressed as a percentage of total proteins added using formula as follows: bound fluorescence/total fluorescence added x 100. One microgram of Td92 was equivalent to 1 x 10^9 cells of *T. denticola*, as judged by SDS-PAGE and subsequently by immunoblotting of aliquots containing various numbers of bacteria. The number of *T. denticola* (OD_{600}=0.2) corresponded to 5 x 10^9 cells/ml, when determined using a Petroff-Hausser counting chamber (Hausser Scientific, Hosham, PA).

To confirm that the Tp92 homologs function as adhesins, binding inhibition of fluorescence-labeled *T. denticola* to epithelial cells by Td92 was tested. KB cells were cultured in 24-well culture plates (1 x 10^5 cells/500 µl) to confluence, washed twice with serum-free medium, and incubated with CFSE-labeled bacteria (100 µl of OD_{600}=0.2, 5 x 10^8 bacteria) in the presence of Td92 (1 to 10 µg) at 37°C under 5% CO_2 for 1 h. The cells were detached and washed three times with PBS by centrifuging at 100 x g, and the fluorescence of the adherent bacteria was determined using a fluorometer as described above. An irrelevant histidine-tagged

recombinant protein (PP4) was used as a negative control. The ratio of *T. denticola* to KB cells used for the binding competition assay was 5,000:1.

To analyze the effect of inhibitory antibodies, cytochalasin D, and Profect P1 on FITC-labeled Td92 binding and internalization into the cells, PMA-differentiated THP-1 cells were seeded at 2 x 10^5 cells/500 μl in 24-well culture plates and were reacted with 150 μl of integrin α5β1 Ab (10 and 20 μg/ml), an anti-mouse IgG (10 μg/ml), or cytochalasin D (1 and 2.5 μM) for 30 min or 1 h. The cells were subsequently treated with FITC-labeled Td92 (10 μg/ml) and were incubated at 37°C for additional 30 min to 1 h. After washing the cells with PBS, the binding of Td92 was analyzed by flow cytometry (FACSCalibur, BD, San Jose, CA, USA). To test of the efficiency of Profect P1 for protein transfection, the cells were treated with pre-incubated mixture of FITC-Td92 (5 μg)-Profect P1 (2.5 μl) for 1 and 4 h and were analyzed by flow cytometry. FITC-Td92-treated cells that had been fixed in 2% paraformaldehyde were used as a negative control for internalization. Trypan blue (4%) was used to quench cell-bound fluorescence and to detect intracellular fluorescence exclusively.

2.15. Real-time qPCR

RNA from the THP-1 cells, PDL cells, and PMA-differentiated THP-1 cells treated with the Tp92 homologs was prepared using an easy-BLUE total extraction kit (iNtRON Biotechnology, Korea) and cDNA was synthesized from 1 μg of RNA

using a Maxime RT PreMix kit (iNtRON Biotechnology, Korea) according to the manufacturer's protocols. For real-time qPCR, cDNA (1 μl) was mixed with 10 μl of SYBR Premix Ex Taq (Takara Bio Inc. Japan) and primer pairs (4 pmol each) in a 20 μl reaction volume, followed by PCR for 40 cycles of a denaturation step at 95°C for 15 sec, an annealing step at 60°C for 15 sec, and an extension step at 72°C for 33 sec in an ABI PRISM 7500 Fast Real-Time PCR System (Applied Biosystems, Foster City, CA, USA). The PCR products were subjected to melting curve analysis to verify the presence of a single amplification product. PCR without RT was performed as a negative control. The housekeeping gene encoding glyceraldehyde dehydrogenase (GAPDH) was used as a reference in order to normalize expression levels and to quantify the changes in gene expression between non-stimulated cells and stimulated cells. The expression level of the gene was normalized against GAPDH and calculated by using the $2^{-\Delta\Delta C}{}_{T}$ method [50]. In the expression of proinflammatory factors in Tp92 homologs-stimulating THP-1 and PDL cells, the data shown fold change to control was expressed as a log2 ratio. The sequences of the primers for real-time qPCR were as follows: 5'-AGC TGT ACC CAG AGA GTC C-3' and 5'-ACC AAA TGT GGC CGT GGT TT-3' for IL-1β; 5'-AAC CTG TCC ACT GGG CAC A-3' and 5'-TCT GGC TCT GAA ACA AAG GAT-3' for IL-6; 5'-GTG AAG GTG CAG TTT TGC CA-3' and 5'-TCT CCA CAA CCC TCT GCA C-3' for IL-8; 5'-CAG GGA CCT CTC TCT AAT CA-3' and 5'-AGC TGG TTA TCT CTC AGC TC-3' for TNF-α; 5'-CTC TGG AGG TTC GAC GTG A-3' and 5'-CTG CAG GAT GTC ATA GGT CA-3' for MMP-9; 5'-AAG CTG GGA AGC CTT CTC TA-3' and 5'-GTG CTG GGC AAA GAA

TGC AA-3' for COX-2; 5'-TGA AGA GGA GTG GAT GGG TT-3' and 5'-TTC AAT GCA CTG GAA TCT GC-3' for NLRP3; 5'-GAT GCG GAA GCT CTT CAG TT-3' and 5'-AGG ATG ATT TGG TGG GAT TG-3' for ASC; 5'-CAG AAC CCT GCT GAC TGA GA-3' and 5'- CCA AAT GGA AAG GTC AAA GG-3' for NLRC4; 5'-CCA AGG GGA ATC AGA ACT CA-3' and 5'-TGG AGC AGG CCC AAA TAT AG-3' for integrin α5; 5'-GTG GTG GAC CTG ACC TGC-3' and 5'-TGA GCT TGA CAA AGT GGT CG -3' for GAPDH.

2.16. Gelatin zymography

To detect MMP-9 expression, gelatin zymography with culture supernatants (25 μl) of THP-1 cells treated with the Td92 homologs was performed as described previously [43]. Culture supernatants of THP-1 cells treated with 10 μg of *E. coli* LPS were used as positive controls. Culture supernatants of nontreated cells or mock extract-treated cells were used as a negative control.

2.17. Determination of ROS level

THP-1 cells (2 x 10^5/ml) were seeded at a 96 well culture plates and differentiated into macrophages by culturing with 160 nM PMA for 72 h, replacing the medium without PMA for 24 h. The cells were switched to serum-free media for 16 h and removed media, and incubated with 10 μM DCF-DA for 30 min at

37℃. The cells then washed with serum-free media, followed by exposure to Td92 (10 μg/ml), LPS (10 μg/ml), or 100 μM H_2O_2 in serum-free media. ROS generation of cells was observed using excitation at 485 nm and emission at 520 nm using FLUO Star OPTIMA (BMG Labtechnologies, Inc. Durham, NC).

2.18. Determination of extracellular ATP level

PMA-differentiated THP-1 cells (2 x 10^6/ml in 6-well plates) were stimulated with Td92, *T. denticola*, fibronectin, GRGDSP peptide, GRADSP peptide (negative control for the RGD peptide), or PP4 for 2 h. The extracellular ATP level was determined using an ATP bioluminescence assay Kit (Roche, Mannheim, Germany) according to the manufacturer's protocol. Briefly, the culture supernatants were mixed with 0.3% TCA and were kept at 4°C for 30 min. After adding four volumes of 250 mM Tris acetate (pH 7.75), the mixture was mixed with the ATP assay reagents as described previously [51]. The luminescence was measured using a Modulus™ Microplate Luminometer (Promega, Madison, WI, USA). In some experiments, the cells were pretreated with the integrin α5β1 Ab for 1 h before Td92 stimulation.

2.19. RNA interference assay

The siRNA duplex was designed by the Invitrogen Block-iT RNAi Designer program. The gene accession numbers are NM-001079821 (NLRP3), NM-013258 (ASC), NM-021209 (NLRC4), NM-138554 (TLR4), NM-002468 (MyD88), NM-182919 (TRIF), and NM-002205 (integrin α5). The sequences were as follows: 5'-AUC ACA GUG GGA UUC GAA ACA CGU G-3' and 5'-CAC GUG UUU CGA AUC CCA CUG UGA U-3' for siNLRP3 duplex; 5'-AAG AGC UUC CGC AUC UUG CUU GGG U-3' and 5'-ACC CAA GCA AGA UGC GGA AGC UCU U-3' for siASC duplex; 5'-UGC AGU UCG AAA UCA AAC UUG UGG G-3' and 5'-CCC ACA AGU UUG AUU UCG AAC UGC-3' for siNLRC4 duplex; 5'-UAA GGU AGA GAG GUG GCU UAG GCU C-3' and 5'-GAG CCU AAG CCA CCU CUC UAC CUU A-3' for siTLR4 duplex; 5'-AUU CCU UGC UCUGCA GGU AAU CAU C-3' and 5'-GAU GAU UAC CUG CAG AGC AAG GAA U-3' for siMyD88 duplex; 5'-UAC AAG AGC UUG UCC UGG CCU GCU G-3' and 5'-CAG CAG GCC AGG ACA AGC UCU UGU A-3' for siTRIF duplex; 5'-UGG CCA UGA UGA GUU UGG CCG AUU U-3' and 5'-AAA UCG GCC AAA CUC AUC AUG GCC A-3' for integrin α5 siRNA duplex. Each of the specific siRNAs and siRNA negative controls were resuspended to a final concentration of 10 μM, and Lipofectamine RNAiMAX diluted in 250 μl of serum-free RPMI 1640 without antibiotics was mixed with an equal volume of diluted siRNA (10 to 30 nM). PMA-differentiated THP-1 cells (2 x 10^6 cells/well) in RPMI 1640 containing 10% FBS without antibiotics in 6-well plates were transfected with the RNAiMAX/siRNA mixtures. Following an 18- to 48-h incubation at 37°C (5%

CO_2 atmosphere) and washing, the cells were treated with Td92 (10 μg/ml), MDP (10 μg/ml), *E. coli* DH5α RNA (5 μg/ml), *S. typhimurium* flagellin (500 ng/ml), or LPS (10 μg/ml) for 6 h as described above. MDP- and LPS-stimulated cells (for TLR4 knockdown experiments) were subsequently pulsed with 2.5 mM ATP for 30 min. To assess cell viability following siRNA transfection, THP-1 cells were stained with Hoechst 33342 after transfection with nonsilencing siRNA using the Lipofectamine RNAiMAX Reagent. The cells appeared healthy and viable after transfection. The knockdown of each gene and protein was analyzed by real-time qPCR and immunoblotting, respectively. The levels of procaspase-1 and proIL-1β in the cell extracts and of their active forms secreted in the supernatant precipitated by 10% TCA were analyzed by immunoblotting.

2.20. Protein transfection

Td92 (10 μg) or flagellin (500 ng) was mixed with 2.5 μl Profect P1, a protein transfection reagent, in 100 μl of serum-free RPMI 1640 medium without antibiotics at room temperature for 20 min. PMA-differentiated THP-1 cells (2 x 10^6 cells/ml in 6-well plates) were stimulated with the mixture for 3 and 6 h. The cells and supernatants were subjected to immunoblotting.

2.21. Determination of cell death

Cell death was measured using the LDH release assay and propidium iodide (PI) uptake. PMA-differentiated THP-1 cells (5 x 10^4 cells/200 µl in a 96-well plates) were stimulated with Td92 (1 to 20 µg/ml), *T. denticola* (MOI of 100 and 1000) or PP4 (10 µg/ml) for 1-40 h. In some experiments, the THP-1 cells were pretreated with KCl (30 to 70 mM), oxATP (300 µM), or the caspase-1 inhibitors Ac-YVAD-cho (1 to 50 µM) and z-YVAD-fmk (1 to 50 µM) prior to stimulation with 10 µg/ml of Td92 for 6 h. Release of cytoplasmic LDH into the supernatant was measured from triplicate samples using an LDH cytotoxicity assay Kit according to the manufacturer's instructions. Cytotoxicity was calculated using the equation 100 × (experimental LDH − spontaneous LDH)/ (maximum LDH release − spontaneous LDH). The maximum release of LDH was obtained by cell lysis with the detergent Triton X-100.

Pore formation in THP-1 cells was determined by the quantification of PI uptake. PMA-differentiated THP-1 cells (2 x 10^5 cells/500 µl in 24-well plates) were treated as described for the LDH release assay. The cells were washed with PBS and were stained with PI (20 µM) and Hoechst 33342 (10 µM) for 30 min. After washing the cells with PBS, images were acquired using fluorescence microscopy (Nikon ECLIPSE TE 200, Tokyo, Japan). PI-positive cells were counted using NIH Image J software, and the pore-forming activity was expressed as the percentage of PI-positive cells in a total of 1000. At least five fields (x 400) were counted.

2.22. Ligand-binding assay

PMA-differentiated THP-1 cells (8 x 10^6cells/5 ml in 100 mm dishes) were lysed with prechilled lysis buffer (25 mM HEPES, pH 7.5, 150 mM NaCl, 1% Nonidet P-40, 0.25% Na-deoxycholate, 10% glycerol, protease inhibitor cocktail). THP-1 cell lysates (1.4 mg in 100 μl) were reacted with Td92 (50 μg), Td92 preincubated with fibronectin (50 μg Td92 + 50 μg fibronectin, 37°C for 1 h), or PP4 (50 μg) in a total reaction volume of 300 μl while slightly inverting at 4°C overnight. The reaction mixtures were then incubated with 30 μl of Ni-NTA agarose at 4°C for 4 h. To minimize the background, the reacted agarose was washed five times with washing buffer A (50 mM HEPES, pH 7.5, 300 mM NaCl, 20 mM imidazol, 0.1 mM PMSF). Proteins bound to the agarose were eluted with elution buffer (Washing buffer A containing 250 mM imidazol). The eluted samples were boiled in 2 x SDS sample buffer and were used for SDS-PAGE followed by immunoblotting for the detection of integrin subunits (α5, αv, β1, and β3), fibronectin, Td92, and PP4 using an integrin α5 Ab, an integrin αv Ab, an integrin β1 Ab, an integrin β3 Ab, a fibronectin Ab, and a histidine Ab (for the detection of the recombinant Td92 and PP4), respectively.

To analyze direct interaction of Td92 with integrin α5β1, the integrin α5β1 Ab (3 μg) or the integrin αvβ3 Ab (3 μg) as a control were incubated with 20 μl of Protein G-agarose (1 mg/ml) at 4°C for 4 h. After washing with washing buffer B (50 mM HEPES pH 7.5, 150 mM NaCl, 1 % Nonidet P40, 0.5% sodium deoxycolate, and 0.1 mM PMSF), the integrin α5β1 Ab bound to agarose was

reacted with recombinant human integrin α5β1 (10 μg), and the integrin αvβ3 Ab bound to agarose was reacted with recombinant human integrin αvβ3 (10 μg) at 4°C overnight. After washing, the agarose was reacted with Td92 (10 μg), fibronectin (20 μg), or PP4 (10 μg) at 4°C overnight. After washing five times, the resultant agarose was boiled in 2 x SDS sample buffer and was used for SDS-PAGE followed by immunoblotting with a histidine Ab, a fibronectin Ab, or an integrin α5 Ab. Control experiments were performed with Protein G-agarose in the absence of integrin α5β1 or integrin αvβ3.

2.23. Detection of fibronectin in macrophages and monocytes

PBMC-derived macrophages, PMA-differentiated THP-1 cells, or undifferentiated THP-1 cells were seeded at 2 x 10^6 cells/ml 6-well plates. After 6 h incubation, the cells were washed with chilled PBS and were lysed in 50 μl of RIPA buffer (10 mM Tris-HC1, pH 7.5, 150 mM NaCl, 1% Triton X-100, 50 mM NaF, 1 mM EDTA, 5 μM Na_3VO_4, and 1 mM PMSF). The lysates were clarified by centrifugation at 13,000 x g for 45 min at 4°C. After precipitation of the proteins in the culture supernatants with 10% TCA, the cleared lysates and precipitates were subjected to immunoblotting using an anti-human fibronectin Ab.

2.24. Endoglycosidase digestion and tunicamycin treatment of THP-1 cells

THP-1 cell lysates (10 μg or 20 μg) were boiled in 20 μl denaturing buffer (1% SDS, 1% 2-mercaptoethanol) at 100 °C for 2 min. After cooling, the lysates were incubated with 1 unit of N-glycosidase F in 0.5% Triton X-100 at 37°C for 2 h. After heat-inactivated at 100 °C for 1min, the protein were boiled in SDS sample buffer, loaded on 8% SDS-PAGE gels, and then transferred onto a PVDF membrane. THP-1 cells (2 x 10^6 cells/ml in 6-well plates) were differentiated into macrophage-like cells in medium containing 10% FBS and 0.5 μM PMA in the presence of 1 μg/ml of tunicamycin which inhibits N-glycosylation of newly synthesized glycoproteins for 3 h. After washing, the cells were incubated in serum-free media in the presence of 1 μg/ml of tunicamycin for additional 6 h. Cells were harvested, rinsed with PBS, and lysed with prechilled lysis buffer (25 mM HEPES, pH 7.5, 150 mM NaCl, 1% Nonidet P-40, 0.25% Na-deoxycholate, 10% glycerol, protease inhibitor cocktail). The cell lysates (20 μg of protein) were subjected to immunoblotting to detect protein deglycosylation and integrin β1. For the glycoprotein detection (lectin blotting), proteins transferred to the PVDF membrane were incubated with 2 μg/ml of biotinylated Phaseolus vulgaris leucoagglutinin for 1 h after blocking with 1% BSA followed by incubation with streptoavidin-HRP for 30 min. The blots were developed with the ECL detection system.

To see the effect of deglycosylation of integrin on Td92 binding, THP-1 cell lysates (1.4 mg in 100 µl) treated with 1 µg/ml of tunicamycin were reacted with Td92 (50 µg) in a total reaction volume of 300 µl while slightly inverting at 4°C overnight. The reaction mixtures were then incubated with 30 µl of Ni-NTA agarose at 4°C for 4 h. To minimize the background, the reacted agarose was washed five times with washing buffer A (50 mM HEPES, pH 7.5, 300 mM NaCl, 20 mM imidazol, 0.1 mM PMSF). Proteins bound to the agarose were eluted with elution buffer (washing buffer A containing 250 mM imidazol). The eluted samples were boiled in 2 x SDS sample buffer and were used for SDS-PAGE followed by immunoblotting for the detection of integrin subunits (α5, β1) and Td92 using an integrin α5 Ab, an integrin β1 Ab, and a histidine Ab (for the detection of the recombinant Td92), respectively.

2.25. Blocking of Td92-induced signaling with the neutralizing integrin α5β1 Ab

PMA-differentiated THP-1 cells (2 x 10^6 cells/ml in 6-well plates) were serum-starved in serum-free media for 24 h. The cells were pretreated with the human integrin α5β1 Ab or the anti-mouse IgG_1 isotype control for 1 h before stimulation with Td92 for 30 min. The cell lysates were subjected to immunoblotting for the detection of p-p38, p-ERK (42/44 kDa), p-JNK (46/54 kDa), IκB-α, and β-Actin using the corresponding antibodies.

2.26. Fibronectin binding assay

To evaluate Td92 binding to soluble fibronectin, 96-well microtiter plates were coated with 100 μl of Td92 (10 μg/ml) or skim milk (5 μg/ml) as a nonspecific binding control at 4°C overnight. After washing with PBS, the wells were blocked with 5% skim milk for 1 h, and 50 μl of FITC-labeled fibronectin (0 to 20 μg/ml) was added at 37°C for 1 h in the presence or absence of non-labeled fibronectin (0 to 10 μg/ml). After washing with PBS, 100 μl of PBS was added to each well, and the fluorescence was measured with a fluorometer (FLUO Star). To evaluate Td92 binding to immobilized fibronectin, 96-well microtiter plates were coated with 100 μl of fibronectin (10 μg/ml) or 100 μl of skim milk (5 μg/ml) at 4°C overnight. After washing with PBS, the wells were blocked with 5% skim milk for 1 h, and FITC-labeled Td92 (0 to 10 μg/ml) was added at 37°C for 1 h. To examine the binding of Td92 to fibronectin was dependent on the RGD sequence, the RGD peptide (GRGDSP, 31 to 250 μg/ml) was added to the wells prior to the addition of 50 μl of FITC-labeled Td92 (5 μg/ml). After washing with PBS, 100 μl of PBS was added to each well and the fluorescence was measured with a fluorometer.

2.27. Integrin α5β1 detection by immunofluorescent staining

THP-1 cells (1 x 10^5 cells/500 μl) were differentiated into macrophages with 0.5 μM of PMA on a cover glass (Φ12 mm) placed in a 24-well plate. The cells

were washed with PBS and pretreated with 2.5 μM cytochalasin D for 30 min before incubation with FITC-labeled Td92 (10 μg/ml) for 2 h. The cells were fixed with 3.8% paraformaldehyde in PBS and were blocked with 2% human serum in PBS. The cells were then incubated with the integrin α5β1 Ab (2 μg/ml) followed by incubation with a Cy3-conjugated secondary Ab (1 μg/ml) in 2% human serum in PBS. To stain the nucleus, the cells were stained with 10 μM Hoechst 33342. The cells were analyzed for colocalization of Td92 with integrin α5β1 on the cell membrane by confocal laser scanning microscopy (x 2000, Olympus FV300, Tokyo, Japan).

To assess the formation of integrin clustering upon Td92 binding, the THP-1 cells (1 x 10^5 cells/500 μl) were differentiated into macrophages with 0.5 μM of PMA on a cover glass (Φ12 mm) placed in a 24-well plate. The cells were treated with Td92 (10 μg/ml), fibronectin (20 μg/ml), or heat-inactivated BSA (10 mg/ml) for 15, 60, and 120 min. After washing, the cells were fixed with 3.8% paraformaldehyde in PBS and immunostained using an integrin α5β1 Ab and a Cy3-conjugated secondary Ab. Cells were analyzed by confocal laser scanning microscopy. A representative cell for each treatment is shown. Magnification, x 2000

2.28. NF-κB activation assay

THP-1 cells (1 x 10^5 cells/500 μl) were seeded on a cover glass (Φ12 mm) placed in a 24-well plate and were differentiated with 0.5 μM PMA for 3 h. The cells that were or not transfected using siRNA specific for MyD88 or TRIF were incubated in serum-free media for 24 h. After washing with PBS, the cells were stimulated with 10 μg/ml of Td92, 10 μg/ml of PP4, MOI 1000 of *T. denticola*, 10 ng/ml of TNF-α, or 10 μg/ml of LPS for 1 h. In some experiments, the cells were pretreated with the integrin α5β1 Ab (10 μg/ml) or the anti-mouse IgG_1 isotype control (10 μg/ml) for 1 h or 300 μM oxATP for 30 min before stimulation for 1 h. After washing with PBS, the cells were fixed with 3.8% paraformaldehyde in PBS, permeabilized with chilled methanol, and blocked with 2% human serum in PBS. The cells were incubated with an anti-human NF-κB p65 Ab (1 μg/ml) and a Cy3-conjugated secondary Ab (1 μg/ml) in 2% human serum in PBS. The nucleus of the cells was stained with 10 μM Hoechst 33342, and the subcellular localization of NF-κB was observed by a confocal laser scanning microscopy (x 2000 and x 400, Olympus FV300, Tokyo, Japan). Images of six microscopic fields per treatment (well) were taken at x 400 magnification, and the percentage of cells with mainly nuclear NF-κB p65 was calculated using NIH Image J. A total of at least 500 cells were counted for each experimental condition.

To determine the relationship between Td92-induced NF-κB activation and caspase-1 activation, PMA-differentiated THP-1 cells (2 x 10^6 cells/ml in 6-well plates) were pretreated with Bay-117082 (5 and 10 μM) for 30 min before stimulation with Td92 (10 μg/ml) or LPS (10 μg/ml) for 6 h. LPS-stimulated cells were pulsed with 2.5 mM ATP for 30 min. Procaspase-1 and proIL-1β in the cell

extracts and their active forms secreted in the supernatant and precipitated by 10% TCA were analyzed by immunoblotting.

2.29. Enyme-linked immunosorbent assay (ELISA)

The culture supernatants of the cells treated with Tp92 homologs were assayed to determine IL-1β, TNF-α, IL-6, IL-8 and PGE_2 levels in the presence or absence of blocking antibodies using the ELISA kits from R&D Systems™ (Minneapolis, MN, USA).

2.30. Statistical analysis

Statistically significant differences between samples were analyzed with an unpaired, one-tailed Student's *t* test. The data are shown as the mean ± SD. A *p* value of < 0.05 was considered statistically significant

2.31. Nucleotide sequence accession number

DNA sequences of the *tp92* gene homologs have been submitted to the GenBank database under accession no. EU057146 for *tl88* of *T. lecithinolyticum*, EU057147 for *tss88* of *T. socranskii* subsp. *socranskii*, and EU057148 for *tm88* of *T. maltophilum*.

3. Results

3.1. Identification and characterization of Tp92 homologs of oral treponemes

3.1.1. Distribution of *tp92* gene homologs in oral treponemes

tp92 gene homologs were identified from the genome sequence of *T. denticola* (ATCC 35405, TDE2601 ORF), which has been denoted as a putative surface antigen, and by sequencing of the PCR products of the genes that were amplified with degenerate and specific primers for *T. lecithinolyticum*, *T. maltophilum*, and *T. socranskii* subsp. *socranskii*. The ORFs of the *tp92* homologs from *T. denticola*, *T. lecithinolyticum*, *T. maltophilum* and *T. socranskii* subsp. *socranskii* were 2457 bp (818 amino acid residues), 2430 (809 aa), 2430 (809 aa), and 2442 bp (813 aa), respectively.

The translated amino acid sequences of the *tp92* homologs in the oral treponemes revealed a significant homology with that of *T. pallidum* Tp92. The Tp92 homologs from the four oral treponemes showed an amino acid sequence identity of 37.9-49.3% and a similarity of 54.5-66.9% with Tp92 (Table 1). The sequence identity and similarity between the Tp92 homologs from the oral treponemes were 41.6-71.6% and 59.9-85.6%, respectively. The Tp92 homologs showed sequence identities of 28.4-30.2% and 22.2-23.7% and similarities of 46.9-49.7% and 37.0-39.4% with two nonoral spirochetes, *Borrelia burgdorferi* B31 and *Leptospira interrogans* serovar Copenhageni, respectively.

All Tp92 homologs have N-terminal signal peptide sequences. The program SignalP identified a 20-aa signal sequence for *T. denticola*, 27-aa for *T. lecithinolyticum*, 25-aa for *T. maltophilum*, and 31-aa for *T. socranskii* subsp. *socranskii*. A cleavable 21-aa N-terminal signal sequence has been identified in Tp92 of *T. pallidum* [18]. PSORTb predicted the localization of the Tp92 homologs from the four oral treponemes to the outer cell membrane with likelihoods of more than 94% (94.5% for *T. denticola*, 100% for *T. lecithinolyticum*, *T. maltophilum*, and *T. socranskii*). The predicted pI and molecular mass of the mature Tp92 homologs were 5.79/91.55-kDa for *T. denticola*, 6.34/88.33-kDa for *T. lecithinolyticum*, 5.54/88.58-kDa for *T. maltophilum*, and 5.46/88.03-kDa for *T. socranskii* subsp. *socranskii*, as predicted by the ProtParam tool from ExPASy. The pI and molecular mass of Tp92 are 8.27/91.97-kDa. The Tp92 homologs were named Td92 for *T. denticola*, Tl88 for *T. lecithinolyticum*, Tm88 for *T. maltophilum*, and Tss88 for *T. socrnaskii* subsp. *socranskii* according to their molecular weights.

.

Table 1. Degrees of amino acid sequence homology of the Tp92 homologs

Bacterium	% Identity/% similarity of Tp92 homologs from the indicated species to Tp92 homolog from:						
	T. denticola	*T. lecithin-olyticum*	*T. malto-philum*	*T. socra-nskii*	*T. pallidum*	*B. burgd-orferi* B31	*L. interrogans* serovar Copenhageni
T. denticola	100						
T. lecithin-olyticum	44.0/63.3	100					
T. maltophilum	43.5/61.2	71.6/85.6	100				
T. socranskii	41.6/59.9	47.3/66.8	46.9/67.2	100			
T. pallidum	49.3/66.9	39.6/57.5	38.2/57.4	37.9/54.5	100		
B.burgd-orferi B31	30.2/46.9	29.2/48.6	29.0/49.7	28.4/47.2	28.6/46.8	100	
L. interrogans serovar Copenhageni	22.7/37.0	23.4/38.6	23.7/39.4	22.2/38.8	22.4/37.8	21.1/38.3	100

3.1.2. Purification of recombinant Tp92 homologs

The *tp92* gene homologs were successfully expressed in *E. coli* using the pQE-30 vector after PCR and TA cloning (Fig. 1). As expected from the deduced amino acid sequence, the molecular size of the recombinant Tp92 homologs was approximately 92-kDa for *T. denticola* and 88-kDa for *T. lecithinolyticum*, *T. maltophilum*, and *T. socranskii* subsp. *socranskii*. The recombinant proteins formed in the inclusion bodies were purified by solubilization, renaturation, and affinity chromatography using Ni-NTA agarose. These proteins were used to study host cell stimulation after further purification to remove any possible *E. coli* LPS contamination by using polymyxin B agarose.

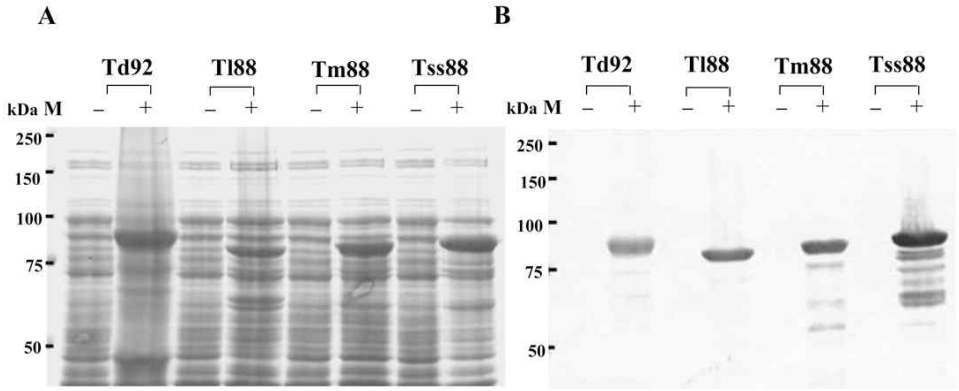

Figure 1. The *tp92* gene homologs are expressed in *E. coli*. The *tp92* gene homologs were cloned in *E. coli* and the expression of histidine-tagged recombinant proteins was analyzed by SDS-PAGE (10% polyacrylamide gel, A) and by immunoblotting with a histidine Ab (B) after induction with IPTG. Lanes: Td92, Tp92 homolog of *T. denticola*; Tl88, Tp92 homolog of *T. lecithinolyticum*; Tm88, Tp92 homolog of *T. maltophilum*; Tss88, Tp92 homolog of *T. socranskii* subsp. *socranskii*. (–), noninduced *E. coli* cell lysates; (+), IPTG-induced *E. coli* cell lysates The positions of protein size markers (M) are indicated.

3.1.3. Cross-reactivity of Tp92 homologs with antiserum raised against Td92

An IgG fraction of antisera raised against recombinant Td92 (Td92 Ab) was purified and tested for reactivity with *T. denticola* and the recombinant Tp92 homologs. Immunoblot analysis showed that the antibodies reacted with a 92-kDa protein band in *T. denticola* lysates and with the recombinant Td92 (Fig. 2A). Immunodot blot analysis showed that the Td92 Ab cross-reacted with Tl88, Tm88, and Tss88 (Fig. 2B), whereas it did not react with an irrelevant histidine-tagged recombinant protein (MspTL) [45] or *E. coli* lysates.

.

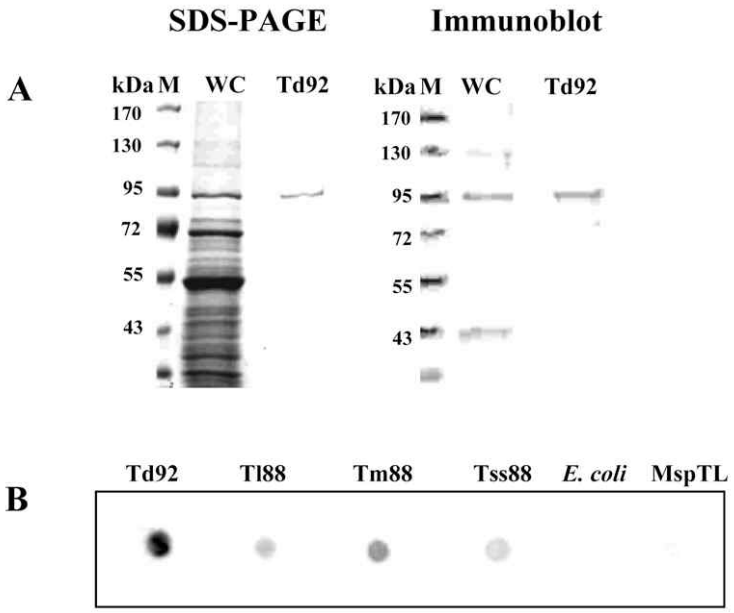

Figure 2. Td92 Ab cross-reacts with *T. denticola* whole cell lysates (WC) and Tp92 homologs. *T. denticola* whole cell lysates (WC, 10 μg) and Td92 were subjected to SDS-PAGE (8% polyacrylamide gel) followed by immunoblotting with a Td92 Ab (A). The applied amounts of Td92 were 500 ng in SDS-PAGE and 100 ng in immunoblot. The cross-reactivity of the Tp92 homologs with the Td92 Ab was examined by an immunodot blot assay. The Tp92 homologs (250 ng in 1 μl) were applied onto a nitrocellulose membrane and reacted with the Td92 Ab. As a negative control, *E. coli* lysates and an irrelevant recombinant protein, MspTL, were included (B). The detection was performed using HRP-labeled mouse anti-rabbit IgG and TMB as HRP substrates.

3.1.4. Outer membrane location of Td92 in *T. denticola*

The computer-assisted analysis using the PSORTb program predicted that the Tp92 homologs were outer membrane proteins as described above. The surface location of *T. denticola* Td92 was empirically evaluated using various techniques. First, the presence of Td92 in the OM isolated from *T. denticola* was examined using a Td92 Ab. As shown in Fig. 3, the Td92 Ab raised against recombinant Td92 recognized a single protein band at 92-kDa in the OM preparation. The FlaA Ab detecting the periplasmic protein FlaA of *T. denticola* did not react with the OM fraction, but it reacted with a 37-kDa protein in the whole cell lysates, verifying the purity of the OM. Second, the ability of the intact bacteria to react with the Td92 Ab was assessed using indirect immunofluorescence. Because of the fragile nature of *Treponema* OM, the Fla Ab was included to control the OM integrity.

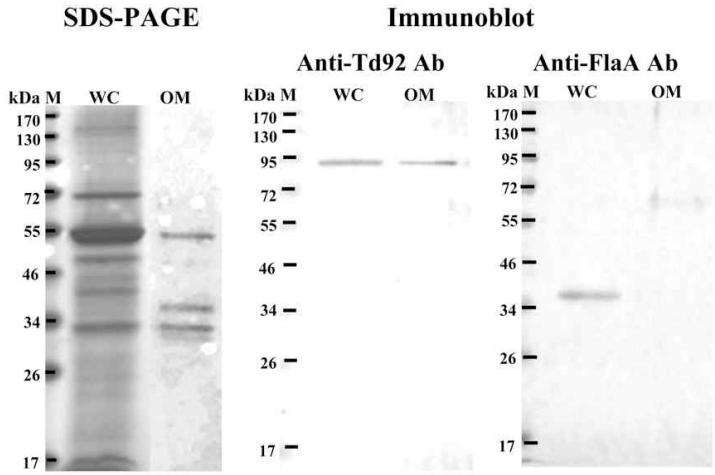

Figure 3. The Td92 is located in the outer membrane of *T. denticola*. *T. denticola* outer membrane was prepared and subjected to SDS-PAGE (10% polyacrylamide gel) followed by immunoblotting with a Td92 Ab and a FlaA Ab. The detection was performed using HRP-labeled mouse anti-rabbit IgG and TMB as HRP substrates. WC, *T. denticola* whole cell lysates (10 μg); OM, outer membrane fraction (2 μg); M, protein size marker.

As shown in Fig. 4, non-fixed *T. denticola* was stained with the Td92 Ab but did not stain with the FlaA Ab. Acetone-fixed and permeabilized *T. denticola* reacted with both antibodies, indicating that the OM of the bacteria was intact and that Td92 was surface-exposed. Furthermore, as shown in Fig. 5, the Td92 Ab reacted with *T. denticola* cells, indicating that the Td92 epitopes were surface-exposed. The antibody also cross-reacted with *T. lecithinolyticum, T. maltophilum*, and *T. socranskii* subsp. *socranskii*, suggesting the presence of common surface epitopes of the homologous proteins in these bacteria. The IgG isotype did not react with the bacteria. The cross-reactivity of the Td92 Ab by immunofluorescence (Fig. 5) was coincident with that observed in immunodot blot assay (Fig. 2B). Immunogold electron microscopy further showed that gold particles bound to the bacterial surface (Fig. 6). Third, flow cytometric analysis using a Td92 Ab showed that more than 80% of non-fixed *T. denticola* cells were immunopositive, while a minor portion of the bacteria was detected with the FlaA Ab (Fig. 7A). Most of the acetone-fixed and permeabilized bacteria were immunopositive with both antibodies (Fig. 7B). Isotype-matched Ab (rabbit IgG) was used as a negative control.

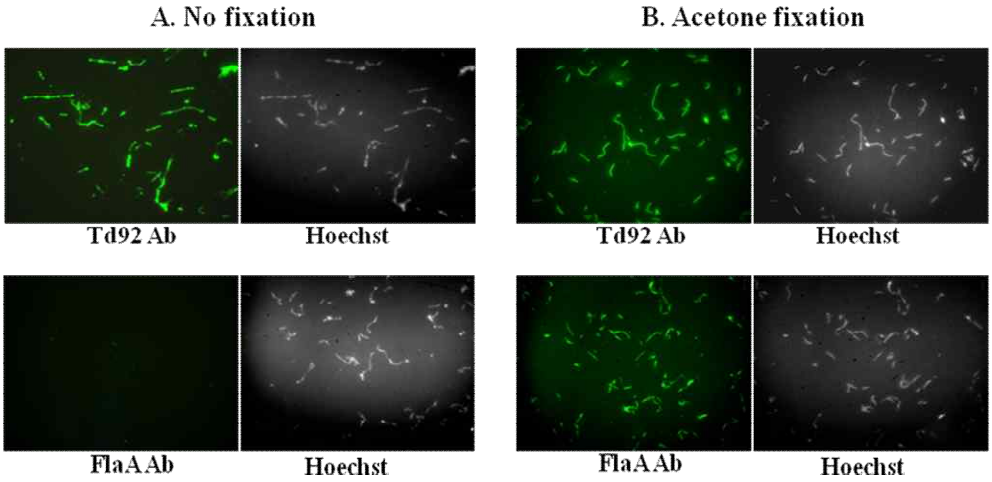

Figure 4. The Td92 is surface-exposed in *T. denticola*. Non-fixed (A) and acetone-fixed/permeabilized *T. denticola* cells (B) were reacted with a Td92 Ab or a FlaA Ab followed by reacting with FITC-labeled anti-rabbit IgG. The same cells were further stained with Hoechst dye, a fluorescent nucleic acid stain. The images of the same fields were obtained from immunoflorescence and Hoechst dye staining. Original magnification x 1000

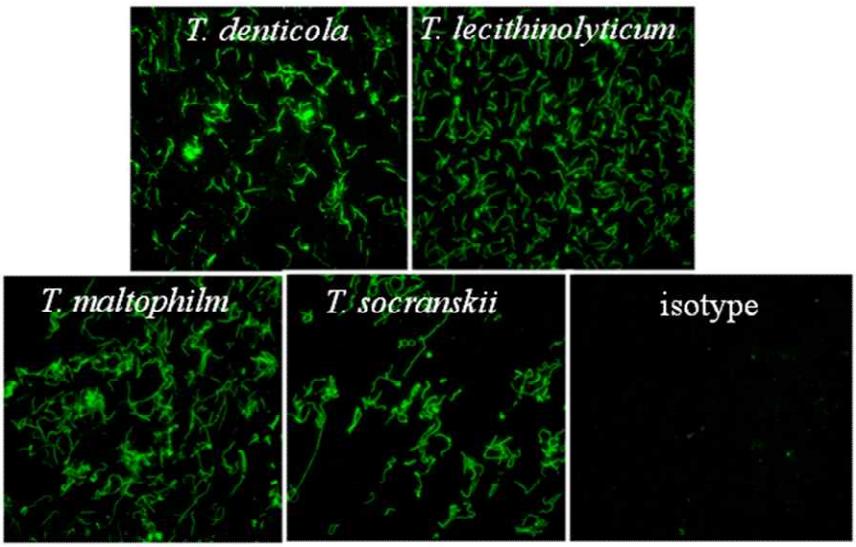

Figure 5. The Td92 Ab cross-reacts with the Tp92 homologs of oral treponemes. Freshly grown *Treponema* species were fixed with 4% paraformaldehyde and reacted with a Td92 Ab or a isotype matched Ab (rabbit IgG; lower right), followed by reacting with FITC-labeled goat anti-rabbit IgG. Original magnification × 1000

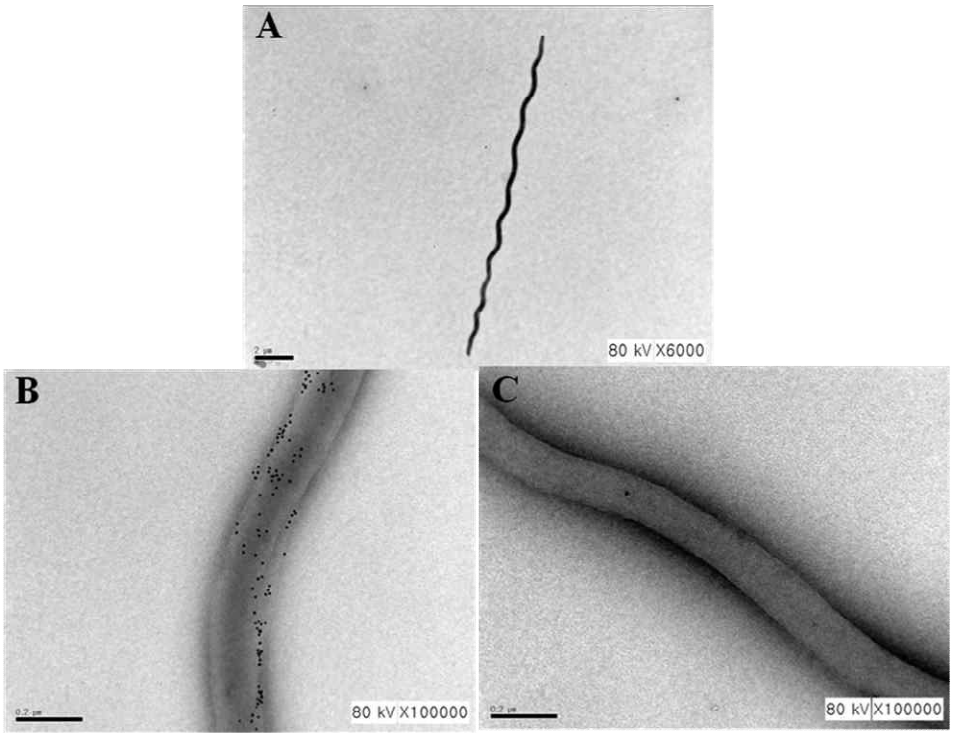

Figure 6. The Td92 Ab binds to the surface of *T. denticola*. *T. denticola* was reacted with a Td92 Ab and subsequently with the anti-rabbit IgG conjugated with 10-nm colloidal gold particles. After negative staining with 1% uranyl acetate, the bacteria were observed by a transmission electron microscopy. *T. denticola* whole cell (A), a part of the bacterium showing immunogold labeling with the Td92 Ab (B), or immunogold labeling with the isotype matched Ab (rabbit IgG) (C). Scale bars represent 2.0 μm (A) and 0.2 μm (B-C).

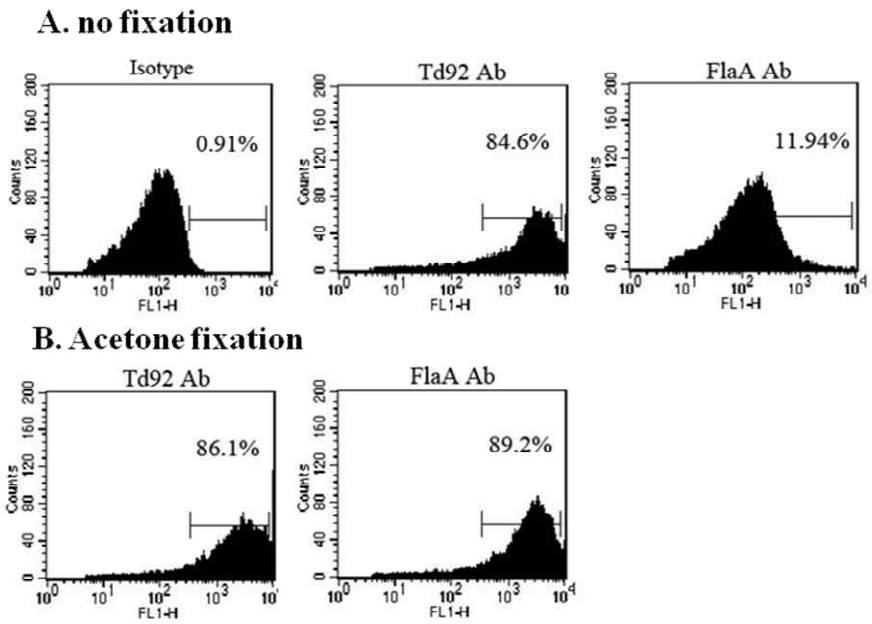

Figure 7. Td92 is expressed in surface of *T. denticola*. Non-fixed (A) and acetone-fixed/permeabilized *T. denticola* cells (B) were reacted with a Td92 Ab or a FlaA Ab followed by reacting with FITC-labeled goat anti-rabbit IgG. The cells were then analyzed by flow cytometry. Isotype-matched Ab (rabbit IgG) was used as a negative control. The experiments were performed three times, and representative data are shown.

3.1.5. Binding of the Tp92 homologs to KB cells

Bacterial binding to the host cells is an initial step in the colonization of pathogens. To determine whether the Tp92 homologs function as adhesins, the binding capacity of the Tp92 proteins to KB cells, an epithelial cell line, was examined. As shown in Fig. 8, the FITC-labeled Tp92 homologs were able to bind to the cells. To test whether this binding was specific, a competitive binding inhibition assay was performed using fluorescently labeled *T. denticola* cells and unlabeled Td92. As shown in Fig. 9, binding of CFSE-labeled *T. denticola* to KB cells was inhibited by unlabeled Td92 in a dose-dependent manner, whereas an irrelevant recombinant protein (PP4) with a histidine tag did not inhibit the binding of *T. denticola* to KB cells.

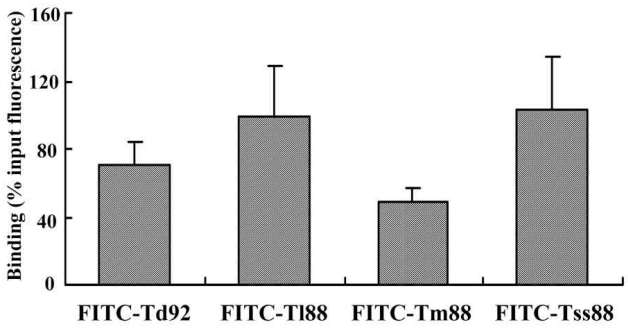

Figure 8. The Tp92 homologs bind to KB cells. KB cells (1 x 10^5/500 μl) were cultured in 24-well plates to confluence, and incubated with FITC-labeled Tp92 homologs (2.5 μg of protein) at 37°C for 1 h. The cells were detached and washed with PBS, and the fluorescence of bound proteins was measured using a fluorometer. Protein adhesion was expressed as a percentage of total proteins added. The experiments were repeated three times and similar results were obtained. The results are presented as means ± SD in triplicate samples.

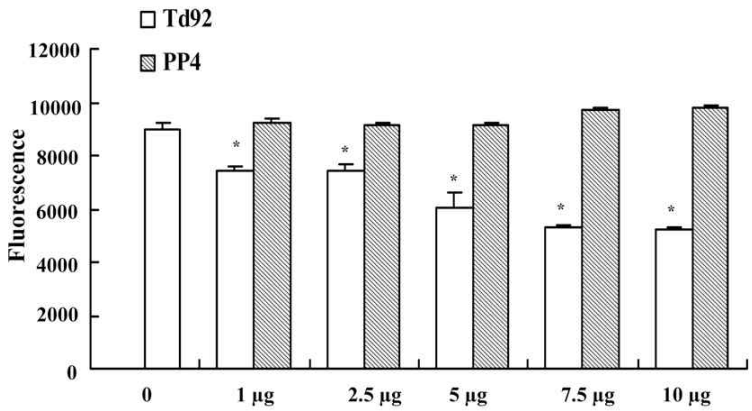

Figure 9. The Td92 inhibits *T. denticola* binding to KB cells. KB cells (1 x 10^5 cells/500 µl) were cultured in 24-well plates and incubated with CFSE-labeled *T. denticola* whole cells (100 µl of a culture with an OD_{600} of 0.2 or 5 x 10^8 bacteria) in the presence of Td92 at different concentrations for 1 h. After the cells were detached and washed with PBS, the fluorescence of bound bacteria was measured by a fluorometer. An irrelevant recombinant protein (PP4) was used as a negative control. The experiments were repeated three times, and similar results were obtained. The results are presented as means ± SD in triplicate samples and are expressed as relative light units. $^{*}p < 0.05$ versus added to PP4

3.1.6. Host cell responses to the Tp92 homologs

Prior to stimulation of the host cells with the recombinant Tp92 homologs, endotoxin decontamination of the recombinant proteins was verified using CHO/CD14/TLR4 cells that expressed CD25 upon TLR4-dependent NF-κB activation. The Tp92 homologs did not cause an increase in CD25 expression in the cells, whereas LPS significantly increased the expression of CD25 (Fig. 10).

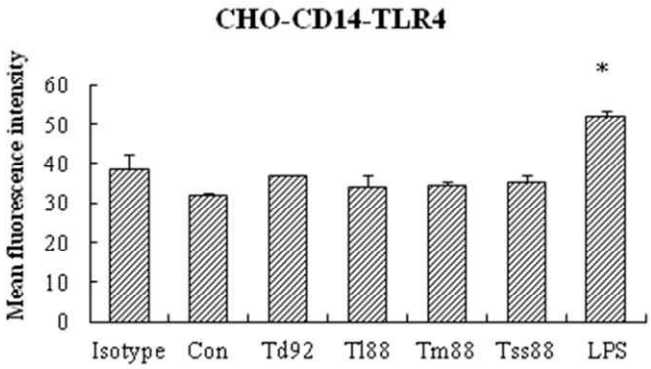

Figure 10. Endotoxin decontamination of Td92 homologs is verified using NF-κB reporter cell line. CHO/CD14/TLR4 cells ($1x10^5$ cells/well) were treated with Tp92 homologs (10 μg/ml), and *E. coli* LPS (1 μg/ml) for 16 h. The cells were stained with FITC-labeled anti-human CD25 Ab for 30 min at 4°C. The expression was analyzed by flow cytometry. The results are presented as means ± SD in triplicate samples. LPS-treated cells were used as a positive control. The results are presented as means ± SD in triplicate samples. $^{*}p < 0.05$ versus nontreated cells (Con)

Using THP-1 and PDL cells, the regulation of representative proinflammatory and osteoclastogenic factors that are known to stimulate RANKL, which is involved in osteoclastogenesis leading to bone resorption, were analyzed. Monocytes are among the early immune cells that react to the local presence of bacteria, and PDL is a supporting tissue linking the root surface and alveolar bone. As shown in Fig. 11, the addition of the Tp92 homologs significantly upregulated IL-1β, TNF-α, IL-6 and IL-8 in THP-1 cells when introduced at a concentration of 10 μg/ml, both at the mRNA and protein levels, as analyzed by real-time qPCR and ELISA, respectively. In PDL cells, IL-6 and IL-8 were upregulated by the Tp92 homologs (Fig. 11). The expression of COX-2 and its product, PGE_2, was also induced by the Tp92 homologs in both THP-1 and PDL cells (Fig. 12). In a gelatin zymography assay, the Tp92 homologs induced a gelatinolytic activity with a molecular mass of 92-kDa, corresponding to MMP-9, in THP-1 cells (Fig. 13).

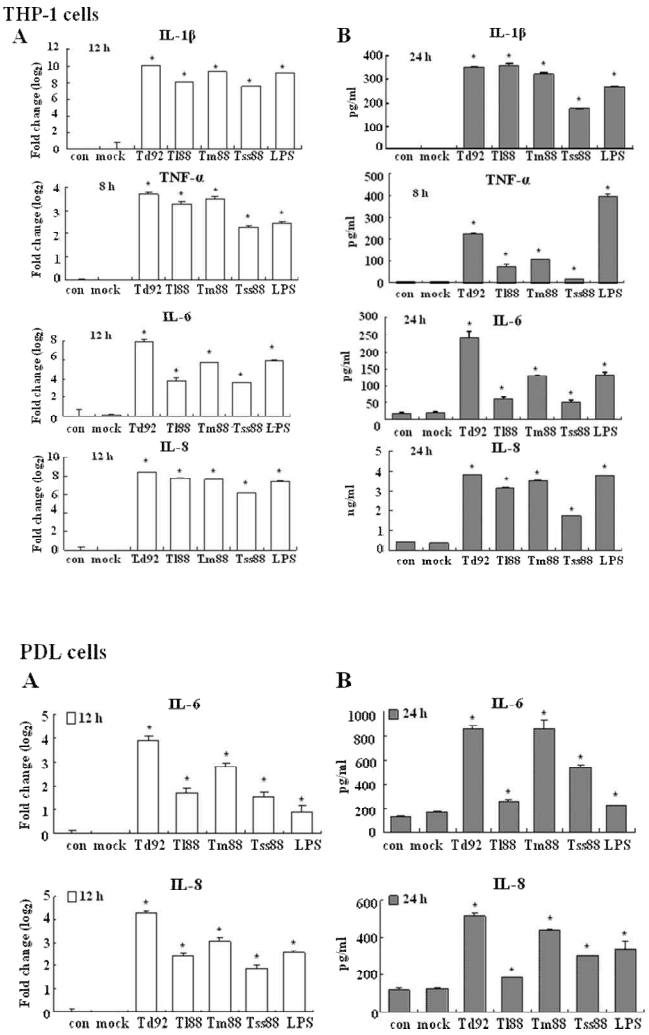

Figure 11. The proinflammatory factors are up-regulated by the Tp92 homologs in THP-1 and PDL cells. THP-1 cells (1 x 10^6/ml) or PDL cells (5 x 10^5/ml) were cultured and treated with the Tp92 homologs (10 μg/ml) or LPS (10 μg/ml) for 8-24 h. RNA was isolated from the cells and subjected to real-time qPCR (A) and the conditioned media were used for ELISA (B). LPS-treated cells were used as a positive control. The results are presented as means ± SD in triplicate samples. $^{*}p < 0.05$ versus untreated cells

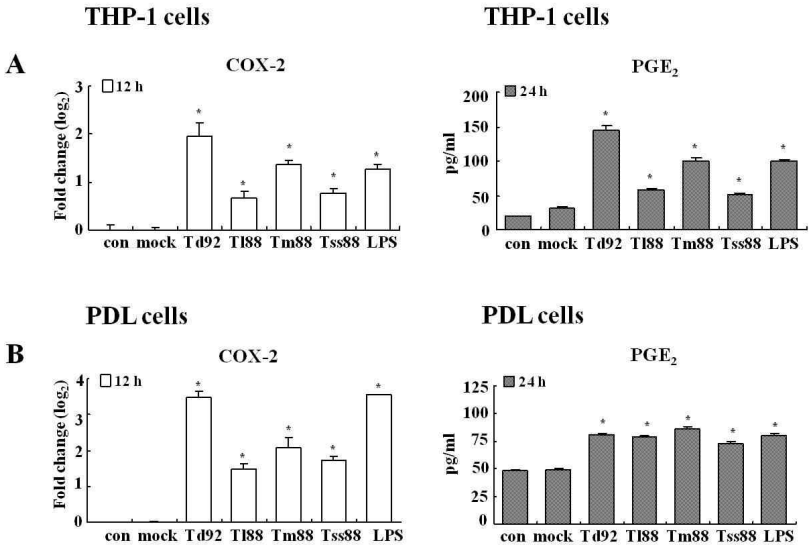

Figure 12. COX-2 and PGE_2 are up-regulated by the Tp92 homologs in THP-1 and PDL cells. THP-1 (A, 1 x 10^6/ml) and PDL cells (B, 5 x 10^5/ml) were cultured and treated with the Tp92 homologs (10 μg/ml) or LPS (10 μg/ml) for 12-24 h. RNA was isolated from the cells and COX-2 mRNA expression was analyzed by real-time qPCR. The conditioned media were used for measuring PGE_2 levels by ELISA. LPS-treated cells were used as a positive control. The results are presented as means ± SD in triplicate samples. $^{*}p < 0.05$ versus untreated cells

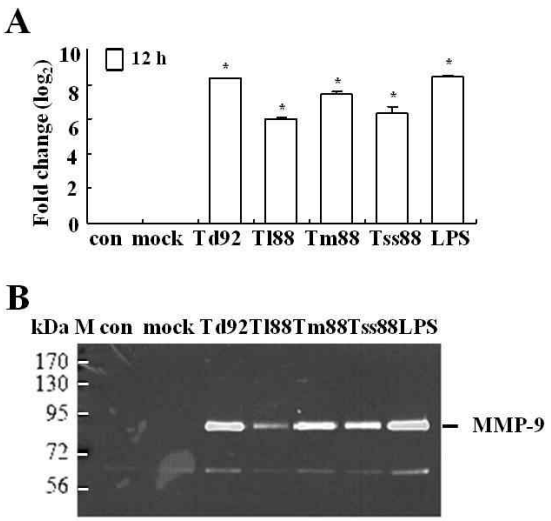

Figure 13. MMP-9 is up-regulated by the Tp92 homologs in THP-1 cells. THP-1 cells (1 x 10^6/ml) were treated with the Tp92 homologs (10 μg/ml) or LPS (10 μg/ml) for 12-24 h. RNA was isolated from the cells and MMP-9 mRNA expression was analyzed by real-time qRT-PCR (A). The conditioned media were used for analyzing MMP-9 expression by gelatin zymography (B). LPS-treated cells were used as positive control. The results are presented as means ± SD in triplicate samples. $^{*}p < 0.05$ versus untreated cells

3.2. A novel function of integrin α5β1 in the activation of innate immune components by Td92

3.2.1. Activation of caspase-1 and IL-1β by *T. denticola* and Td92

As shown Fig. 11, Td92, a Tp92 homolog of *T. denticola*, induced IL-1β mRNA expression and secretion in the monocyte cell line THP-1. Because IL-1β is secreted in the mature form and IL-1β maturation occurs by cleavage of the N-terminal 116-amino acids of the inactive cytosolic proIL-1β (p31) by caspase-1, it was firstly determined whether Td92 and *T. denticola* could activate caspase-1 and induce proIL-1β maturation in THP-1 cells. Caspase-1 is also expressed as a proenzyme (45-kDa) composed of three domains, the N-terminal pro-domain, the p20 subunit (20-kDa), and the p10 subunit (10-kDa), of which the latter two domains are the essential caspase catalytic domains and form a catalytic tetramer [52]. Because caspase-1 is constitutively activated in undifferentiated THP-1 cells and monocytes but not in macrophages [53, 54],

PMA-differentiated THP-1 cells were used throughout this study to assess the effect of Td92 on caspase-1 activation and IL-1β secretion. As shown in Fig. 14A, Td92 activated caspase-1 in a dose-dependent manner in THP-1 cells, and the level of the processed p20 subunit in the culture supernatants increased with increased Td92, as detected by immunoblotting. An irrelevant recombinant protein (PP4), which is a C-terminal partial peptide of the surface protein MspTL of *Treponema lecithinolyticum*, an oral spirochete that does not have a cell-stimulating activity [45], was used as a negative control. All of the chemicals used for the preparation

of PP4 were from the same batches that were used for the Td92 preparation. MDP plus ATP was used as a positive control. Truncated recombinant Td92 polypeptides were also included to examine their ability to activate caspase-1. Td92 was divided into two fragments according to the structural analysis of the protein using MODELLER [55]: the G-domain (Td-G, 46-kDa) corresponded to the amino acid positions 1-400 and the B-domain (Td-B, 45.5-kDa) corresponded to the amino acid positions 401-798. According to the structure prediction, the G-domain is a globular domain expected to perform a specific biological function, and the B-domain is a membrane-spanning beta-barrel domain. The G-domain activated caspase-1 and induced proIL-1β expression, but the B-domain did not. The Tp92 homologs of oral treponemes also activated caspase-1 and induced proIL-1β expression (Fig. 14B). These results strengthen the hypothesis that Td92 has specific effects on caspase-1 activation and proIL-1β expression. Dose-dependent caspase-1 activation was also observed when THP-1 cells were treated with live *T. denticola* at a multiplicity of infection (MOI) of 100, 500, or 1000. The dose- and time-dependent release of active IL-1β following the addition of Td92 or live bacteria was detected in culture supernatants by ELISA (Fig. 14C and 14D). A significant release of IL-1β was observed after a 3 h treatment with Td92 (10 μg/ml) and *T. denticola* at MOI of 1000 (Fig. 14D).

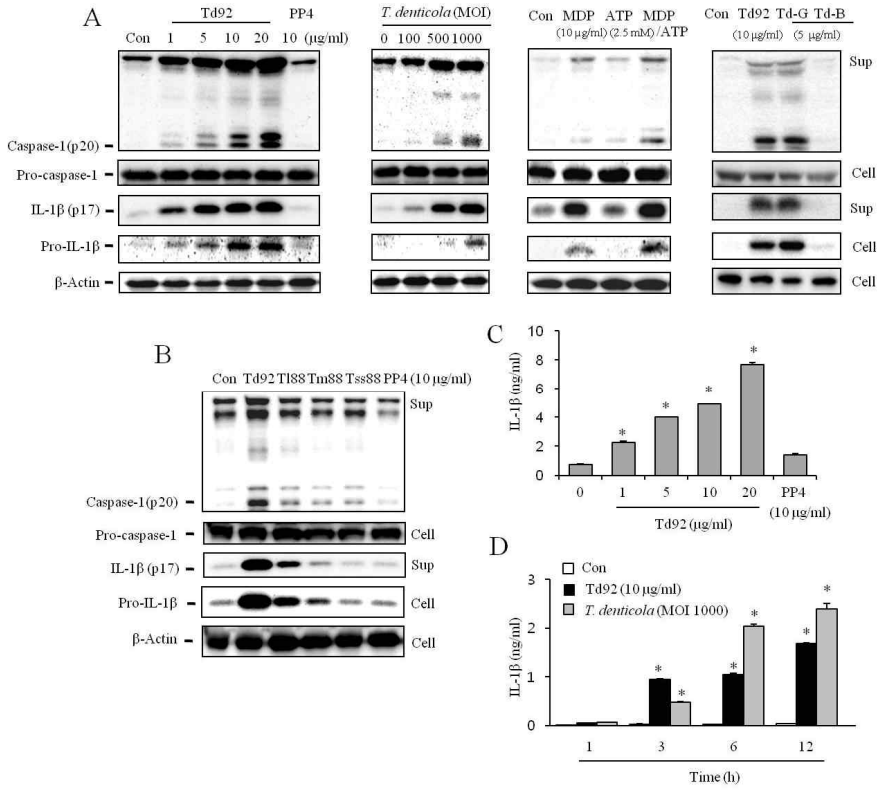

Figure 14. **Tp92 homologs and live *T. denticola* induce caspase-1 activation and IL-1β secretion.** THP-1 cells were treated with Tp92 homologs (Td92, Tl88, Tm88, and Tss88), live T. *denticola*, PP4, truncated Td92 (Td-G and Td-B domain), or MDP for 1 to 12 h (6 h in A-C). MDP-stimulated cells were then pulsed with 2.5 mM ATP for 30 min. Caspase-1 and IL-1β secreted into the culture supernatants (sup) and procaspase-1, proIL-1β, and β-Actin in the cell lysates (cell) were detected by immunoblotting. The β-Actin was used as a loading control (A-B). The IL-1β level in the culture supernatants was analyzed by ELISA. The data are shown as the means ± SD of one representative experiment of three performed in triplicate. $^{*}p < 0.01$ versus unstimulated cells (C-D)

To confirm that the Td92-induced IL-1β activation was caused by caspase-1 activation, the cells were pretreated with the caspase-1-specific inhibitors z-YVAD-fmk and ac-YVAD-cho prior to Td92 treatment. As shown in Fig. 15, z-YVAD-fmk and ac-YVAD-cho inhibited the caspase-1 activation and IL-1β secretion induced by Td92, indicating that IL-1β activation by Td92 is caspase-1-dependent.

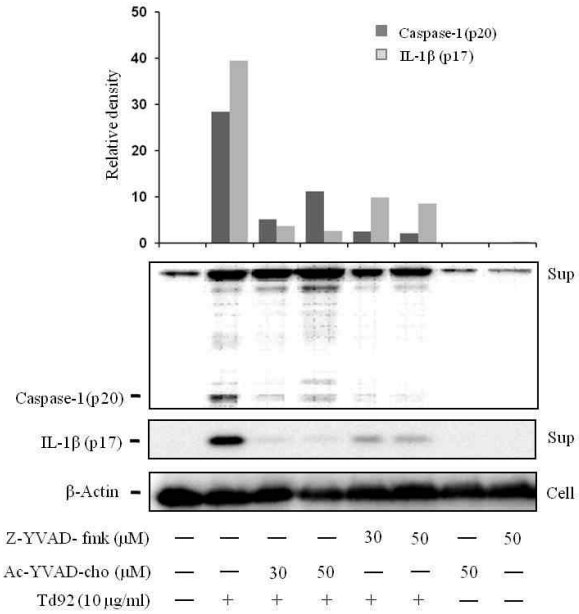

Figure 15. Td92-induced IL-1β activation was caused by caspase-1 activation. THP-1 cells were pretreated with z-YVAD-fmk or ac-YVAD-cho for 30 min before stimulation with Td92 for 6 h. Caspase-1 and IL-1β in the culture supernatants (sup) and β-Actin in the cell lysates (cell) were detected by immunoblotting. The band intensities on the immunoblots were quantified using NIH Image J software and are presented as the relative ratio to β-Actin.

In addition to caspase-1 activation, Td92 and *T. denticola* induced proIL-1β expression in the cells (Fig. 14A). Because recombinant Td92 was used, control experiments were performed to verify that the Td92 activity was not attributable to endotoxin contamination. First, IL-1β secretion in response to native and recombinant Td92 after heating (95°C for 1 h) was compared. Similar to the recombinant Td92, heat-treated native Td92 significantly reduced IL-1β secretion, but not completely, compared with the untreated native Td92 (Fig. 16). Native and recombinant Td92 from three independent purifications were used and provided similar results. In repeated experiments, heated Td92 (10 μg/ml) reduced IL-1β secretion by 56-65%. In contrast to that of LPS, the activity of Td92 was remarkably reduced by heating but not by polymyxin B, an endotoxin inhibitor (Fig. 17). The activity of Td92 to induce IL-1β secretion was not altered after extraction with 1% Triton X-114, which is an efficient method to dissociate endotoxins from biomolecules, whereas LPS completely lost its activity after Triton X-114 extraction (Fig. 18). The endotoxin activity of the recombinant Td92 was 0.37 EU/μg of the protein and approximately 1/30,000 that of *Escherichia coli* LPS in the same amount as measured by a Limulus amoebocyte lysate assay.

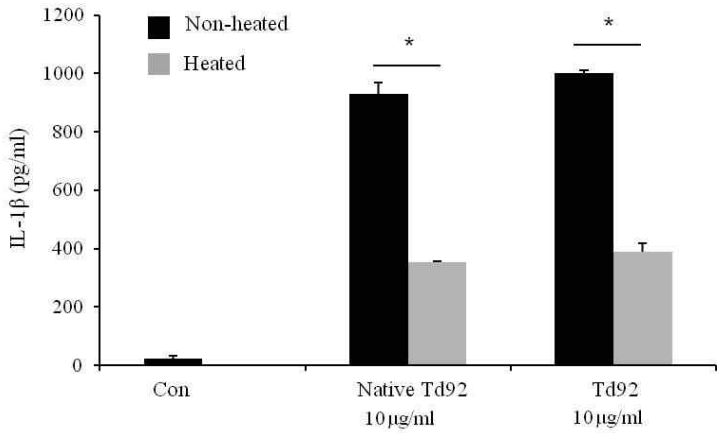

Figure 16. Heat treatment significantly reduces Td92-induced IL-1β secretion. PMA-differentiated THP-1 cells (1 x 10^6 cells/500 μl in 12-well plates) were treated with native or recombinant Td92 before or after heating (95°C for 1 h) for 6 h. The IL-1β level in the culture supernatants was analyzed by ELISA. The experiments were performed three times and representative data are shown. $^{*}p <$ 0.01 versus non-heated Td92-stimulated cells

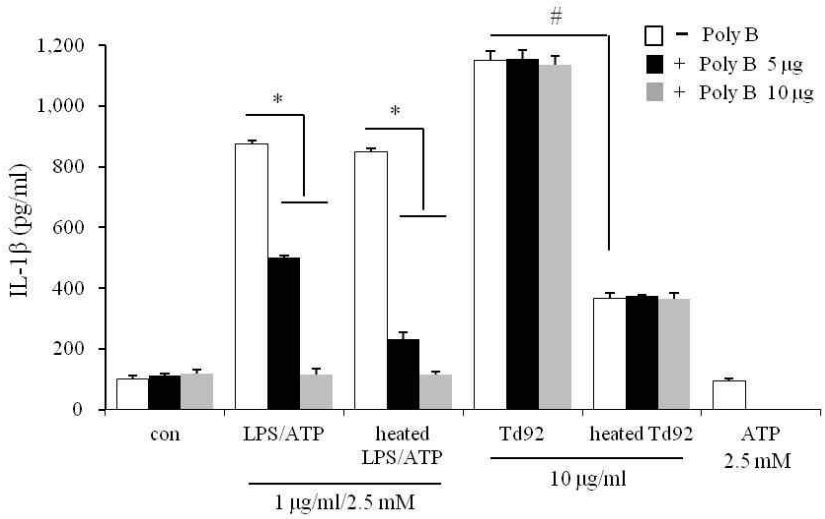

Figure 17. Polymyxin B treatment does not affect Td92-induced IL-1β secretion. PMA-differentiated THP-1 cells (1 x 10^6 cells/500 μl in 12-well plates) were pretreated with polymyxin B (5 and 10 μg/ml) for 1 h before stimulation with LPS (1 μg/ml), heated LPS (1 μg/ml), Td92 (10 μg/ml), or heated-Td92 (10 μg/ml) for 6 h. The IL-1β level in the culture supernatants was analyzed by ELISA. LPS-treated cells were incubated with 1% FBS and pulsed with 2.5 mM ATP for 30 min. LPS and Td92 were heated at 95°C for 1 h. The experiments were performed three times, and representative data are shown. $^{*}p < 0.01$ versus LPS-stimulated cells; $^{\#}p < 0.01$ versus Td92-stimulated cells

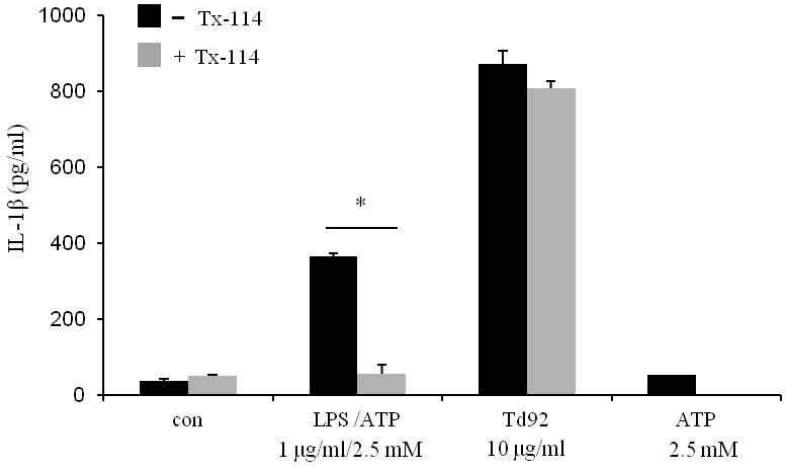

Figure 18. Triton X-114-extracted Td92 maintains its ability to induce IL-1β secretion. Td92 (250 μg) or LPS (100 μg) was mixed with 1% Triton X-114 in a total volume of 1 ml and incubated at 4°C for 30 min with constant stirring. After further incubation at 37°C for 10 min, the samples were centrifuged at 16,000 x g for 30 min at 25°C and the upper aqueous phase was carefully removed. The Triton X-114 extraction was repeated for two more cycles, and the resulting aqueous phase were used for cell treatments. As a control, PBS extracted with Triton X-114 was included. PMA-differentiated THP-1 cells (1 x 10^6 cells/500 μl in 12-well plates) were treated with Td92 (10 μg/ml) or LPS (1 μg/ml) for 6 h. The IL-1β level in the culture supernatants was analyzed by ELISA. The experiments were performed three times and representative data are shown. $^{*}p < 0.01$ versus LPS-stimulated cells

Furthermore, transfection with TLR4 siRNA did not affect Td92-induced proIL-1β expression, whereas it inhibited *E. coli* LPS-induced proIL-1β expression compared to nontransfected cells (Fig. 19). I also tested whether native Td92 extracted from *T. denticola* induces proIL-1β expression and activates caspase-1. Native Td92 exerted the same activities as the recombinant protein (Fig. 20). These results indicate that Td92 induces both proIL-1β expression and caspase-1 activation to increase IL-1β secretion.

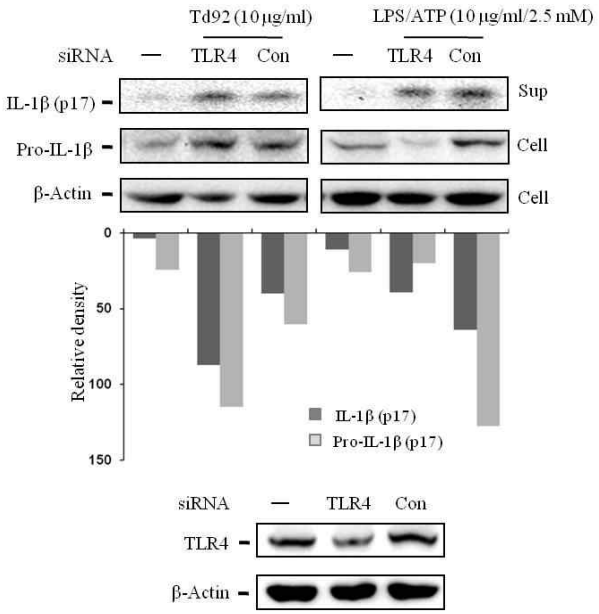

Figure 19. Knockdown of TLR4 does not affect Td92-induced proIL-1β expression. THP-1 cells transfected with TLR4 siRNA were treated with Td92 or LPS for 6 h. LPS-stimulated cells were then pulsed with 2.5 mM ATP for 30 min. IL-1β secreted into the culture supernatants (sup), proIL-1β and β-Actin in cell lysates (cell), and TLR4 knockdown by siRNA (lower panel) were detected by immunoblotting. The band intensities on the immunoblots were quantified using NIH Image J software and are presented as the relative ratio to β-Actin.

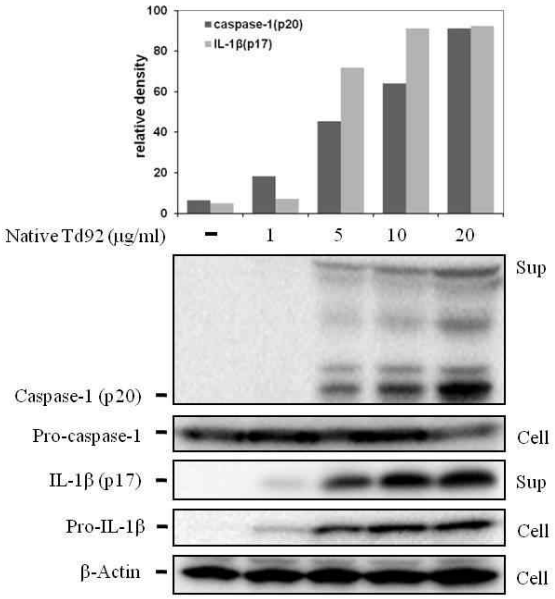

Figure 20. Native Td92 induces caspase-1 activation and IL-1β secretion. THP-1 cells were stimulated with various concentrations of native Td92 for 6 h. Caspase-1 and IL-1β in the culture supernatants (sup) and procaspase-1, proIL-1β, and β-Actin in the cell lysates (cell) were detected by immunoblotting. The band intensities on the immunoblots were quantified using NIH Image J software and are presented as the relative ratio to β-Actin.

3.2.2. Td92-induced caspase-1 activation via the NLRP3 inflammasome

Caspase-1 activation is initiated by the different inflammasome components. NLRs, such as NLRP3 and NLRC4, are the representative inflammasome components that have been shown to be involved in caspase-1 activation. To determine the component of inflammasome involved in Td92-induced caspase-1 activation, the roles of NLRP3, ASC, and NLRC4 were examined using siRNA technology. Because ASC is known to be an essential component of the NLRP3 inflammasome, the ASC knockdown experiment was also performed. Transfection of THP-1 cells with each siRNA resulted in a marked reduction in the expression of the corresponding mRNA and protein as assessed by real-time qPCR and immunoblotting, respectively, compared to cells transfected with control siRNA (Fig. 21). When Td92 was added to THP-1 cells transfected with NLRP3-specific siRNA (Fig. 21A) or ASC-specific siRNA (Fig. 21B), the p20 subunit of caspase-1 was markedly decreased, while the knockdown of NLRC4 did not affect the active caspase-1 level induced by Td92 (Fig. 21C). Accordingly, the decrease in the active form of caspase-1 resulted in a decrease in IL-1β secretion. MDP/ATP, *Salmonella typhimurium* flagellin, and *E. coli* RNA were used as positive controls for NLRP3 inflammasome-, NLRC4 inflammasome-, and ASC-dependent caspase-1 activation, respectively. The present results indicate that Td92 activates the NLRP3 inflammasome.

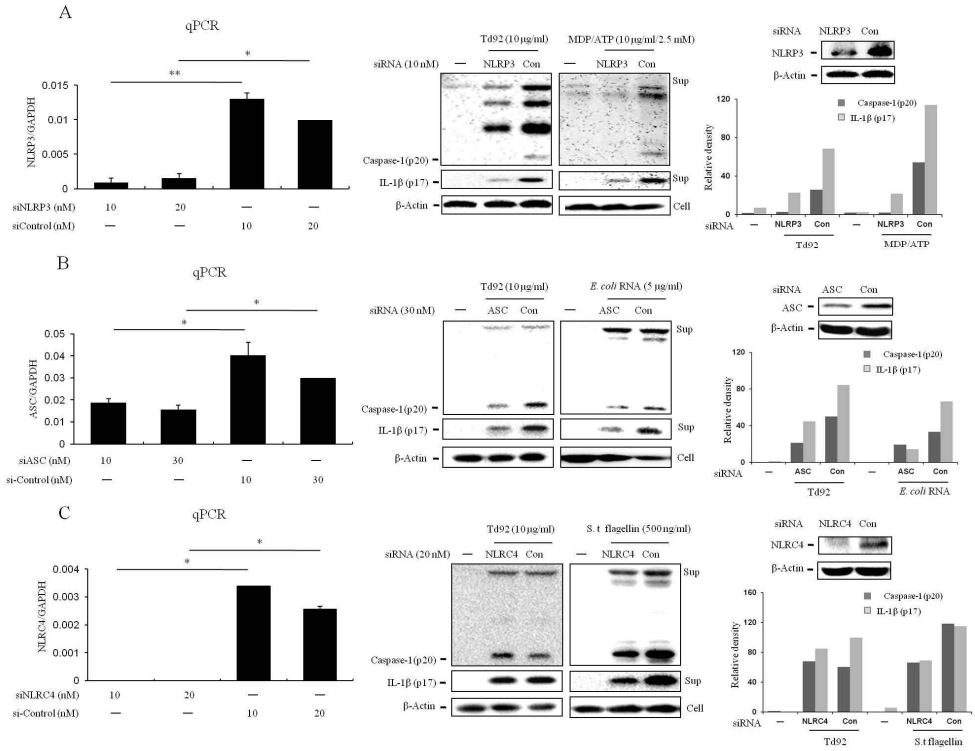

Figure 21. Td92-induced IL-1β activation is mediated via NLRP3. THP-1 cells were transfected with NLRP3 siRNA (A), ASC siRNA (B), NLRC4 siRNA (C), or control siRNA for 18 to 48 h. To confirm RNA interference, half of the cells were used for RNA extraction followed by real-time qPCR, and the other half of the cells were subjected to immunoblotting with antibodies for NLRP3 (A), ASC (B), and NLRC4 (C). Also, siRNA-transfected cells were treated with Td92, MDP, *E. coli* RNA, or *S. typhimurium* flagellin for 6 h (flagellin was delivered into the cytosol using the Profect P1 protein transfection reagent). MDP-stimulated cells were pulsed with 2.5 mM ATP for 30 min. Caspase-1 and IL-1β in the culture supernatants (sup) and β-Actin in cell lysates (cell) were detected by immunoblotting. The real-time qPCR data are shown as the means ± SD of one

representative experiment of three performed in triplicate. The band intensities on the immunoblots were quantified using NIH Image J software and are presented as the relative ratio to β-Actin. $^{*}p < 0.05$ and $^{**}p < 0.01$ versus control siRNA-transfected cells

3.2.3. ROS generation by Td92

Reactive oxygen species (ROS) are among the most important factors of inflammasome activation. Recently, it has been reported that inflammasome activation is triggered by reactive oxygen species, which are generated by a NADPH oxidase upon particle phagocytosis. ROS are generated by a NADPH oxidase, which is implicated in NALP3 inflammasome activation [56]. To determine whether ROS are generated by Td92, THP-1 cells were incubated with the ROS-sensitive fluorescent dye 2'.7'-dichlorodihydrofluorescein diacetate (DCF-DA) before treatment with Td92. As shown in Fig. 22A, the production of ROS was triggered by stimulation with Td92, compared with no treatment. To further examine whether Td92 induced ROS generation through NADPH oxidase in inflammasome activation, THP-1 cells were pretreated with ROS inhibitors (NAC and PDTC) and NADPH oxidase inhibitors (apocynin and DPI) before stimulation with Td92. As shown in Fig. 22B, the Td92-induced caspase-1 and IL-1β secretion were partially reduced by ROS inhibitors (NAC and PDTC) and by NADPH oxidase inhibitors (Apocynin and DPI). Although Td92-induced caspase-1 activation could not be completely inhibited by these inhibitors, the Td92-induced ROS generation is involved in caspase-1 activation.

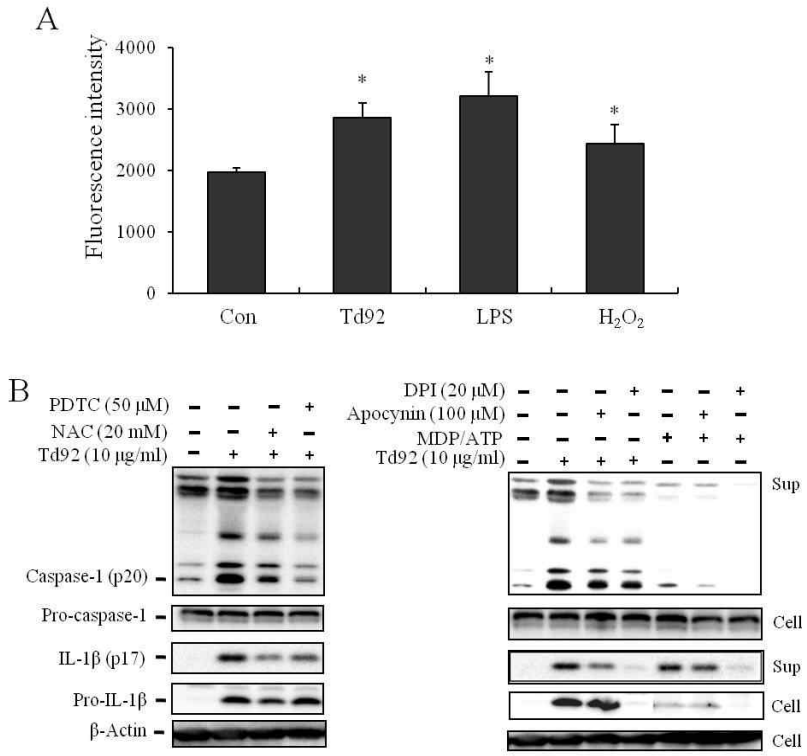

Figure 22. Td92 induces ROS generation through NADPH oxidase. THP-1 cells ($2x10^5$cells/ml) were seeded at 96-well culture plates and differentiated into macrophages with 160 nM PMA for 72 h. The cells were incubated with 10 μM DCF-DA at 37°C for 30 min and then the cells were washed with serum-free media followed by exposure to Td92 (10 μg/ml), LPS (10 μg/ml), or H_2O_2 (100 μM) for 1 h. ROS generation of cells was detected using a fluorometer (excitation at 485nm and emission at 520nm). The experiments were repeated three times and similar results were obtained. The results are presented as means ± SD in triplicate samples. $^*p < 0.05$ versus unstimulated cells (A) THP-1 cells (2×10^6/ml) were pretreated with 20 mM NAC, 50 μM PDTC, 100 μM apocynin, or 20 μM DPI for 30 min and

cells were then stimulated with Td92 (10 μg/ml), or MDP (10 μg/ml) for additional 6 h. MDP-stimulated cells were then pulsed with 2.5 mM ATP for 30 min. Caspase-1 and IL-1β secreted into the culture supernatants (Sup) and procaspase-1, proIL-1β, and β-Actin in the cell lysates (Cell) were detected by immunoblotting. The β-Actin was used as a loading control (B).

3.2.4. Association of ATP with Td92-induced caspase-1

The NLRP3 inflammasome can be specifically activated by a danger signal, such as ATP, which is released from stressed cells [35, 57, 58]. Extracellular ATP is an inflammatory mediator that binds to the P2X7 receptor and is involved in caspase-1 activation in macrophages and epithelial cells. To examine whether Td92 induces ATP release, which in turn leads to caspase-1 activation, THP-1 cells were treated with Td92 or *T. denticola*, and the ATP levels in the culture supernatants were measured. Td92 (10 μg/ml) and live *T. denticola* at an MOI of 100 and 1000 significantly induced ATP release, whereas PP4 did not enhance ATP production (Fig. 23A). To determine whether there is a link between the ATP produced by Td92 and caspase-1 activation, THP-1 cells were treated with oxATP, the irreversible P2X7 antagonist that blocks the interaction of ATP with the P2X7 receptor. As shown in Fig. 23B, oxATP at 300 μM completely blocked caspase-1 and IL-1β activation induced by Td92, indicating that Td92-induced caspase-1 activation is mediated by ATP. Furthermore, oxATP treatment inhibited the induction of proIL-1β by Td92. These results suggest that ATP has a critical role in both NLRP3 inflammasome activation and proIL-1β induction by Td92.

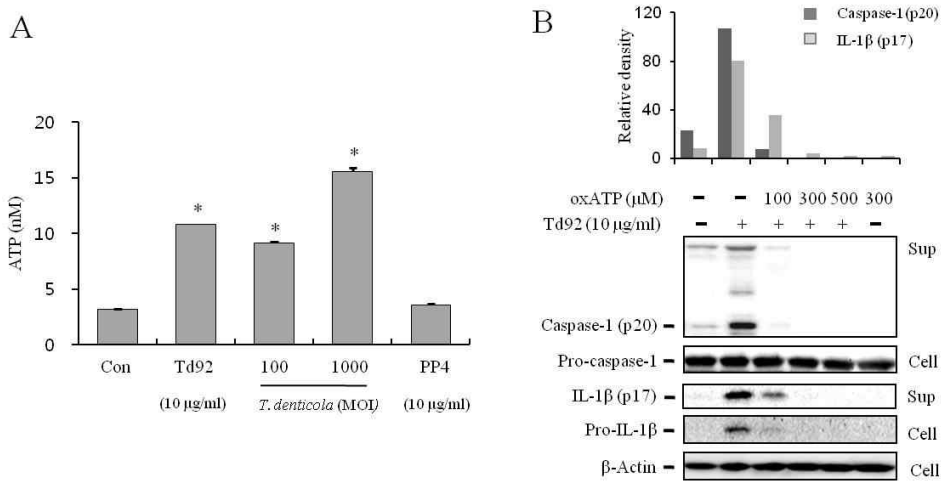

Figure 23. ATP is involved in Td92-induced NLRP3 activation. THP-1 cells were stimulated with Td92, live *T. denticola*, or PP4 for 2 h. Extracellular ATP levels were determined by using an ATP bioluminescence assay Kit. The data are shown as the means ± SD of one representative experiment of three performed in triplicate. $^{*}p < 0.01$ versus unstimulated cells (A) For the inhibition assay, the cells were pretreated with oxATP for 30 min prior to stimulation with Td92 for 6 h. Caspase-1 and IL-1β secreted into the culture supernatants (sup) and procaspase-1, proIL-1β, and β-Actin in the cell lysates (cell) were detected by immunoblotting. The band intensities of the immunoblots were quantified using NIH Image J software and are presented as the relative ratio to β-Actin (B).

3. 2.5. K^+ efflux as a mechanism of Td92-induced inflammasome activation

Depletion of intracellular K^+ is one of the mechanisms that leads to NLRP3 inflammasome activation, and *in vitro*, millimolar amounts of ATP induce a rapid collapse of ionic gradients by activating the purinergic receptor P2X7R, an ATP-gated cation channel, and cause K^+ efflux [35, 59]. To examine the role of K^+ efflux in the Td92-induced inflammasome activation, THP-1 cells were treated with Td92 in the presence of high concentrations of KCl in the culture medium that would block K^+ efflux from the cells. KCl treatment significantly reduced Td92-mediated caspase-1 activation and proIL-1β expression (Fig. 24A).

To further examine the role of K^+, caspase-1 activation was analyzed after THP-1 cells were treated with Td92 in the presence of the ATP-sensitive potassium channel blockers glybenclamide (also known as glyburide*)* and tolbutamide. As shown in Fig. 24B and 24C, both inhibitors decreased the extent of caspase-1 activation induced by Td92. These results indicate that Td92 increases plasma membrane permeability via ATP, resulting in K^+ efflux. K^+ efflux is sensed by NLRP3 and is followed by caspase-1 recruitment, inflammasome formation, and caspase-1 activation. Interestingly, proIL-1β expression in the cell extracts was decreased by glybenclamide but not by tolbutamide. Glybenclamide inhibited the caspase-1 activation, and IL-1β secretion induced by LPS plus ATP, targeting a signaling component downstream of the P2X7 receptor [60].

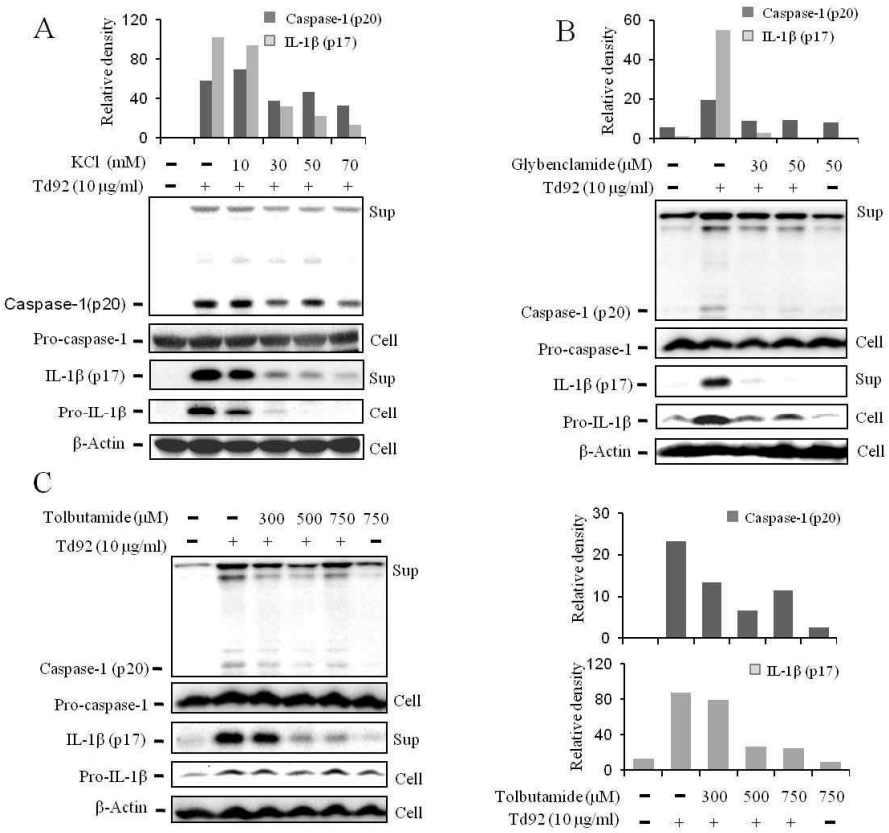

Figure 24. K^+ efflux is involved in Td92-induced NLRP3 activation. THP-1 cells were stimulated with Td92 for 6 h after pretreatment with KCl (A), glybenclamide (B), or tolbutamide (C) for 30 min prior to stimulation with Td92 for 6 h. Caspase-1 and IL-1β secreted into the culture supernatants (sup) and procaspase-1, proIL-1β, and β-Actin in the cell lysates (cell) were detected by immunoblotting. The band intensities of the immunoblots were quantified using NIH Image J software and are presented as the relative ratio to β-Actin.

3. 2.6. Caspase-1-dependent proinflammatory cell death induced by Td92

In addition to processing the proinflammatory cytokines proIL-1β and proIL-18 into their mature forms, caspase-1 can initiate a proinflammatory cell death called pyroptosis. Because *T. denticola* and Td92 activate caspase-1 via the NLRP3 inflammasome, the release of lactate dehydrogenase (LDH), a marker of cell death, from THP-1 cells was measured to determine whether pyroptosis is induced by *T. denticola* and Td92. Td92 and *T. denticola* significantly induced LDH release in THP-1 cells, whereas an irrelevant recombinant protein, PP4, had no effect (Fig. 25A). The LDH release was increased in a dose- and time-dependent manner by Td92 stimulation (Fig. 25B and 25C). Approximately 70% cell death was observed upon treatment with Td92 for 40 h. LDH release induced by Td92 was decreased in the presence of high extracellular K^+ (Fig. 25D) or the caspase-1 inhibitors ac-YVAD-cho and z-YVAD-fmk (Fig. 25E). Pyroptosis is characterized by the insertion of pores into the cell membrane, which can be detected by the uptake of a low-molecular-weight dye, such as propidium iodide (PI). Td92 increased PI uptake in the cells, and this increase was inhibited by the addition of oxATP, KCl, or caspase-1 inhibitors (Fig. 25F). Taken together, these results show that Td92 induces pore formation in the cell membrane and that the cell death is the result of caspase-1 activation rather than the direct cytotoxicity of Td92.

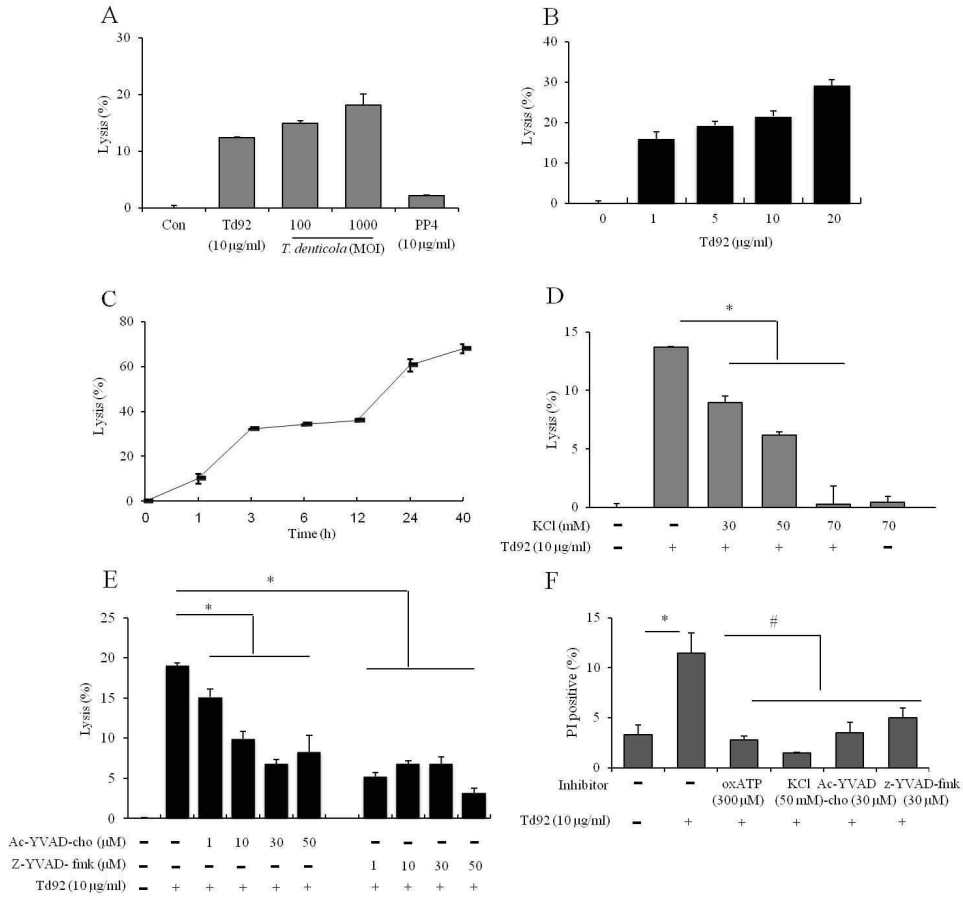

Figure 25. Td92 induces pyroptosis, caspase-1-dependent cell death. THP-1 cells were treated with Td92, live *T. denticola*, or PP4 for 6 h (A-B). THP-1 cells were treated with Td92 (10 μg/ml) for 1 to 40 h (C). THP-1 cells were pretreated with KCl, Ac-YVAD-cho, and z-YVAD-fmk for 30 min prior to stimulation with Td92 for 6 h (D-E). Cell supernatants were evaluated for the release of the cytoplasmic enzyme LDH using the LDH-cytotoxicity assay Kit. Cytotoxicity is expressed as the percentage of total LDH released as determined by lysing the cells with Triton X-100 detergent. The data are shown as the means ± SD of one representative experiment of three performed in triplicate (A-E). $^{*}p < 0.01$ versus

Td92-treated cells (D-E) THP-1 cells were pretreated with oxATP, KCl, Ac-YVAD-cho, and z-YVAD-fmk for 30 min prior to stimulation with Td92 for 3 h. The cells were stained with propidium iodide (PI, 20 μM) and Hoechst 33342 dye (10 μM) for 30 min, and images were acquired using fluorescence microscopy. PI-positive cells were counted out of at least 1000 total cells using the Image J software, and the data are presented as the means ± SD of the percentage of PI-positive cells in one representative experiment of three performed in triplicate. $^{*}p < 0.05$ versus unstimulated controls; $^{\#}p < 0.05$ versus Td92-stimulated cells (F)

3.2.7. Effect of intracellular delivery of Td92 on caspase-1 activation

Flagellin is one of a few protein ligands that activates caspase-1 in an NLRC4-dependent manner, and it must be internalized into the cytosol of the cell to exert its activity. To determine whether Td92 internalization is a prerequisite for NLRP3 activation, Td92 was delivered into THP-1 cells for 3 and 6 h using a transfection reagent Profect P1, which forms non-covalent complexes with proteins sized between 10-540 kDa and enables the translocation of intact proteins to cross the cell membrane, and caspase-1 activation was analyzed. Unexpectedly, internalization decreased the level of caspase-1 activation induced by Td92, whereas the intracellular delivery of *S. typhimurium* flagellin with the transfection reagent markedly enhanced caspase-1 activation compared to instances in which flagellin was added without the transfection reagent (Fig. 26A). ProIL-1β expression induced by Td92 was also decreased by the transfection reagent. An increased time for transfection (from 3 to 6 h) did not affect the results. Accordingly, the level of IL-1β secretion by Td92-treated cells was remarkably reduced by the transfection reagent, whereas flagellin-induced IL-1β secretion was increased by the transfection reagent. The enhanced Td92 internalization into the cells was confirmed by flow cytometry using FITC-labeled Td92 after extracellular fluorescence quenching with trypan blue. For the assay, paraformaldehyde-fixed cells, which do not allow endocytic internalization, were used as a negative control. The mean fluorescence intensity of the THP-1 cells treated with FITC-labeled Td92 was remarkably higher in the presence of Profect P1 than in the absence of Profect P1 and increased with time, thereby showing efficient internalization of

Td92 into the cells (Fig. 26B, top two panels). To elucidate the relationship between Td92 internalization and caspase-1 activation, further experiments were tested using cytochalasin D, an inhibitor of actin polymerization, which can delay or prevent protein internalization. The pretreatment of THP-1 cells with cytochalasin D resulted in a dose-dependent decrease in FITC-labeled Td92 internalization, when analyzed by flow cytometry (Fig. 26B, bottom panel). However, immunoblot analysis showed that cytochalasin D treatment did not affect Td92-induced caspase-1 activation, proIL-1β expression, or cell death (Fig. 26C and Fig. 27A).

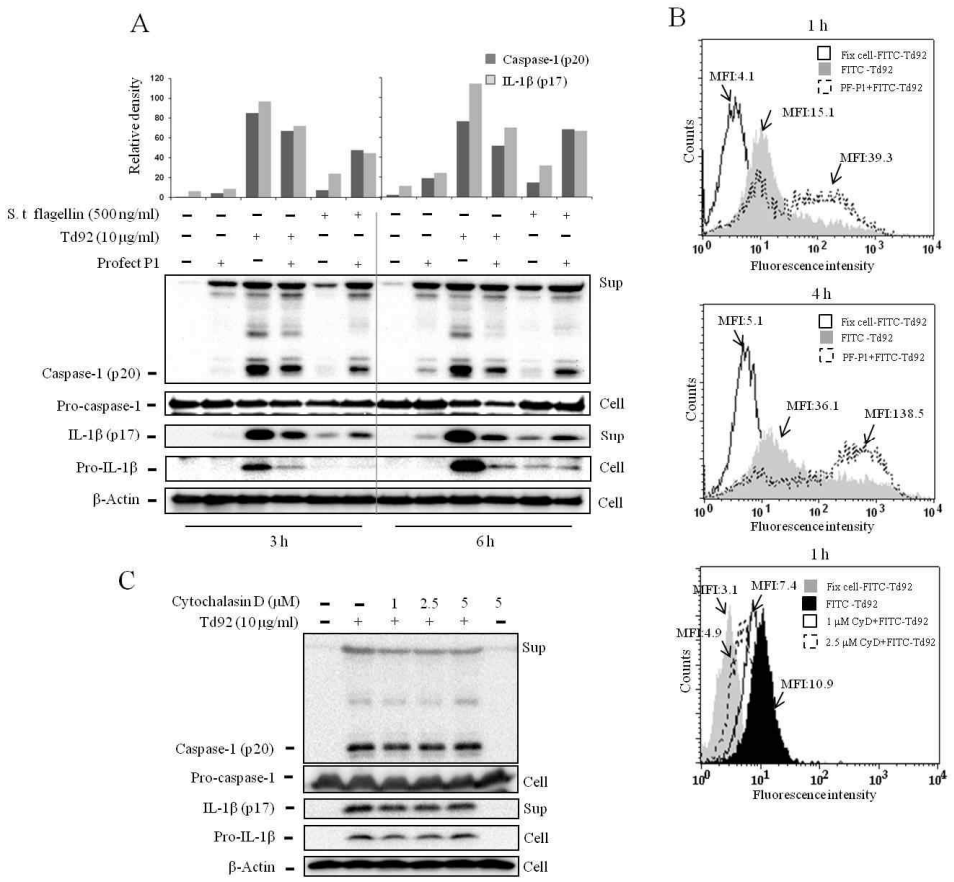

Figure 26. Td92 internalization into the cells is not required for caspase-1 activation or proIL-1β expression. THP-1 cells were stimulated with Td92 or *S. typhimurium* flagellin, which was premixed with or without Profect P1 for 3 and 6 h. Caspase-1 and IL-1β in the culture supernatants (sup) and procaspase-1, proIL-1β, and β-Actin in the cell lysates (cell) was detected by immunoblotting (A). THP-1 cells were incubated with FITC-labeled Td92, which was premixed with or without Profect P1 (top two panels), or THP-1 cells were pretreated with cytochalasin D for 30 min (bottom panel) before FITC-labeled Td92 treatment for

1 or 4 h. Internalization of Td92 was analyzed by flow cytometry. Paraformaldehyde-fixed THP-1 cells treated with FITC-Td92 were used as a negative control for internalization. The data are presented as the mean fluorescence intensities (MFI) from one representative of three independent experiments (B). THP-1 cells were pretreated with cytochalasin D for 30 min prior to Td92 treatment for 6 h. Caspase-1 and IL-1β in the culture supernatants (sup) and procaspase-1, proIL-1β, and β-Actin in the cell lysates (cell) were detected by immunoblotting (C).

Because *S. typhimurium* flagellin is known to induce pyroptosis [61], the LDH release from the cells treated with Td92 and flagellin was compared in the presence or absence of Profect P1 (Fig. 27B). Td92-treated THP-1 cells released approximately 17% of the total LDH, and the addition of Profect P1 increased LDH release to 25%. Because Profect P1 alone caused release of approximately 10% of the LDH, the increased LDH release by Td92 plus Profect P1 could be due to the mild cytotoxic effect of Profect P1. Flagellin-treated THP-1 cells released less than 3% of LDH in the absence of Profect P1, but the addition of Profect P1 strongly increased the LDH release (26%), indicating that cytosolic flagellin efficiently induces caspase-1 activation. These results support the data indicating that, unlike flagellin, internalization of Td92 is not critical in activating caspase-1 and causing cell death.

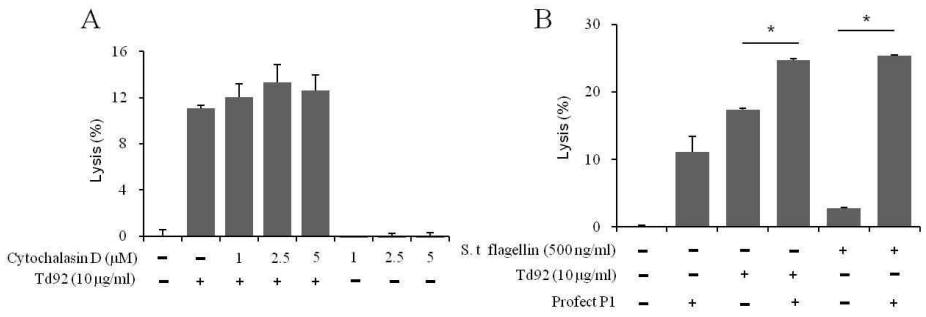

Figure 27. Td92 internalization into the cells is not required for cell death. THP-1 cells were pretreated with cytochalasin D for 30 min prior to Td92 treatment for 6 h. LDH released into the culture supernatants was measured (A). LDH released into the culture supernatants of Td92- or *S. typhimurium* flagellin-stimulated cells with or without the addition of Profect P1 for 6 h (B). The data are presented as the means ± SD of one representative experiment of three performed in triplicate. $^{*}p < 0.05$ versus without Profect P1

3.2.8. Activation of NLRP3 inflammasome by Td92 via interaction with the cellular receptor integrin α5β1

The present results indicate that Td92 binding, not internalization, is important for both caspase-1 activation and IL-1β transcription. Profect P1 caused the rapid uptake of protein into the cells without binding to the cells, and cytochalasin D blocked Td92 internalization without affecting caspase-1 activation and proIL-1β expression. It is hypothesized that Td92 binding to a membrane receptor is essential for the caspase-1 activation and the transcriptional/posttranscriptional regulation of IL-1β. As shown in this study, Td92 was able to bind to KB cells, an epithelial cell line, and it contributed to the binding of *T. denticola* to the cells. Additionally, Td92 was able to bind to immobilized fibronectin, which is known to be recognized by integrins, including α5β1 and αvβ3. Therefore, to identify the cellular receptor for Td92 that is involved in caspase-1 activation, an affinity ligand-binding assay was performed using Ni-NTA agarose, which binds histidine-tagged recombinant Td92. Ni-NTA-bound Td92 was mixed with THP-1 cell lysates, and the cellular proteins bound to Td92 were then eluted and subjected to immunoblotting with an anti-human fibronectin Ab and an anti-human integrin Abs. Because fibronectin was detected only in the culture supernatants of differentiated THP-1 cells but not in the cell lysates (Fig. 28), fibronectin was added to the ligand-binding assay mixture to test whether Td92 binds to integrin indirectly via fibronectin (Fig. 29A, lane 4). Td92 bound to both the α5 and β1 subunits (individual subunits) of the integrins, regardless of the presence of fibronectin (Fig. 29A, lane 4 and 5). The detection of integrin α5β1 in lane 4 was the result of both

direct binding of the integrin to Td92 and indirect binding of the integrin to Td92 via fibronectin. The detection of integrin α5β1 in lane 5 was the result of direct binding of Td92 to the integrin. Td92 did not bind directly to the integrin subunits αv or β3, but it bound to these integrins in the presence of fibronectin. The irrelevant recombinant protein PP4 did not bind to any subunit of the integrins (Figure 29A, lane 6). To further assess the specificity of the interaction of Td92 with the integrin α5β1, the anti-human integrin α5β1 Ab-coated Protein G agarose was incubated with recombinant human integrin α5β1 followed by Td92, fibronectin, or PP4. Following this experiment, the direct binding of Td92 to integrin α5β1 was confirmed by immunoblotting (Fig. 29B, lane 2). Fibronectin was used as a positive control and could be detected bound to integrin α5β1 (Fig. 29B, lane 3), whereas PP4 did not bind to integrin α5β1 (Fig. 29B, lane 4). Td92 was not detected when it was reacted with the Ab-coated Protein G agarose in the absence of integrin α5β1 (Fig. 29B, lane 8).

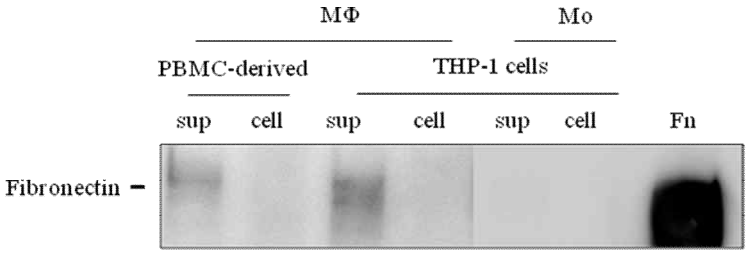

Figure 28. Macrophages secrete fibronectin. Expression of fibronectin was detected by immunoblotting in the cell lysates (cell) and the supernatants (sup) of human PBMC-derived macrophages, PMA-differentiated THP-1 cells (Mϕ), or THP-1 cells (Mo). Human plasma fibronectin (2 μg) was used as a control.

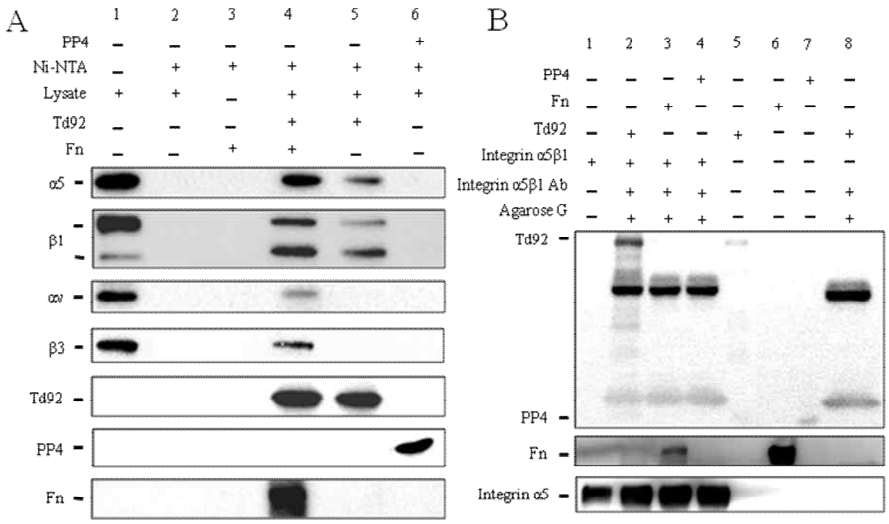

Figure 29. Integrin α5β1 directly interacts with Td92 to activate caspase-1. (A) THP-1 cell lysates (1.4 mg in 100 μl) were reacted with Td92 (50 μg), Td92 preincubated with fibronectin (Fn, 50 μg), or PP4 (50 μg) while slightly inverting at 4°C overnight. The reaction mixtures (300 μl) were incubated with 30 μl of Ni-NTA agarose at 4°C for 4 h. Agarose-bound proteins were eluted and subjected to immunoblotting for the detection of integrin subunits (α5, αv, β1, and β3), fibronectin (Fn), Td92, and PP4. (B) Protein G-agarose (20 μg) was incubated with an integrin α5β1 Ab (3 μg) at 4°C for 4 h and, subsequently, with recombinant human integrin α5β1 (10 μg) at 4°C overnight. After incubating the agarose with Td92 (10 μg), fibronectin (Fn, 20 μg), or PP4 (10 μg) at 4°C overnight, the proteins bound to the integrin α5β1-coated agarose were analyzed by immunoblotting using a histidine Ab (for the detection of recombinant Td92 and PP4), a fibronectin Ab or an integrin α5 Ab.

Using a polyclonal integrin β1 Ab, the β1 subunit of integrins from THP-1 cells was detected as two distinct bands, which were recognized by both Td92 and fibronectin. The β1 integrin undergoes variable glycosylation according to cell type [62]. Indeed, the deglycosylation of THP-1 cell lysates using N-glycosidase F, which cleaves between the innermost *N*-acetylglucosamine and asparagine residues of oligosaccharides from N-linked glycoproteins, resulted in a single β1 integrin form that had a decreased molecular mass (approximately 95-kDa) when analyzed by immunoblotting (Fig. 30A), suggesting that the molecular mass difference in the two forms of β1 integrin may be completely attributed to the levels of glycosylation. Lysates of THP-1 cells treated with tunicamycin, which inhibits N-glycosylation of newly synthesized glycoproteins, were reacted with Ni-NTA-bound Td92, and the cellular proteins bound to Td92 were detected by immunoblotting with an anti-human integrin β1 Ab. Td92 binding to the unglycosylated form of β1 integrin was not observed (Fig. 30B), indicating that inhibition of glycosylation of integrin α5β1 affects the binding of Td92. Although Td92 and fibronectin recognized both forms of β1 integrin, the lower band of β1 integrin was preferentially pulled down over the upper band. As a control, recombinant integrin αvβ3 was included. Integrin αvβ3 Ab-coated Protein G agarose was incubated with recombinant human integrin αvβ3 and subsequently with Td92, fibronectin, or PP4. Td92 and PP4 were not found to bind integrin αvβ3 (Fig. 31), whereas fibronectin did bind integrin αvβ3, suggesting specific interactions between Td92 and integrin α5β1.

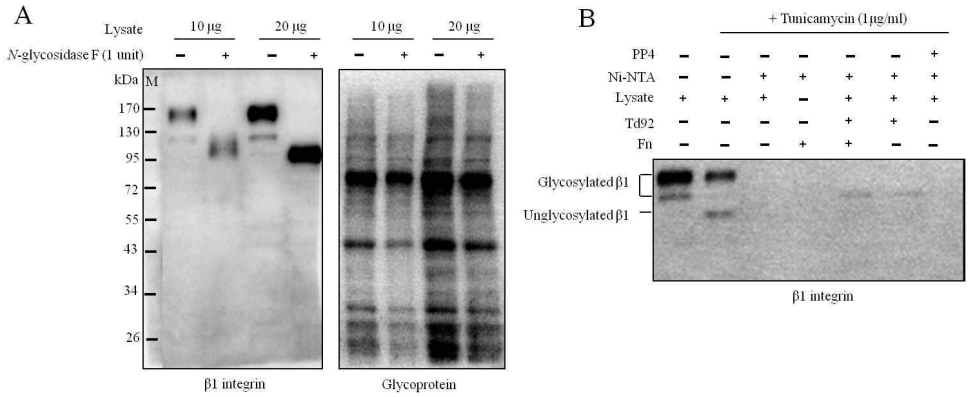

Figure 30. Td92 does not bind to unglycosylated integrin β1. THP-1 cell lysates (10 μg or 20 μg) were incubated with 1 unit of N-glycosidase F and subjected to SDS-PAGE followed by immunoblotting using an integrin β1 Ab and biotinylated Phaseolus vulgaris Leucoagglutinin (PHA-L) (A). THP-1 cells were treated with 1 μg/ml tunicamycin during differentiation with PMA for additional 6 h before lysis. THP-1 cell lysates (1.4 mg in 100 μl) were reacted with Td92 (50 μg), Td92 preincubated with fibronectin (Fn, 50 μg), or PP4 (50 μg) while slightly inverting the reaction mixture at 4°C overnight. The reaction mixtures (300 μl) were incubated with 30 μl of Ni-NTA agarose at 4°C for 4 h. Agarose-bound proteins were eluted and subjected to immunoblotting for the detection of integrin β1 (B).

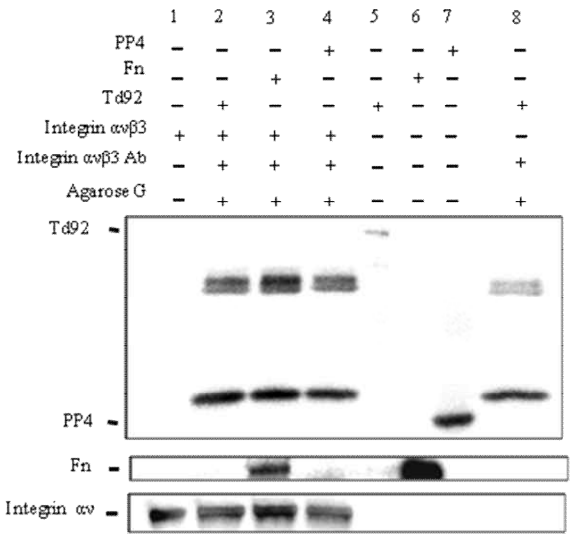

Figure 31. Integrin αvβ3 does not interact with Td92. Protein G-agarose (20 μg) was incubated with an integrin αvβ3 Ab (3 μg) at 4°C for 4 h and then with recombinant human integrin αvβ3 (10 μg) at 4°C overnight. After incubating the agarose with Td92 (10 μg), fibronectin (Fn, 20 μg), or PP4 (10 μg) at 4°C overnight, the proteins bound to the integrin αvβ3-coated agarose were analyzed by immunoblotting using a histidine Ab (for the detection of recombinant Td92 and PP4), a fibronectin Ab, or an integrin αv Ab (The heavy and light chains of the antibody are also detected).

Ligand binding of the integrin receptor induces clustering of the integrins and recruitment of focal adhesion-associated proteins. To assess the formation of integrin α5β1 clustering upon Td92 binding, THP-1 cells were treated with Td92, fibronectin (a positive control), or bovine serum albumin (BSA, a negative control) at different times and observed by confocal microscopy after staining with an integrin α5β1 Ab and a Cy3-labeled secondary antibody. A uniform distribution of integrin α5β1 was observed in unstimulated cells (Fig. 32). However, upon stimulation of THP-1 cells with Td92 or fibronectin, extensive aggregation of integrin α5β1 on the cell surface was observed in more than 80% of the cells after 15 min, whereas the BSA treatment did not induce integrin aggregation over the time course up to 2 h. Because cytochalasin D prevented Td92 internalization, THP-1 cells were pretreated with cytochalasin D prior to FITC-labeled Td92 treatment to visualize Td92 binding to integrin α5β1. Upon incubating the THP-1 cells with Td92 for up to 2 h, the colocalization of Td92 with integrin α5β1 was clearly observed, whereas without cytochalasin D pretreatment, Td92 was observed in the cells as well as on the cell surface (Fig. 33). To validate these data that showing the involvement of integrin α5β1 in Td92-induced caspase-1 activation, an experiment was performed with integrin siRNA. Because the intact integrin α5 is known to be essential for α5β1 dimer formation, expression on the cell surface, and its biological function [63], siRNA specific for integrin α5 was used. Caspase-1 activation and proIL-1β expression induced by Td92 were remarkably inhibited in THP-1 cells that were transfected with integrin α5 siRNA (Fig. 34).

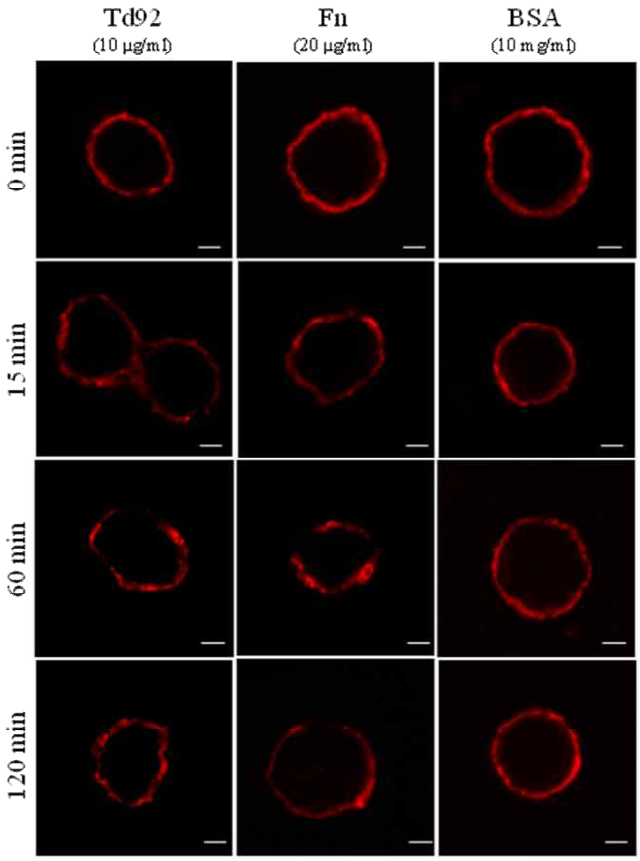

Figure 32. Td92 binding to the cells induces integrin clustering. THP-1 cells were treated with Td92, fibronectin (Fn), or heat-inactivated BSA for 15, 60, and 120 min. After washing, the cells were fixed with 3.8% paraformaldehyde in PBS and immunostained using an integrin α5β1 Ab and a Cy3-conjugated secondary Ab. Cells were analyzed by confocal laser scanning microscopy. A representative cell for each treatment is shown. Magnification, x 2000 Scale bars represent 2.5 μm.

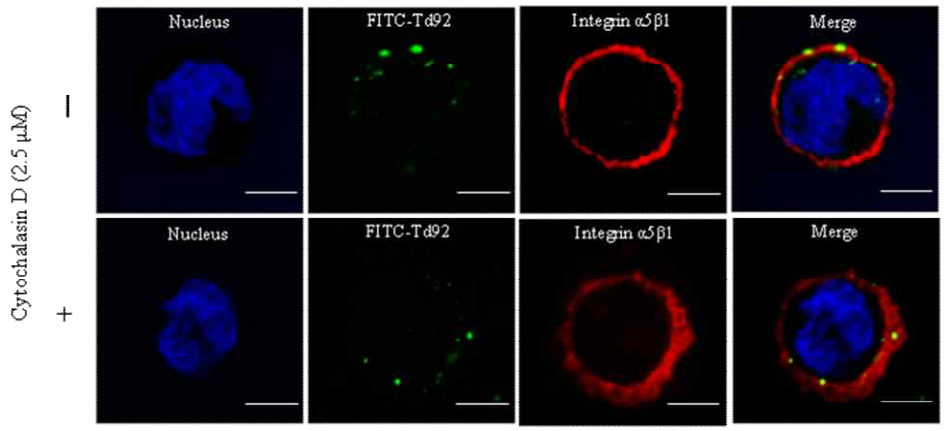

Figure 33. Colocalization of Td92 with integrin α5β1 is clearly observed with or without cytochalasin D. THP-1 cells cultured on a cover glass were pretreated with cytochalasin D for 30 min and then incubated with FITC-labeled Td92 (10 μg/ml) for 2 h. After fixation with 3.8% paraformaldehyde in PBS, the cells were incubated with an integrin α5β1 Ab followed by a Cy3-conjugated secondary Ab with the nuclear staining with Hoechst 33342 and were observed by confocal microscopy (x 2000). Scale bars represent 5 μm.

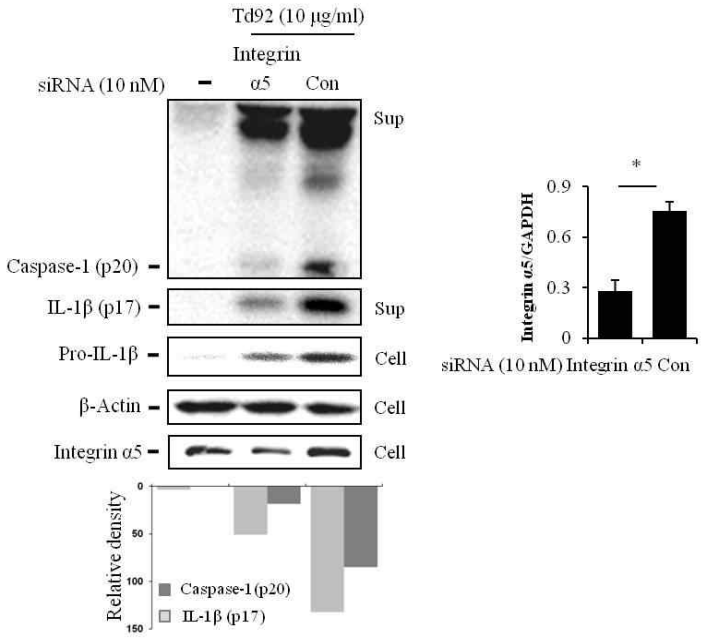

Figure 34. Knockdown of integrin α5 affects Td92-induced inflammasome activation. THP-1 cells were transfected with α5 siRNA or control siRNA for 36 h. To confirm RNA interference, the cells were used for RNA extraction followed by real-time qPCR. Also, siRNA-transfected cells were treated with Td92, Caspase-1 and IL-1β in the culture supernatants (sup) and proIL-1β, β-Actin, and integrin α5 in the cell lysates (cell) were detected by immunoblotting. The real-time qPCR data are shown as the means ± SD of one representative experiment of three performed in triplicate. The band intensities on the immunoblots were quantified using NIH Image J software and are presented as the relative ratio to β-Actin. $^{*}p < 0.05$ versus control siRNA-transfected cells

To further confirm that Td92 bound to the cells via integrin α5β1, a neutralizing integrin α5β1 Ab was used. The integrin α5β1 Ab inhibited FITC-labeled Td92 binding to THP-1 cells as analyzed by flow cytometry (Fig. 35A). Although the integrin α5β1 Ab did not completely inhibit Td92 binding to the cells, we observed that the antibody inhibited Td92 binding in a dose-dependent manner and that more than 60% of Td92 binding was inhibited at a concentration of 25 μg/ml of the antibody (Fig. 35B), suggesting integrin α5β1 is the major cellular receptor for Td92.

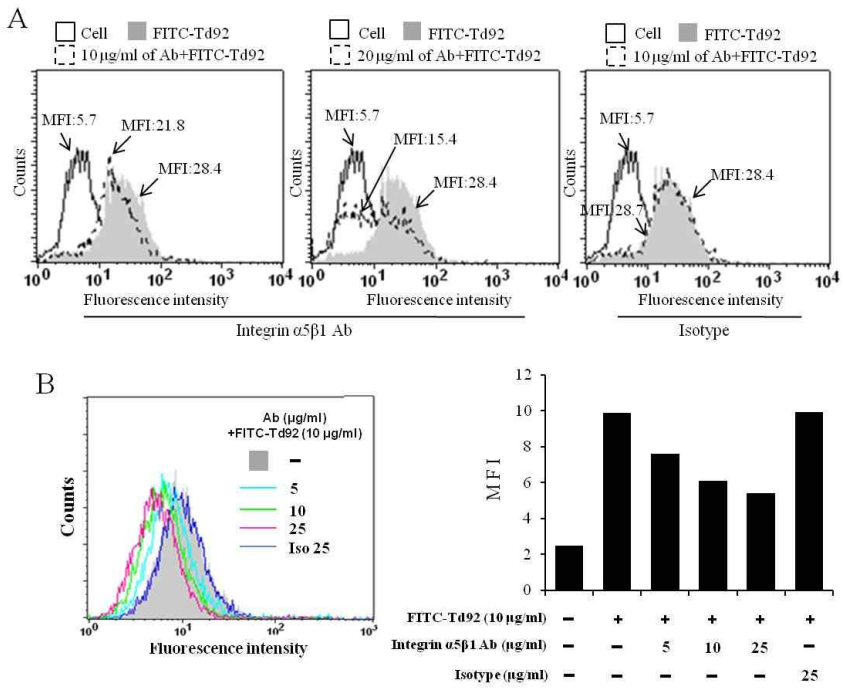

Figure 35. Integrin α5β1 Ab inhibits FITC-Td92 binding to THP-1 cells. THP-1 cells were incubated with an integrin α5β1 Ab (10 and 20 μg/ml: A; 5 to 25 μg/ml: B) or the anti-mouse IgG_1 isotype control (10 μg/ml: A; 25 μg/ml: B) for 1 h prior to incubation with FITC-labeled Td92 (10 μg/ml) for 30 min, and Td92 binding was analyzed by flow cytometry. The data are presented as the mean fluorescence intensities (MFI) from one representative of three independent experiments.

In addition, the integrin α5β1 Ab remarkably reduced caspase-1 activation and IL-1β secretion in a dose-dependent manner (Fig. 36A and 36B), whereas a neutralizing integrin αvβ3 Ab did not affect Td92 binding to cells, caspase-1 activation, or IL-1β secretion (Fig. 37). Td92-induced caspase-1 activation and proIL-1β expression in THP-1 cells pretreated with cytochalasin D were inhibited by the integrin α5β1 Ab (Fig. 38). These results confirm that Td92 internalization is not required for these mechanisms. The integrin α5β1 Ab also significantly reduced *T. denticola*-induced IL-1β secretion. The addition of the integrin α5β1 Ab at 2, 5, 10, and 20 μg/ml reduced the level of *T. denticola*-induced IL-1β secretion by 12, 17, 36, and 45% compared with the same concentration of IgG_1 isotype Ab (Fig. 39D). The level of proIL-1β transcription was also reduced by the integrin α5β1 Ab (Fig. 36A). Additionally, neutralizing effects of the integrin α5β1 Ab on native Td92 and *T. denticola* whole bacteria–induced caspase-1 activation and proIL-1β expression were observed (Fig. 39A and 39B). However, the integrin α5β1 Ab did not affect *S. typhimurium* flagellin-induced IL-1β secretion (Fig. 39C).

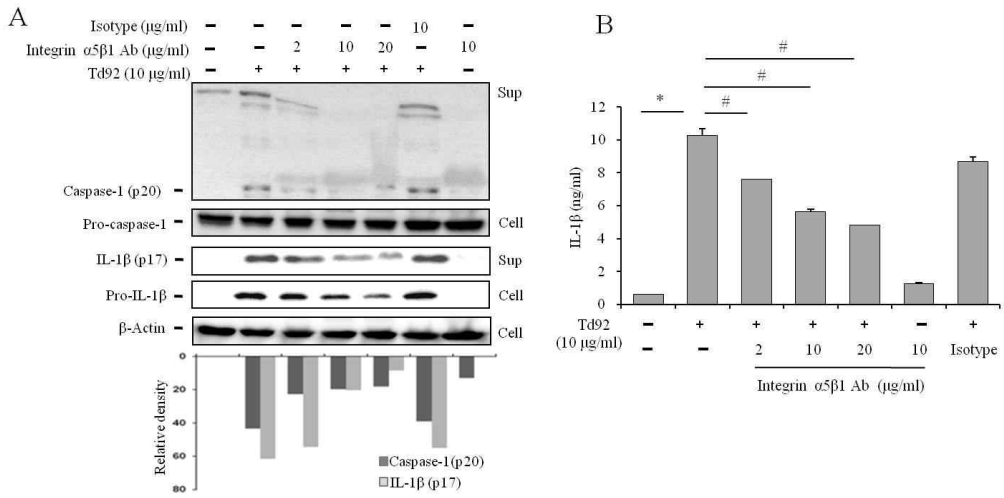

Figure 36. Integrin α5β1 Ab inhibits Td92-induced inflammasome activation. THP-1 cells were pretreated with an integrin α5β1 Ab (2 to 20 μg/ml) or the anti-mouse IgG_1 isotype control (10 μg/ml) for 1 h prior to stimulation with Td92 (10 μg/ml) for 6 h (A-B). Caspase-1 and IL-1β in the culture supernatants (sup) and procaspase-1, proIL-1β, and β-Actin in the cell lysates (cell) were detected by immunoblotting (A), and the IL-1β level in the culture supernatants was measured by ELISA (B). The band intensities on the immunoblots were quantified using NIH Image J software and are presented as the relative ratio to β-Actin (A). The data are shown as the mean ± SD of one representative experiment of three performed in triplicate. $^{*}p < 0.05$ versus unstimulated cells; $^{\#}p < 0.05$ versus Td92-stimulated cells (B)

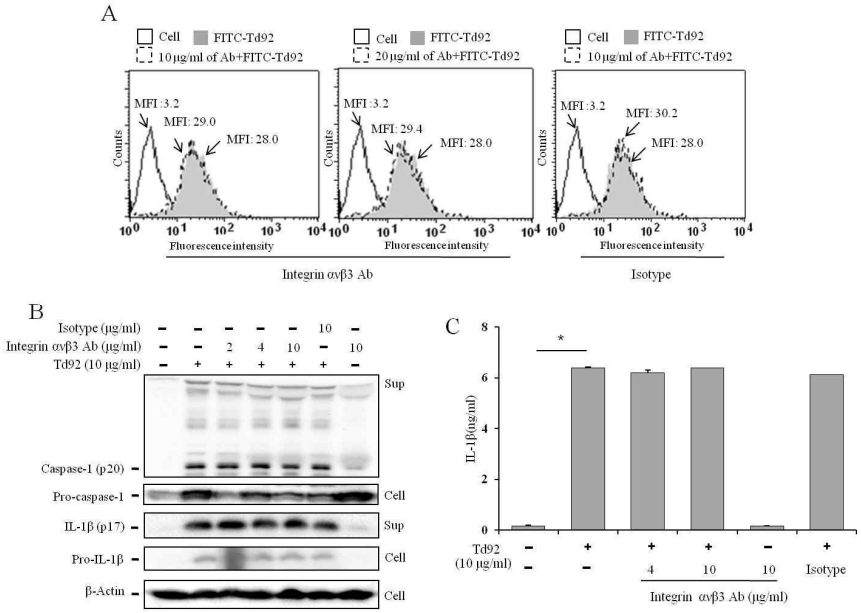

Figure 37. Integrin αvβ3 is not involved in Td92-induced NLRP3 activation. THP-1 cells were pretreated with an anti-human integrin αvβ3 Ab (10 and 20 μg/ml) or the anti-mouse IgG_1 isotype control (10 μg/ml) for 1 h prior to incubation with FITC-labeled Td92 (10 μg/ml) for 30 min, and Td92 binding was analyzed by flow cytometry. The data are presented as the mean fluorescence intensities (MFI) from one representative of three independent experiments (A). THP-1 cells were pretreated with an anti-human integrin αvβ3 Ab (2 to 10 μg/ml) or the anti-mouse IgG_1 isotype control (10 μg/ml) for 1 h prior to stimulation with Td92 for 6 h (B-C). Caspase-1 and IL-1β in the culture supernatants (sup) and procaspase-1, proIL-1β, and β-Actin in the cell lysates (cell) were detected by immunoblotting (B), and the IL-1β level in the culture supernatants was measured by ELISA (C). The data are shown as the means ± SD of one representative experiment of three performed in triplicate. $^{*}p < 0.01$ versus unstimulated cells (C)

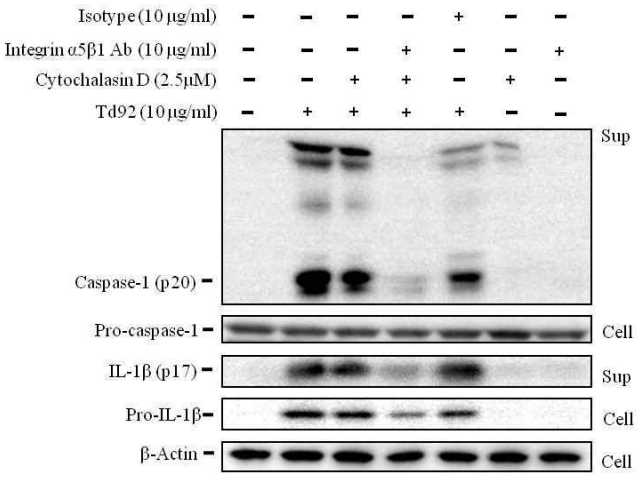

Figure 38. Td92-induced caspase-1 activation and proIL-1β expression in THP-1 cells pretreated with cytochalasin D are inhibited by an integrin α5β1 Ab. THP-1 cells were pretreated with cytochalsin D for 30 min and subsequently with an integrin α5β1 Ab for 1 h before treatment of the cells with Td92 for 6 h. Caspase-1 and IL-1β secreted into the culture supernatants (sup) and procaspase-1, proIL-1β, and β-Actin in the cell lysates (cell) were detected by immunoblotting.

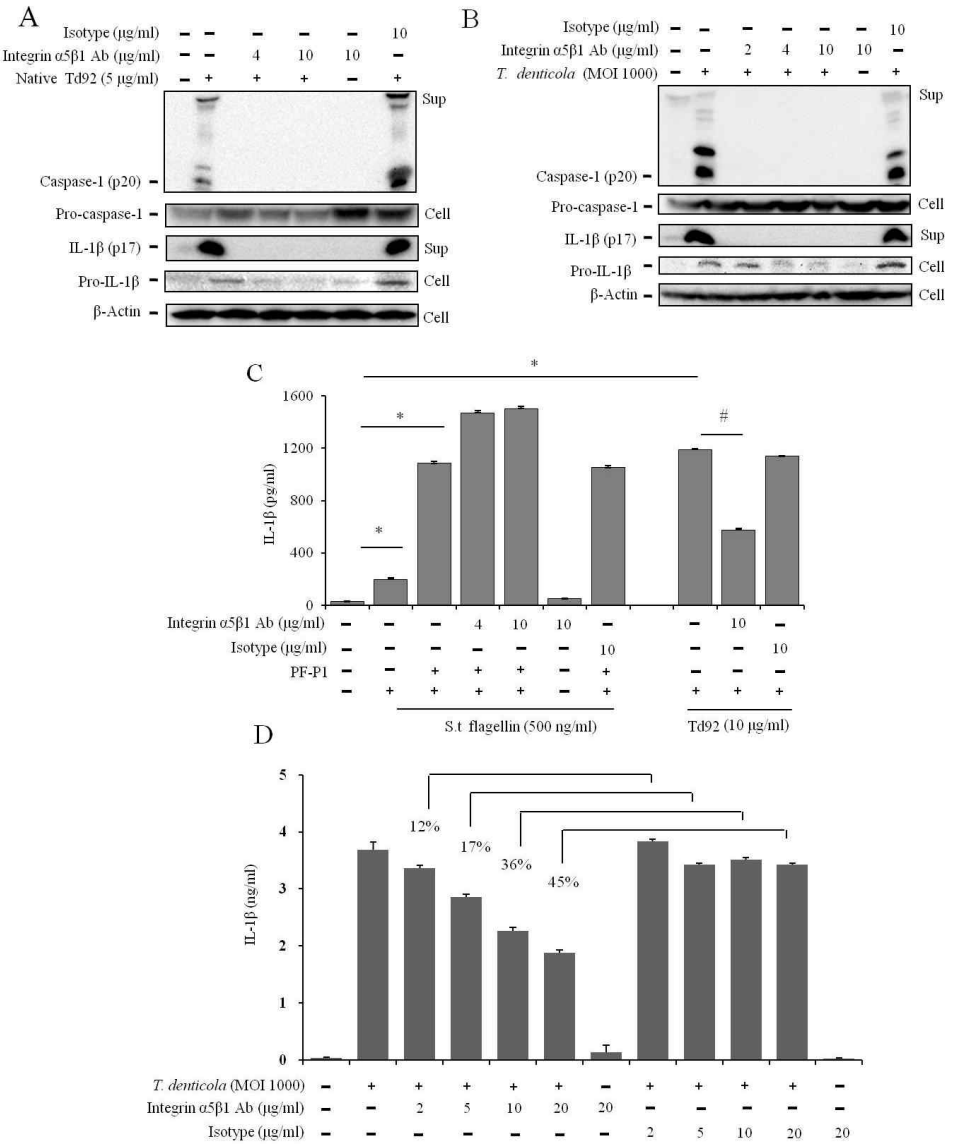

Figure 39. Integrin α5β1 is involved in caspase-1 activation by native Td92 and *T. denticola*, but not by flagellin. THP-1 cells were pretreated with an anti-human integrin α5β1 Ab (2 to 10 μg/ml: A-C; 2 to 20 μg/ml: D) or the anti-mouse IgG_1 isotype control (10 μg/ml: A-C; 2 to 20 μg/ml: D) for 1 h prior to stimulation with native and recombinant Td92 (10 μg/ml), live *T. denticola* (MOI 1000), or *S.*

typhimurium flagellin (500 ng/ml) for 6 h. *S. typhimurium* flagellin was premixed with Profect P1 before cell stimulation. Caspase-1 and IL-1β in the culture supernatants (sup) and procaspase-1, proIL-1β, and β-Actin in the cell lysates (cell) were detected by immunoblotting (A-B). The IL-1β level in the culture supernatants was analyzed by ELISA. The data are shown as the mean ± SD of one representative experiment of three performed in triplicate. $^{*}p < 0.05$ versus unstimulated cells; $^{\#}p < 0.05$ versus Td92-stimulated cells (C-D)

To test that integrin α5β1 was also involved in Td92-induced caspase-1 activation in PBMC-derived macrophages, freshly isolated PBMCs were differentiated into macrophages and stimulated with Td92. Td92 induced caspase-1 activation and IL-1β secretion, and the integrin α5β1 Ab markedly reduced caspase-1 activation and IL-1β secretion by Td92 in PBMC-derived macrophages (Fig. 40). In contrast to the findings in THP-1 cells, proIL-1β expression in untreated PBMC-derived macrophages was similar to that in Td92-treated cells, and the neutralization effect by the integrin Ab was not observed.

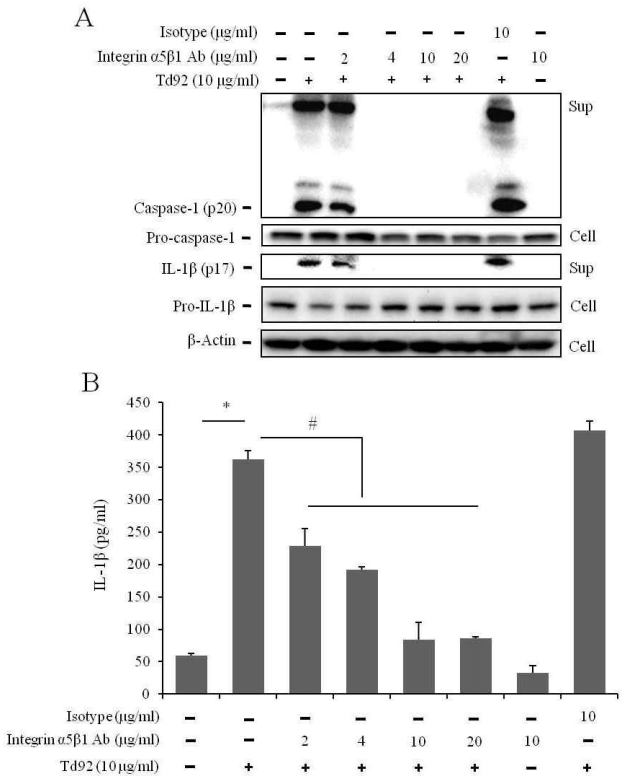

Figure 40. Td92 induces IL-1β secretion in human PBMC-derived macrophages. Human PBMC-derived macrophages were pretreated with an integrin α5β1 Ab (2 to 20 μg/ml) or the anti-mouse IgG_1 isotype control (10 μg/ml) for 1 h prior to stimulation with Td92 (10 μg/ml) for 6 h. Caspase-1 and IL-1β in the culture supernatants (sup) and procaspase-1, proIL-1β, and β-Actin in the cell lysates (cell) were detected by immunoblotting (A). The IL-1β level in the culture supernatants was analyzed by ELISA. The data are shown as the mean ± SD of one representative experiment of three performed in triplicate. $^{*}p < 0.05$ versus unstimulated cells; $^{\#}p < 0.05$ versus Td92-stimulated cells (B)

Because Td92-induced ATP is a critical factor in NLRP3 inflammasome activation by Td92, the effect of the integrin α5β1 Ab on Td92-induced ATP production was analyzed. The antibody reduced the release of ATP by Td92 to the control level (Fig. 41). The neutralizing fibronectin Ab did not affect caspase-1 activation, proIL-1β expression, or IL-1β secretion, although the binding of Td92 was reduced by the addition of the fibronectin Ab (Fig. 42). The binding of Td92 to soluble and immobilized fibronectin was confirmed by ELISA using FITC-labeled Td92 and fibronectin (Fig. 43). The FITC-labeled fibronectin in solution was bound to immobilized Td92, and non-labeled fibronectin competed with FITC-labeled fibronectin to bind Td92. FITC-labeled Td92 also bound to immobilized fibronectin, and the RGD peptide (GRGDSP) did not interfere with the binding of Td92 to fibronectin. These results indicate that although Td92 is able to bind to both integrin α5β1 and fibronectin, Td92-induced NLRP3 activation is mediated via direct binding to integrin α5β1, but not by binding to fibronectin, indicating that the interaction between Td92 and integrin α5β1 plays a critical role for NLRP3 inflammasome activation.

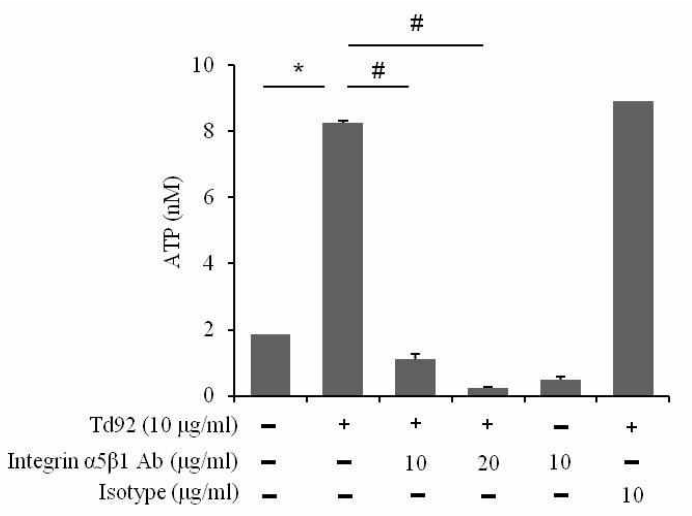

Figure 41. Integrin α5β1 is involved in ATP release by Td92. THP-1 cells were pretreated with an integrin α5β1 Ab (10 and 20 µg/ml) or the anti-mouse IgG_1 isotype control (10 µg/ml) for 1 h before stimulation with Td92 (10 µg/ml) for 2 h. Extracellular ATP levels were determined using an ATP bioluminescence assay Kit. The data are shown as the means ± SD of one representative experiment of three performed in triplicate. $^{*}p < 0.05$ versus unstimulated cells; $^{\#}p < 0.05$ versus Td92-stimulated cells

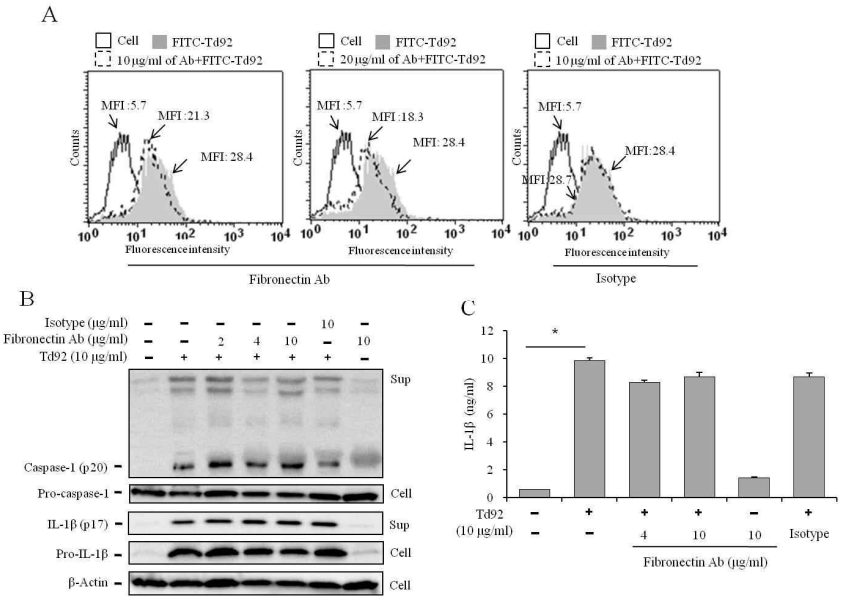

Figure 42. Td92 binding to fibronectin does not affect caspase-1 activation. THP-1 cells were pretreated with a fibronectin Ab (10 and 20 μg/ml) or the anti-mouse IgG_1 isotype control (10 μg/ml) for 1 h prior to incubation with FITC-labeled Td92 (10 μg/ml) for 30 min, and the Td92 binding was analyzed by flow cytometry. The data are presented as the mean fluorescence intensities (MFI) of one representative of three independent experiments (A). THP-1 cells were pretreated with a fibronectin Ab (2 to10 μg/ml) or the anti-mouse IgG_1 isotype control (10 μg/ml) for 1 h prior to stimulation with Td92 for 6 h (B-C). Caspase-1 and IL-1β secreted in the culture supernatants (sup) and procaspase-1, proIL-1β, and β-Actin in the cell lysates (cell) were detected by immunoblotting (B). The IL-1β level in the culture supernatants was measured by ELISA. The data are presented as the means ± SD of one representative experiment of three performed in triplicate. $^{*}p < 0.05$ versus unstimulated cells (C)

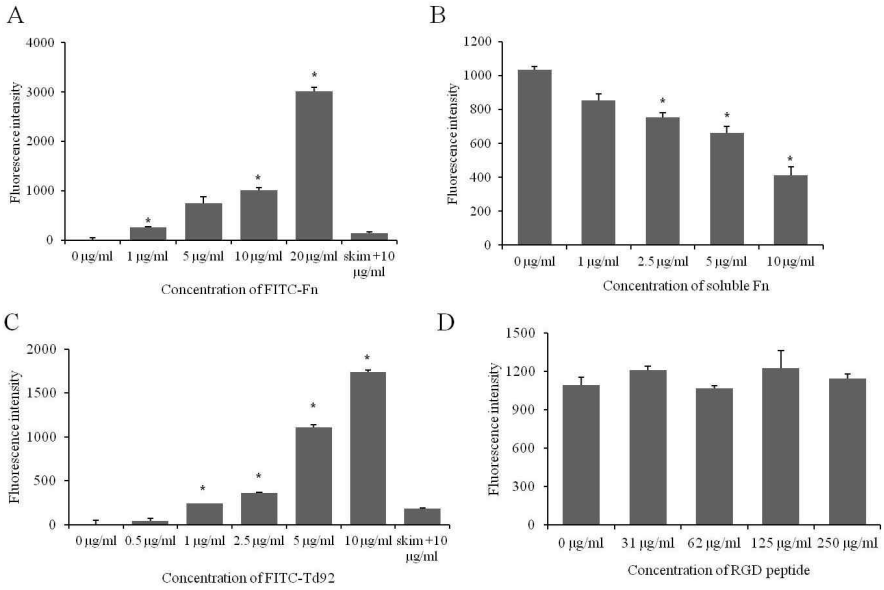

Figure 43. Td92 binds to soluble and immobilized fibronectin. Ninety-six well microtiter plates were coated with 100 µl of Td92 (10 µg/ml) or skim milk (5 µg/ml). FITC-labeled fibronectin (1 to 20 µg/ml) was added to the wells at 37°C for 1 h (A). FITC-labeled fibronectin (10 µg/ml) was added in the presence of non-labeled fibronectin (1 to 10 µg/ml) (B). Ninety-six well microtiter plates were coated with 100 µl of human plasma fibronectin (10 µg/ml) or skim milk. FITC-labeled Td92 (0.5 to 10 µg/ml) was added to the wells at 37°C for 1 h (C). The RGD peptide was added to the wells for 30 min prior to the addition of FITC-labeled Td92 (5 µg/ml) for 1 h (D). The fluorescence of fibronectin bound to Td92 and Td92 bound to immobilized fibronectin was measured with a fluorometer. $^{*}p <$ 0.01 versus the control in each experiment (no addition of FITC-labeled fibronectin in A; no addition of non-labeled fibronectin in B; no addition of FITC-labeled Td92 in C)

To determine whether the priming of integrin α5β1 by other ligands induces NLRP3 activation, THP-1 cells were treated with representative integrin α5β1 ligands, such as fibronectin (a soluble form) and the RGD peptide (GRGDSP), and the ligands were analyzed for their ability to activate caspase-1. Fibronectin (5-20 μg/ml) and the RGD peptide (10 and 100 μg/ml) induced caspase-1 activation without the addition of ATP, whereas the non-RGD peptide (GRADSP) did not induce caspase-1 activation (Fig. 44A). The addition of ATP did not affect caspase-1 activation by fibronectin or the RGD peptide (Fig. 44B). As expected, fibronectin and the RGD peptide significantly induced the release of ATP in THP-1 cells (Fig. 45). The addition of the integrin α5β1 Ab or oxATP markedly inhibited the caspase-1 activation induced by fibronectin or the RGD peptide (Fig. 46A and 46B). However, an integrin αvβ3 Ab did not inhibit caspase-1 activation by fibronectin (Fig. 47). Neither fibronectin nor the RGD peptide induced proIL-1β expression at the concentrations used in this study (Fig. 44A).

Taken together, the results above confirm that integrin α5β1 is the principle receptor for NLRP3 activation, and ATP is the primary regulator. Because there is no RGD motif in Td92, the Td92 binding site for integrin α5β1 is most likely distinct from that of fibronectin and, possibly, that of other RGD-containing proteins. The interaction between Td92 and integrin α5β1 is similar to the interaction between fibronectin/RGD and integrin α5β1 in terms of caspase-1 activation, but it differs in the induction of proIL-1β expression.

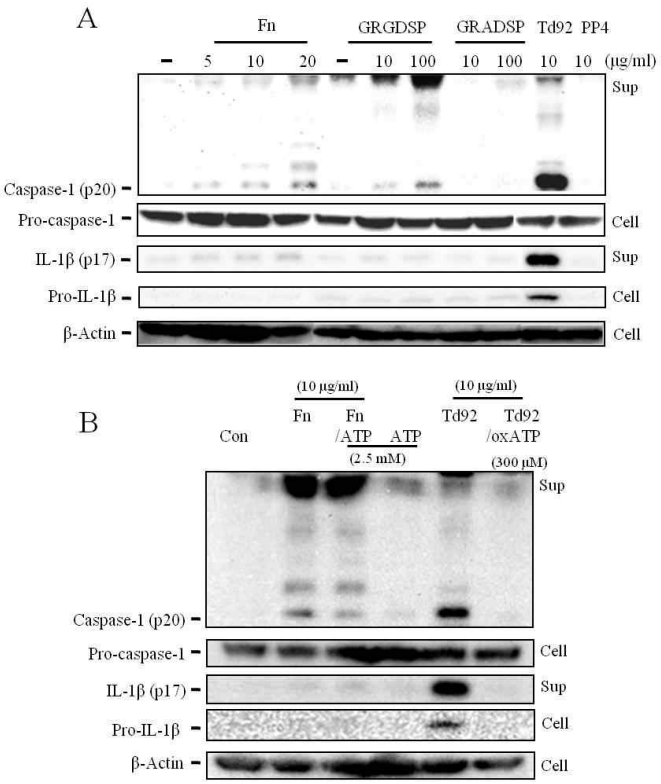

Figure 44. Priming of integrin α5β1 by other ligands induces NLRP3 activation. THP-1 cells were treated with fibronectin (Fn, 5 to 20 μg/ml), GRGDSP peptide (10 and 100 μg/ml), GRADSP peptide (10 and 100 μg/ml), Td92 (10 μg/ml), or PP4 (10 μg/ml) for 6 h (A). THP-1 cells were treated with fibronectin or Td92 (10 μg/ml) for 6 h. In some experiments, Fn-stimulated cells were pulsed with 2.5 mM ATP for 30 min and the Td92-stimulated cells were pretreated with oxATP (300 μM) for 30 min before stimulation with Td92 for 6 h (B). Caspase-1 and IL-1β in the culture supernatants (sup) and procaspase-1, proIL-1β, and β-Actin in the cell lysates (cell) were detected by immunoblotting.

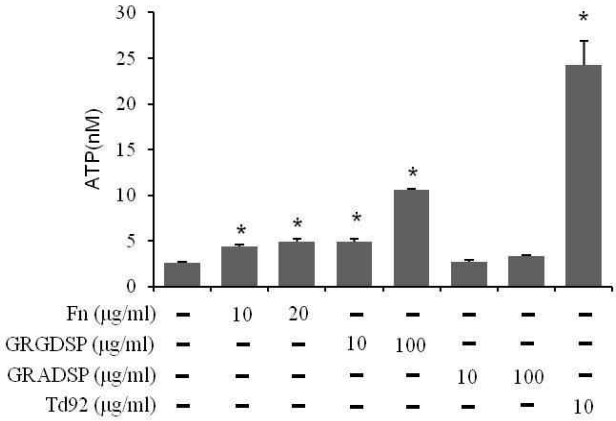

Figure 45. Integrin α5β1 ligands induce extracellular ATP release. Extracellular ATP levels were determined in the supernatants of fibronectin (Fn)-, GRGDSP-, GRADSP-, or Td92-incubated cells for 2 h. The data are shown as the means ± SD of one representative experiment of three performed in triplicate. $^{*}p <$ 0.05 versus unstimulated cells

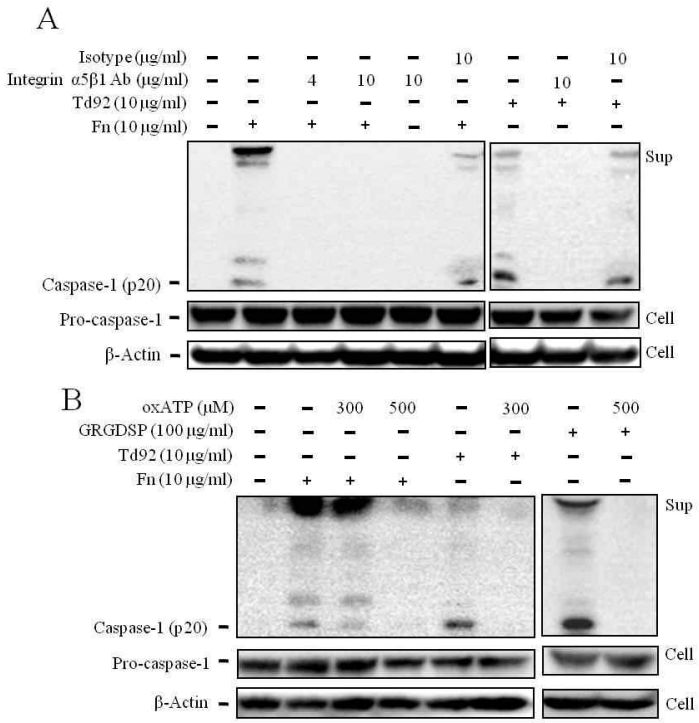

Figure 46. Interaction between Fibronectin/RGD and integrin α5β1 induces NLRP3 activation. THP-1 cells were pretreated with an integrin α5β1 Ab (4 and 10 μg/ml) or the anti-mouse IgG_1 isotype control (10 μg/ml) for 1 h (A) or oxATP (300 and 500 μM) for 30 min (B) prior to stimulation with fibronectin (Fn), GRGDSP, or Td92 for 6 h. Caspase-1 in the culture supernatants (sup) and procaspase-1 and β-Actin in the cell lysates (cell) were detected by immunoblotting.

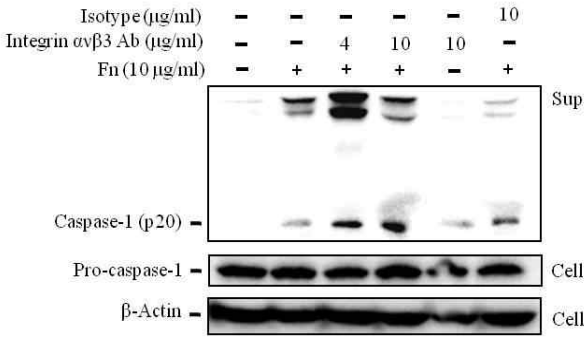

Figure 47. The integrin αvβ3 Ab does not inhibit fibronectin-induced caspase-1 activation. THP-1 cells were pretreated with an integrin αvβ3 Ab (4 and 10 μg/ml) or the anti-mouse IgG_1 isotype control (10 μg/ml) for 1 h prior to stimulation with fibronectin (Fn) for 6 h. Caspase-1 in the culture supernatants (sup) and procaspase-1 and β-Actin in the cell lysates (cell) were detected by immunoblotting.

3.2.9. NF-κB activation by Td92 for the proIL-1β expression and NLRP3 activation

These results suggest that the binding of Td92 to cell membrane integrin α5β1 is a critical step for NLRP3 inflammasome activation via ATP release, which causes K^+ efflux. Because anti-human integrin α5β1 Ab also reduces the expression of proIL-1β induced by Td92, NF-κB and MAP kinase inhibitors were used to determine whether these signaling pathways are involved in proIL-1β expression following Td92 binding to integrin. The induction of proIL-1β expression by Td92 was inhibited by pretreatment of the cells with inhibitors of NF-κB (TPCK and BAY-117082) and MAP kinases, including p38 (SB202190 and SB203580), ERK (PD98059), and JNK (SP600125) (Fig. 48A). Pretreatment of the cells with the integrin α5β1 Ab markedly inhibited IκBα degradation and reduced the phosphorylation of p38, ERK, and JNK (Fig. 48B). NF-κB translocation into the nucleus using NF-κB p65 Ab was observed by confocal microscopy in the cells treated with Td92, *T. denticola*, LPS (a positive control), or TNF-α (a positive control). PP4, used as a negative control, did not induce NF-κB translocation (Fig. 49A). To assess the inhibitory effect of the integrin α5β1 Ab and oxATP, the number of cells with NF-κB translocation were counted following pretreatment of THP-1 cells with the integrin α5β1 Ab for 1 h or oxATP for 30 min prior to treatment with Td92 or *T. denticola* for 1 h. The integrin α5β1 Ab and oxATP significantly reduced the induction of NF-κB translocation by Td92 or *T. denticola*, but not by LPS (Fig. 49B and C). The integrin α5β1 Ab and oxATP did not inhibit LPS-induced proIL-1β expression (Fig. 50A and B).

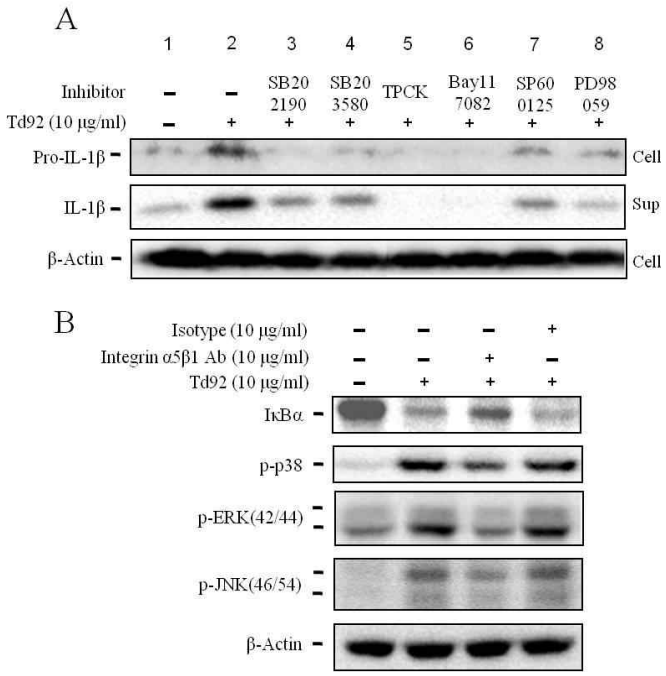

Figure 48. NF-κB and MAP kinase signaling pathways are involved in proIL-1β expression following Td92 binding to integrin. THP-1 cells were pretreated with various inhibitors (Lanes: 3, SB202190 20 μM; 4, SB203580 30 μM; 5, TPCK 30 μM; 6, BAY-117082 10μM; 7, SP600125 20 μM; 8, PD98059 50 μM) for 30 min prior to stimulation with Td92 for 6 h. IL-1β in the culture supernatants (sup) and proIL-1β and β-Actin in the cell lysates (cell) were detected by immunoblotting (A). THP-1 cells were pretreated with an integrin α5β1 Ab (10 μg/ml) or the anti-mouse IgG_1 isotype control (10 μg/ml) for 1 h prior to stimulation with Td92 for 30 min. The cell lysates were subjected to immunoblotting for IκBα degradation and MAPK phosphorylation (B).

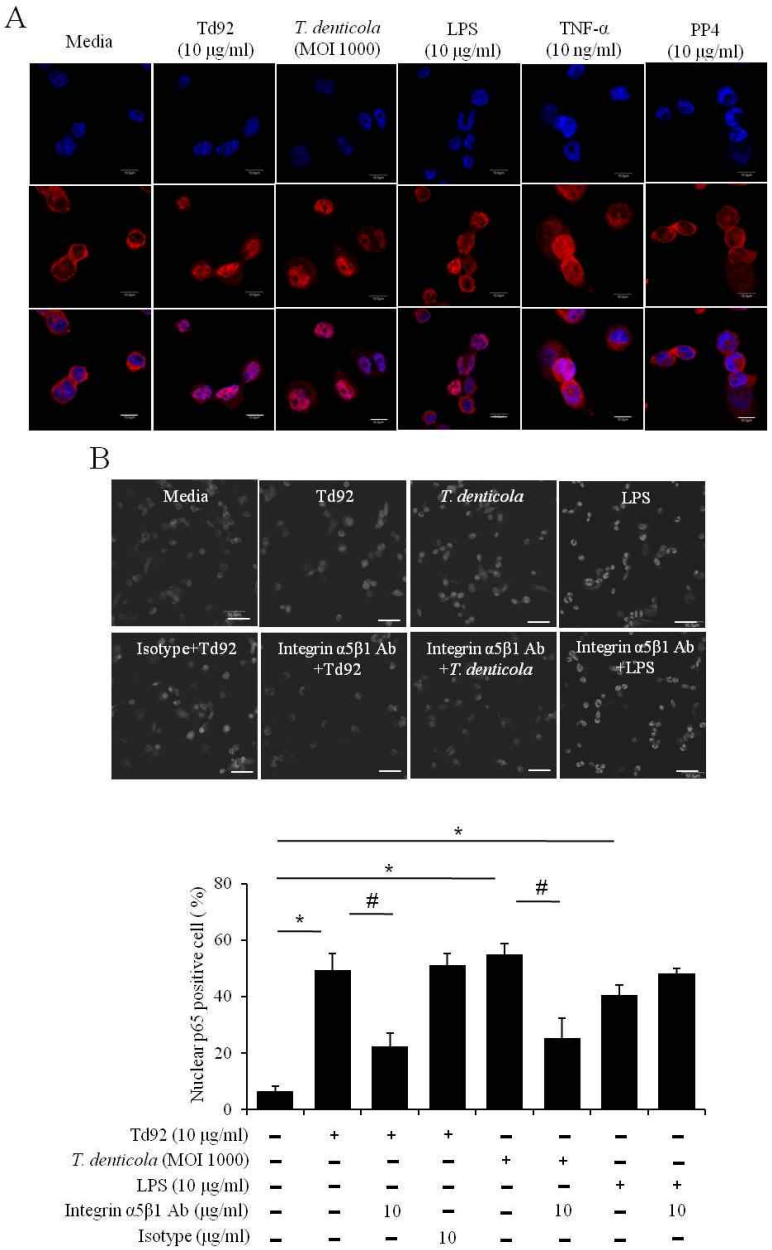
A
Media
Td92 (10 μg/ml)
T. denticola (MOI 1000)
LPS (10 μg/ml)
TNF-α (10 ng/ml)
PP4 (10 μg/ml)
B
Media
Td92
T. denticola
LPS
Isotype+Td92
Integrin α5β1 Ab +Td92
Integrin α5β1 Ab +T. denticola
Integrin α5β1 Ab +LPS
Nuclear p65 positive cell (%)
0
20
40
60
80
*
#
Td92 (10 μg/ml)
T. denticola (MOI 1000)
LPS (10 μg/ml)
Integrin α5β1 Ab (μg/ml)
Isotype (μg/ml)

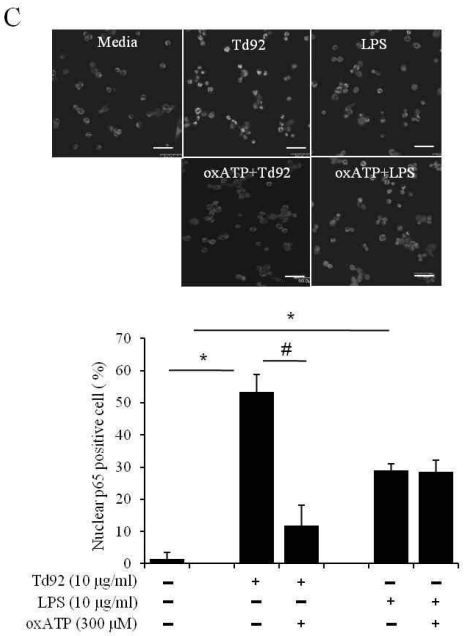

Figure 49. Td92 and *T. denticola* binding to integrin α5β1 induces NF-κB translocation. THP-1 cells were stimulated with Td92, *T. denticola*, LPS, TNF-α, or PP4 for 1 h, and NF-κB localization was detected using a NF-κB p65 Ab and a Cy3-conjugated secondary Ab with nuclear staining with Hoechst 33342 (A-C). NF-κB translocation into the nucleus of the cells was observed using confocal laser scanning microscopy (A). The number of cells positive for NF-κB activation after pretreatment with the integrin α5β1 Ab (B, 10 μg/ml) or oxATP (C, 300 μM) was counted out of a total of at least 500 cells with the NIH Image J software, and the data are presented as the means ± SD of one representative experiment of three performed in triplicate. $^{*}p < 0.05$ versus unstimulated cells; $^{\#}p < 0.01$ versus Td92 or *T. denticola*-treated cells (B-C) Scale bars represent 10 μm in (A) and 50 μm in (B-C).

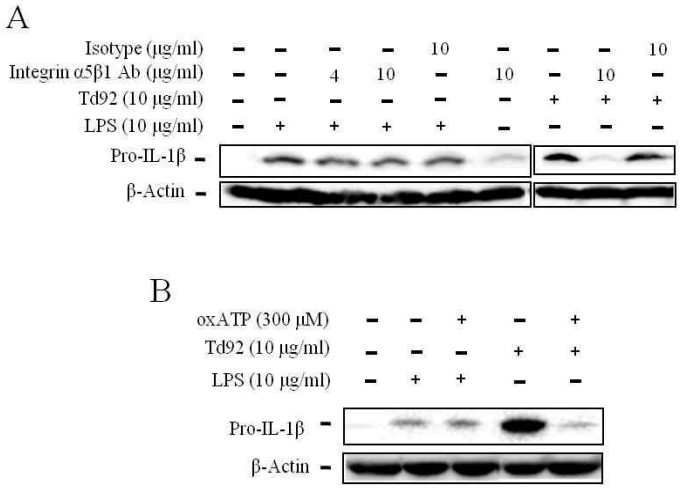

Figure 50. Integrin α5β1 Ab and oxATP did not affect LPS-induced proIL-1β expression. THP-1 cells were pretreated with an integrin α5β1 Ab (4 and 10 μg/ml), the anti-mouse IgG_1 isotype control (10 μg/ml), or oxATP (300 μM) for 30 min (B) or 1 h (A) prior to stimulation with LPS or Td92 for 6 h. ProIL-1β and β-Actin in the cell lysates were detected by immunoblotting (A-B).

Because the integrin α5β1 Ab and oxATP reduced both the caspase-1 activation and the proIL-1β expression induced by Td92 and because the NF-κB pathway has an important role in Td92-induced proIL-1β expression, the NF-κB pathway was tested for its involvement in the Td92-induced caspase-1 activation. As shown in Fig. 51A, Td92-induced caspase-1 activation was reduced by a specific NF-κB inhibitor, Bay-117082, suggesting a key role of NF-κB for IL-1β production and secretion. Proinflammatory stimuli, including TLR ligands (LPS, Pam3CSK4, and poly(I:C)) and TNF-α, have been reported to induce NLRP3 expression, which is thought to be a limiting factor for NLRP3 activation and to be mediated by NF-κB activation [64]. Td92 induced NLRP3 expression, and this was inhibited by an NF-κB inhibitor that was also tested. Td92 induced NLRP3 expression at the gene (Fig. 51B) and protein (Fig. 51C) levels, and this induction was inhibited by the specific NF-κB inhibitor Bay-117082. Td92-induced NLRP3 expression was also reduced by incubation with an integrin α5β1 Ab or oxATP (Fig. 51C). These results indicate that Td92 fulfills all of the requirements for the activation of the NLRP3 inflammasome and IL-1β secretion by priming the cell through integrin α5β1 and NF-κB activation. Marginal upregulation of NLRP3 expression was observed when the cells were treated with fibronectin (Fig. 51C). Although TLR4 is not involved in Td92-induced proIL-1β expression, further experiments were performed to determine whether any TLRs could be primed with Td92 to induce NF-κB activation and proIL-1β expression. Because TLR signaling is transmitted through the adaptor proteins myeloid differentiation factor 88 (MyD88) and/or Toll/IL-1 receptor domain-containing adapter inducing interferon-

β (TRIF) to activate NF-κB, the THP-1 cells transfected with siRNA specific for MyD88 or TRIF were treated with Td92 or LPS. MyD88 or TRIF knockdown significantly inhibited LPS-induced NF-κB translocation into the nucleus, but it did not affect Td92-induced NF-κB translocation (Fig. 52A). To examine the effect of MyD88 or TRIF knockdown on Td92-induced proIL-1β expression, the effect of the knockdown of these genes on Td92-induced proIL-1β expression was also observed. Td92-induced proIL-1β expression was not changed by MyD88 or TRIF knockdown, whereas LPS-induced proIL-1β expression was markedly decreased (Fig. 52B). These results exclude the involvement of any TLRs in Td92-induced NF-κB activation and proIL-1β expression.

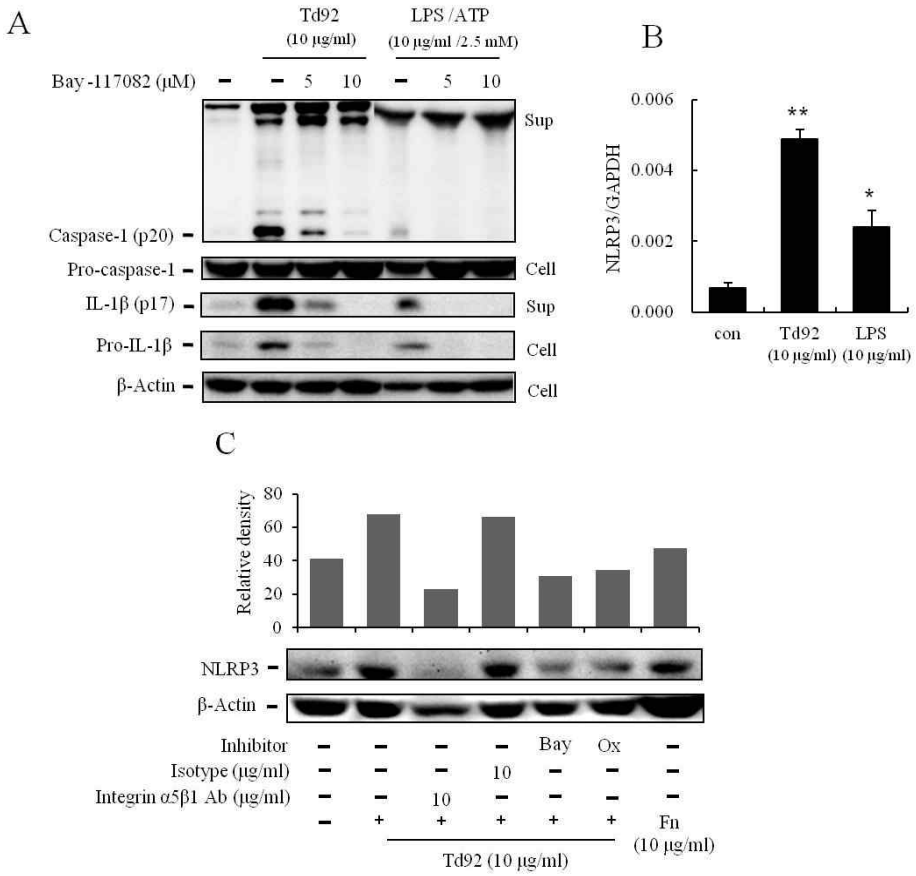

Figure 51. Priming of the cells by Td92 through integrin α5β1 and NF-κB activation fulfills the activation of NLRP3 inflammasome. THP-1 cells were pretreated with Bay-117082 for 30 min before stimulation with Td92 and LPS for 6 h. LPS-stimulated cells were pulsed with 2.5 mM ATP for 30 min. Caspase-1 and IL-1β in the culture supernatants (sup) and procaspase-1, proIL-1β, and β-Actin in the cell lysates (cell) were detected by immunoblotting (A). THP-1 cells were stimulated with Td92 or LPS for 4 h. The cells were subjected to RNA extraction followed by real-time qPCR to detect NLRP3 mRNA expression. The real-time qPCR data are shown as the means ± SD of one representative experiment of three

performed in triplicate (B). THP-1 cells were pretreated with an integrin α5β1 Ab (10 μg/ml), the anti-mouse IgG_1 isotype control (10 μg/ml), Bay-117082 (Bay, 10 μM), or oxATP (Ox, 300 μM) for 30 min or 1 h prior to stimulation with Td92 (10 μg/ml) for 6 h. The cells were subjected to immunoblotting for the detection of NLRP3 expression. Fibronectin (Fn, 10 μg/ml)-stimulated cells were also included (C). $^{**}p < 0.01$ and $^{*}p < 0.05$ versus unstimulated cells (B).

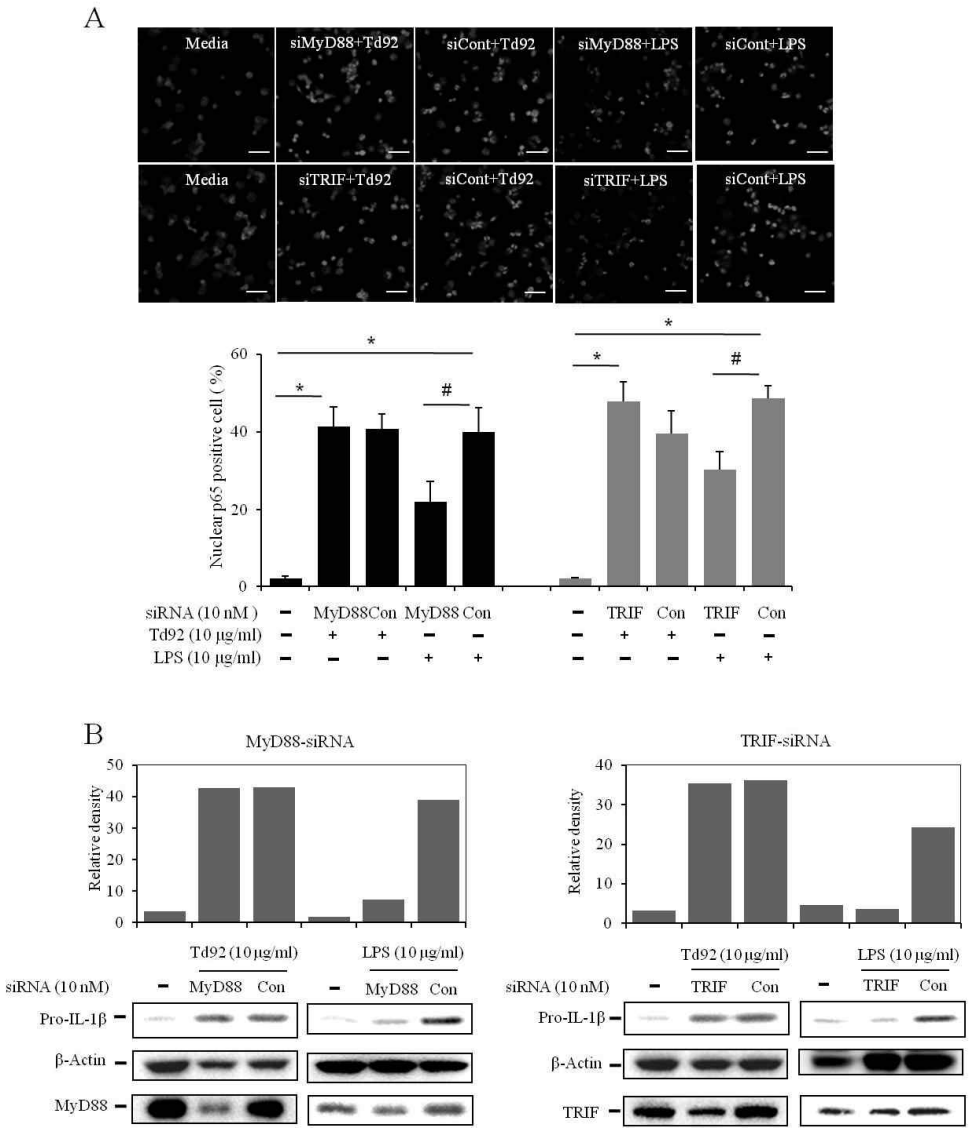

Figure 52. Knockdown of MyD88 or TRIF does not affect Td92-induced NF-κB activation and proIL-1β expression. The THP-1 cells transfected with MyD88 or TRIF siRNA were treated with Td92 or LPS for 1 h, and NF-κB localization was detected using a NF-κB p65 Ab and a Cy3-conjugated secondary Ab with nuclear staining with Hoechst 33342. NF-κB translocation into the nucleus

of the cells was observed by confocal microscopy. The number of cells positive for NF-κB activation was counted out of a total of at least 500 cells using the NIH Image J software, and the data are presented as the means ± SD of one representative experiment of three performed in triplicate. $^{*}p < 0.05$ versus unstimulated cells; $^{\#}p < 0.01$ versus control siRNA-transfected cells Scale bars represent 50 μm (A). The THP-1 cells transfected with MyD88 or TRIF siRNA were treated with Td92 or *E. coli* LPS for 6 h. Knockdown of MyD88 and TRIF by siRNA and the expression of proIL-1β, MyD88, TRIF, and β-Actin in cell lysates were detected by immunoblotting. The band intensities on the immunoblots were quantified using NIH Image J software and are presented as the relative ratio to β-Actin (B).

4. Discussion

Microbial genome projects have unraveled the genome sequences of an expanding number of pathogens, including major oral pathogens [1], and the comparison of genes between bacterial species allows for the determination of gene function by amino acid similarity and conserved functional domains. The information on bacterial genome sequences facilitates the elucidation of bacterial physiology, biosynthesis and metabolic pathways. With comparative genomics, it is also possible to determine the virulence factors involved in pathogenesis. The enormous diversity of oral treponemes, even within a single periodontitis patient, has been a roadblock to the study of their common pathogenicity. Recently, the whole genome sequence of *T. denticola*, the most intensively studied oral spirochete, has been deciphered [65]. Genomic information is being used to search for conserved surface antigens present in representative oral spirochetes associated with periodontitis and to examine their functional roles, thus leading to insights on a common pathogenesis that would be useful for developing of a strategy for growth inhibition or eradication. Identification and functional analysis of conserved OMPs are therefore important for understanding the common mechanisms of pathogenesis in the extremely diverse collection of oral spirochetes. In this study, highly conserved surface antigens of oral spirochetes that are homologous to Tp92 with an opsonic potential in *T. pallidum* [18] were identified and characterized for their virulence. The Tp92 homologs from oral spirochetes showed high homology with Tp92, and the antibody raised against Td92, a Tp92 homolog of *T. denticola*,

cross-reacted with the Tp92 homologs of *T. lecithinolyticum*, *T. maltophilum*, and *T. socranskii* subsp. *socranskii*. Td92 is an outer membrane protein with a surface-exposed epitope that could be detected using a Td92 Ab. The fact that anti-Td92 recognized other *Treponema* species included in this study suggests that the Tp92 homologs from oral spirochetes share a similar surface structural motif.

In spite of high homology with Tp92, the Tp92 homologs of oral spirochetes have distinct characteristics. First, the Tp92 homologs of oral spirochetes have no serine-rich region at the C-terminal, which is a signature sequence in the *T. pallidum* Tp92. The C-terminus of Tp92 encompassing the serine repeat signature sequence (245 aa) was not expressed in *E. coli*. However, the full length *tp92* gene homologs of oral spirochetes were expressed in *E. coli*, showing the expected molecular masses. Second, the calculated pI of the Tp92 homologs was different from that of Tp92. The pI of the Tp92 homologs was in the acidic range between 5.46-6.34, while the pI of Tp92 was 8.27. Third, a cysteine residue is absent in the Tp92 homologs of oral spirochetes, and only one is present in the case of *T. lecithinolyticum* and *T. maltophilum*, while three cysteine residues are present in Tp92, implying the possible formation of an intramolecular disulfide bond. It will be interesting to examine whether these differences are linked to distinct functions.

T. denticola, along with *Porphyromonas gingivalis* and *Tannerella forsythia*, belongs to the red cluster according to the classification by Socransky et al. [3], who defined bacterial groups in dental plaque biofilms with respect to their reciprocal association and sequential formation. The red complex produces

significant amounts of proteases, including trypsin-like peptidase activity, and is in contact with the gingival junctional epithelium. In this study, it has been observed that the Tp92 homologs adhered to epithelial cells, suggesting that the encoded proteins mediate the binding of *Treponema* cells to host cells and thus accelerate their pathologic effects. Several surface proteins of *T. denticola* have been reported to attach to host cells or extracellular matrix (ECM) proteins. The best studied of proteinis the 53-kDa Msp, which is able to bind epithelial cells, fibroblasts and ECM proteins, such as fibronectin, keratin, laminin, collagen, fibrinogen, hyaluronic acid, and heparin [13, 66]. CTLP has been demonstrated to bind to PDL epithelial cells [6] and to *P. gingivalis* fimbriae, implicating it in the coaggregation of *T. denticola* and *P. gingivalis* [67]. The leucine-rich repeat protein LrrA has been demonstrated to attach to human epithelial cells [68]. OppA (70 kDa) bound soluble plasminogen and fibronectin [14]. In the present study, Td92 significantly inhibited *T. denticola* adhesion to epithelial cells. This fact suggests that Td92 is a *T. denticola* adhesin.

The Tp92 homologs upregulated IL-1β, TNF-α, IL-6, IL-8, PGE_2, and MMP-9 in THP-1 cells. These factors are proinflammatory and osteoclastogenic factors, and they have been reported to be stimulated by periodontopathogens, including the red complex. IL-1β and TNF-α are representative proinflammatory cytokines associated with periodontal disease characterized by a loss of connective tissue attachment and bone resorption, leading to alveolar bone loss [69]. IL-1β is a potent stimulator of bone resorption and an inhibitor of bone formation that enhances osteoclast differentiation and acts as a survival factor for mature

osteoclasts [27, 70, 71]. It has been shown to activate RANKL in PDL cells [72]. TNF-α promotes the production of RANKL and macrophage colony-stimulating factor by stromal cells and induces osteoclast formation. In experimental periodontitis, IL-1 and TNF antagonists have been demonstrated to inhibit the inflammatory response and bone loss [69]. IL-6, together with IL-1β and TNF-α, is a major mediator of the host response to tissue destruction and bone resorption. IL-6 binds to its receptor, existing in either a membrane-bound form (CD126) or a soluble form (sIL-6R alpha). This complex subsequently binds to a signal transducing protein, gp130 [73], leading to upregulation of RANKL in osteoblasts, which is a key factor in osteoclastogenesis. IL-8 is a representative chemokine and leads inflammatory cells to infection sites, playing an important role in initiating the inflammatory reactions. PGE_2 stimulates osteoclastogenesis through stimulation of RANKL production, inhibition of osteoprotegerin secretion by osteoblasts, and stimulation of IL-6 production [74, 75]. PGE_2 was synergistically stimulated by IL-1 and TNF in human gingival fibroblasts [76]. MMP-9 is a zinc-dependent proteinase and has been demonstrated to play an important role in the bone resorption process by dissolving the bone matrix, releasing the chemotactic factor on osteoclasts, and activating the cytokines involved in bone resorption [77]. Although various periodontopathogens have been shown to induce all these host factors, only a few bacterial factors have been identified at the molecular level. LPS is a prominent molecule that induces proinflammatory cytokines and bone resorbing factors. LPS or LPS-like molecules of periodontopathogens have been demonstrated to modulate biological activities, including the upregulation of IL-1,

TNF-α, IL-6, IL-8, PGE_2 and MMP-9 in various host cell types [78-81]. These factors are found at significantly higher levels in the tissues and GCF of periodontitis patients than those of in healthy subjects [82, 83]. Among surface proteins, the outer membrane protein 100 of *Aggregatibacter* (*Actinobacillus*) *actinomycetemcomitans* and fimbrillin of *P. gingivalis* (41 and 67 kDa) have been demonstrated to induce proinflammatory cytokines in host cells, including epithelial cells and macrophages [84-86]. The 67-kDa *P. gingivalis* fimbriae protein induced osteoclast differentiation, and blocking of IL-1, TNF and IL-6 induced by the protein reduced osteoclast differentiation. Recently, it has been reported that the major surface protein MspTL of *T. lecithinolyticum* induced IL-1β, TNF-α, IL-6 and PGE_2 in THP-1 cells [15, 45]. Although the Tp92 homologs are not abundant surface proteins, such as Msp of *T. denticola* and MspTL of *T. lecithinolyticum*, when judged by SDS-PAGE profiles, they are widely distributed in oral spirochetes, and the coexistence of various species of oral spirochetes in a single patient or at a single site may result in the amplification of the cytopathological effects on host cells.

In this study, it has been demonstrated that the direct interaction of integrin α5β1 and *T. denticola* Td92, which is a bacterial surface protein of a periodontopathogen, induces NLRP3 activation in THP-1 cells and PBMC-derived macrophages, which have been well characterized in terms of inflammasome activation [56, 57]. Td92-induced caspase-1 activation caused pyroptosis, an inflammatory cell death. Although integrins are not conventional pathogen recognition receptors, as are TLRs, retinoic acid inducible gene I, NLRs, and C-

type lectins, many pathogens directly or indirectly exploit integrin α5β1 for adherence and invasion. Group A streptococcus, *Staphylococcus aureus*, and *E. coli* interact with integrin α5β1 via fibronectin to invade cells by actin rearrangement [87-89]. The type IV secretion system (T4SS) pilus-associated CagL of *Helicobacter pylori* binds to integrin α5β1 via its RGD motif [90]. However, CagY and CagA, which are components of the cag-T4SS, interact with β1 integrin independently of the RGD motif [91]. The *Orientia tsutsugamushi* outer membrane protein TSA56 interacts with integrin α5β1 via fibronectin for the invasion of host cells [92]. The bacterial surface of *Porphyromonas gingivalis*, a major periodontopathogen, binds to integrin α5β1 and is taken up into the cells via lipid rafts [93]. *P. gingivalis* type II fimbriae has a high affinity for integrin α5β1, causing marked adhesion of the bacteria to epithelial cells and high serum IL-1β levels in a mouse abscess model [94]. However, the role of integrin α5β1 in NLRP3 inflammasome activation has not yet been reported.

This study showed that fibronectin, a representative integrin ligand, and the RGD peptide also activate caspase-1 via interaction with integrin α5β1 and ATP release, as was shown for Td92-induced caspase-1 activation. Because Td92 does not contain an RGD-motif, this motif is not required for the activation of caspase-1 following the interaction of Td92 with integrin α5β1, indicating that the binding site for integrin α5β1 of Td92 is different from that of fibronectin or that of other RGD-containing proteins. Td92 can bind to cells via fibronectin, but this interaction does not seem to be critical for Td92-induced caspase-1 activation because a neutralizing anti-fibronectin Ab inhibited cell binding but not caspase-1

activation. Otherwise, the effect of Td92 on caspase-1 activation via fibronectin may be shielded by the direct interaction between Td92 and integrin α5β1. Further work to identify the sites through which Td92 binds to integrin α5β1 and fibronectin will yield new insight into the nature of the interaction between the integrin and its ligands that activates the NLRP3 inflammasome. Using the truncated Td92, it has been shown that the amino terminal half of Td92 possesses the activities for caspase-1 activation and proIL-1β expression.

Td92 binding alone without internalization leads to NLRP3 activation, and proIL-1β expression has been shown using cytochalasin D, which inhibits actin polymerization. Interestingly, the clustering of integrin α5β1 induced by Td92 was not blocked by cytochalasin D. Buensuceso et al. [95] showed that fibrinogen binding to CHO cells stably expressing integrin αIIbβ3 induces αIIbβ3 clustering, which is not inhibited by cytochalasin D. These results were interpreted to mean that the actin cytoskeleton imposes basal constraints on fibrinogen binding function, and prevention of actin polymerization releases those constraints and increases ligand binding. Stable interaction between integrin αvβ3 and vitronectin was observed in the absence of actin polymerization [96].

Inflammation is essential for host defense against infections, but the chronic or excessive production of IL-1β by dysregulation of the inflammasome caused by mutations in NLRP3 and P2X7 is associated with heritable and acquired inflammatory diseases, such as type 2 diabetes, gout, and cryopyrin-associated periodic syndromes, including familial cold autoinflammatory syndrome, Muckle-

Wells syndrome, and chronic infantile cutaneous neurological articular syndrome [35, 97-99]. IL-1β or IL-1β receptor antagonists are thus potential therapeutics for the treatment of inflammatory diseases through the targeting of the NLRP3 activation pathway [100]. IL-1β is a key mediator for gingival inflammation and is a strong enhancer of tissue levels of PGE_2 and TNF-α, leading to the degradation of the extracellular matrix of the periodontal tissues and alveolar bone, which are the characteristics of periodontitis [101]. Because IL-1β is tightly controlled by the separate regulation of transcription/translation and secretion, the simultaneous induction of proIL-1β and its maturation by Td92 could lead to uncontrollable inflammation. Td92 and homologous proteins are found in diverse oral *Treponema* species associated with periodontitis, and multiple *Treponema* species can be found in a single periodontitis patient or a single diseased site, implying that the coexistence of several *Treponema* species expressing Td92 homologous proteins could additively enhance IL-1β production, thus amplifying the cytopathological effects on host cells [102]. The significant reduction in *T. denticola*-induced IL-1β secretion upon the addition the integrin α5β1 Ab may indicate the specific contribution of Td92 to the overall *T. denticola*-induced IL-1β production. IL-1β is found at significantly higher levels in periodontal tissue and in the gingival crevicular fluid of periodontitis patients compared to healthy subjects, and its levels are markedly reduced after periodontal therapy [31, 103]. There is also a positive correlation between an IL-1β gene polymorphism and increased risk of developing periodontitis [104, 105].

ProIL-1β induction by microbial stimuli usually involves NF-κB activation, which is independent of inflammasome activation. However, a recent report demonstrated that proIL-1β induction also potentiated NLRP3 inflammasome activity by the NF-κB-dependent induction of NLRP3 in murine macrophages [64]. According to this report, the level of NLRP3 expression was critical for the activation of NLRP3 by its activators, including ATP, pore-forming toxins, and crystalline activators. NLRP3 activators alone cannot activate NLRP3 without the priming of the cells to stimulate NLRP3 transcription via transcriptionally active signaling receptors, such as TLRs and TNFR, which is dependent on the NF-κB signaling pathway. Consistent with this study, Td92 induced proIL-1β and NLRP3 expression via NF-κB activity, which also affected caspase-1 activation. NLRP3 mRNA expression in gingival tissues has been shown to be significantly higher in patients with gingivitis, chronic periodontitis, and generalized aggressive periodontitis than in periodontally healthy subjects, and the levels of NLRP3 mRNA positively correlate with IL-1β mRNA [106]. Upon the infection of bone marrow-derived murine macrophages by *Vibrio vulnificus* or *Vibrio cholerae*, NF-κB activation has been shown to be required for NLRP3 activation [107]. NF-κB activation for NLRP3 activation is TLR-dependent in *V. vulnificus* and TLR-independent in *V. cholera*. However, the upregulation of NLRP3 expression was not observed with caspase-1 activation by these pathogens. Notably, ATP release was not found to be involved in NLRP3 activation by *Vibrio* infection. Td92-induced NF-κB activation is TLR-independent.

The involvement of integrin α5β1 in the transcriptional regulation of IL-1β has been demonstrated in human promonocytic U937 cells through the activation of protein kinase C and the induction of AP-1 but not NF-κB [108]. Soluble fibronectin or a 120-kDa RGD-containing peptide obtained by chymotrypsin digestion of fibronectin induced IL-1β transcription via integrin α5β1 in U937 cells, and an RGD peptide inhibited fibronectin-induced IL-1β gene expression. Furthermore, an integrin α5 Ab alone induced IL-1β gene transcription, but the antibody did not enhance IL-1β expression when the cells were treated with fibronectin. Chen et al. [109] reported that RGD peptides, such as linear Arg-Gly-Asp-Ser (RGDS) and cyclic Arg-Gly-Asp-Phe (RGDF), induced the mRNA expression of the interleukin-1β-converting enzyme (caspase-1) and apoptosis in the glomerular mesangial cells of adult human kidneys. Taken together, these results imply that integrin priming could lead to the induction of IL-1β expression. Although fibronectin and the RGD peptide induced caspase-1 activation in this study, they did not induce proIL-1β. The discrepancy between the present results and the results observed in previous studies using U937 cells and glomerular mesangial cells may be attributable to the different types of cells that were used or different doses of fibronectin used for cell treatment.

A diverse variety of bacteria induce NLRP3 activation in the presence of ATP [110]. For example, *P. gingivalis* induces IL-1β synthesis in primary gingival epithelial cells, but IL-1β secretion via NLRP3 activation by the bacteria is dependent on the addition of ATP [58]. In contrast, Td92 triggers the release of ATP, which causes NLRP3 activation. The integrin α5β1 Ab inhibited Td92-

induced ATP. ATP release induced by hypotonic stress has also been shown to be inhibited by the integrin α5β1 Ab in human umbilical cord vein endothelial cells, whereas ATP release induced by lysophosphatidic acid in the same cells was not affected by the Ab [111], even though hypotonic stress and lysophosphatidic acid use the same signaling molecules, RhoA/Rho-kinase and FAK/paxillin, to induce ATP release. This is because lysophosphatidic acid has a specific receptor that is not integrin α5β1. These results imply that integrin α5β1 binding is one mechanism for ATP release.

Solini et al. [112] reported that the increased P2X7 reactivity and increased ATP release of fibroblasts from type 2 diabetes patients enhanced the intracellular accumulation and the extracellular release of fibronectin. Additionally, ATP caused increased YO-PRO uptake, cell swelling and shrinkage in the fibroblasts of type 2 diabetes patients compared with cells from healthy subjects. Taken together, these results imply a possible connection between fibronectin and caspase-1 activation as well as cell death. However, a clear connection between these three components has been missing. In this study, the role of fibronectin in caspase-1 activation has been elucidated by demonstrating that the interaction between fibronectin and integrin α5β1 resulted in ATP release, which can cause caspase-1 activation and lead to cell death. It has been observed that fibronectin increased ATP release and vice versa. ATP release in response to fibronectin might be an autocrine or paracrine signal to stimulate further fibronectin expression, thereby resulting in enhanced caspase-1 activation.

Caspase-1 activation by Td92 is associated with membrane pore formation and the release of LDH, which are characteristics of pyroptosis, a proinflammatory cell death. Pyroptosis is an innate immune response to efficiently clear intracellular pathogens, including *S. typhimurium* and *Legionella pneumophila*, in a manner independent of proinflammatory cytokines, such as IL-1β and IL-18 [61]. Td92-induced cell death is inhibited by the inhibitors of Td92-induced NLRP3 activation. *T. denticola* is not an intracellular organism, and persistent stimulation of cells with the *T. denticola* surface protein Td92 induces the related processes of IL-1β secretion and cell death, contributing to chronic nature of periodontitis.

Currently, three models for NLRP3 activation have been proposed. In the channel model, the agonists activate the P2X7 ATP-gated ion channel, which triggers K^+ efflux from the cells and recruits the pore-forming pannexin 1 hemichannel. The agonists enter the cells through the pannexin 1 hemichannel and interact with NLRP3 in the cytoplasm [110, 113, 114]. In the lysosome rupture model, large particulate agonists, such as alum and silica, are inefficiently cleared from the host after phagocytosis, and the remaining particles induce phagosomal destabilization and lysosomal rupture, which allows the activation of NLRP3 via cathepsin B release [115, 116]. Finally, in the ROS model, all of the NLRP3 agonists trigger the generation of a common component, possibly ROS, which leads to NLRP3 activation [56, 57, 59, 117, 118]. Because Td92-induced NLRP3 activation includes ATP release from the host cells and K^+ efflux, the channel model should be considered. However, the interaction of Td92 with a cell membrane receptor was sufficient to signal NLRP3 inflammation activation, and

Td92 internalization into the cytosol is not necessary. Therefore, the third model could possibly apply to Td92-induced NLRP3 activation. Td92-induced ROS have been observed. Although the activation of caspase-1 by Td92 is completely negated by the ATP antagonist oxATP, ROS production was only partially reduced by this compound. The elucidation of the mechanisms of NLRP3 activation via integrin priming to NF-κB activation may provide new insights into the process of NLRP3-dependent caspase-1 activation.

In summary, Tp92 homologs are surface-exposed outer membrane proteins that are common among the four oral *Treponema* species strongly associated with periodontitis. These proteins have the potential to bind to host cells and stimulate host factors that contribute to inflammation and osteoclastogenesis, which are major characteristics of periodontitis. As shown in Fig. 53, Td92 of *T. denticola* directly binds to integrin α5β1, which is a heterodimeric cell membrane receptor, leading to the activation of signaling pathways, such as the NF-κB pathway and the MAPK pathway, as well as ATP release. Activation of NF-κB and MAPK stimulate the expression of the IL-1β and NLRP3 genes, corresponding to the "signal 1". ATP released by Td92 binds to the P2X7 receptor, which causes K^+ efflux. Assembly of the NLRP3 inflammasome due to the K^+ efflux results in autocatalytic cleavage of procaspase-1 to active caspase-1, corresponding to "signal 2". The active caspase-1 can convert proIL-1β to its bioactive form and form pores in the plasma membrane. Thus, the active IL-1β can be secreted into the extracellular space. The simultaneous activation of IL-1β transcription and NLRP3

activation is required for IL-1β secretion, which can lead to uncontrolled IL-1β levels that may exaggerate inflammation, a characteristic of periodontitis.

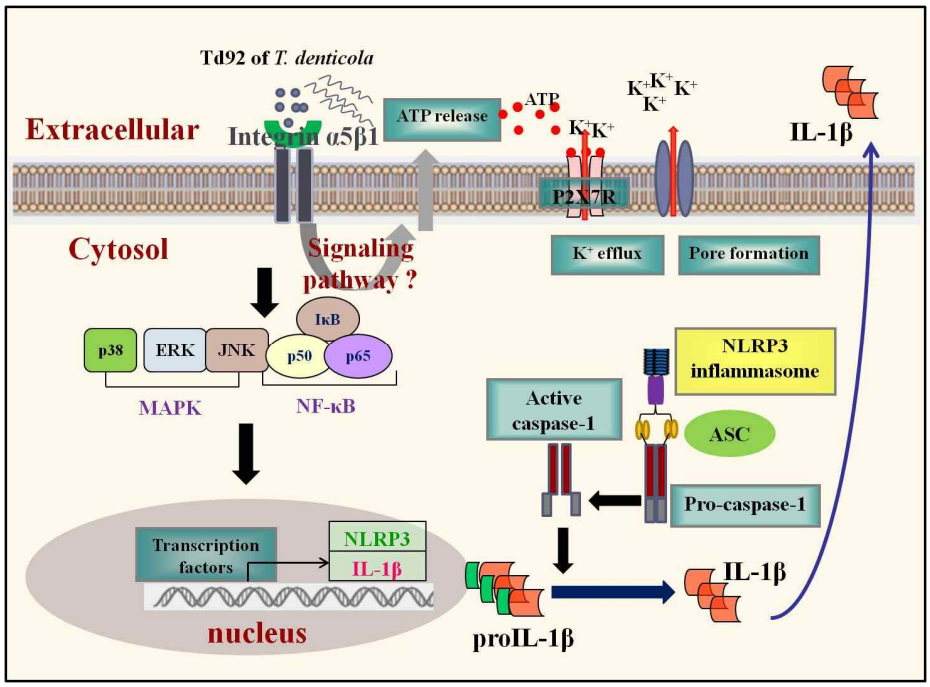

Figure 53. Integrin α5β1 is a principle receptor for the NLRP3 activation and IL-1β transcription by *T. denticola* Td92.

5. Conclusion

The coexistence of various *Treponema* species in a single periodontal pocket may result in an accumulation of multiple Tp92 homologs and may amplify the pathological effects in periodontitis. The role of integrin α5β1 in NLRP3 activation by Td92 of *T. denticola* may provide new insight into understanding the activation and regulation of the inflammasome. Strategies that control NLRP3 activation via integrin α5β1 and related signaling molecules may have potential for controlling periodontal disease.

6. Referneces

1. Ellen RP, Galimanas VB: **Spirochetes at the forefront of periodontal infections**. *Periodontol 2000* 2005, **38**:13-32.
2. Moter A, Riep B, Haban V, Heuner K, Siebert G, Berning M, Wyss C, Ehmke B, Flemming TF, Goebel UB: **Molecular epidemiology of oral treponemes in patients with periodontitis and in periodontitis-resistant subjects**. *J Clin Microbiol* 2006, **44**(9):3078-3085.
3. Socransky SS, Haffajee AD, Cugini MA, Smith C, Kent RL: **Microbial complexes in subgingival plaque**. *J Clin Periodontol* 1998, **25**(2):134-144.
4. Dewhirst FE, Tamer MA, Ericson RE, Lau CN, Levanos VA, Boches SK, Galvin JL, Paster BJ: **The diversity of periodontal spirochetes by 16S rRNA analysis**. *Oral Microbiol Immunol* 2000, **15**(3):196-202.
5. Asai Y, Jinno T, Ogawa T: **Oral treponemes and their outer membrane extracts activate human gingival epithelial cells through toll-like receptor 2**. *Infect Immun* 2003, **71**(2):717-725.
6. Fenno JC, Hannam PM, Leung WK, Tamura M, Uitto VJ, McBride BC: **Cytopathic effects of the major surface protein and the chymotrypsinlike protease of *Treponema denticola***. *Infect Immun* 1998, **66**(5):1869-1877.
7. Lee SH, Kim JS, Jun HK, Lee HR, Lee D, Choi BK: **The Major Outer Membrane Protein of a Periodontopathogen Induces IFN-β and IFN-Stimulated Genes in Monocytes via Lipid Raft and TANK-Binding Kinase 1/IFN Regulatory Factor-3**. *The Journal of Immunology* 2009, **182**(9):5823-5835.
8. Miyamoto M, Ishihara K, Okuda K: **The *Treponema denticola* surface protease dentilisin degrades interleukin-1β (IL-1β), IL-6, and tumor necrosis factor alpha**. *Infect Immun* 2006, **74**(4):2462-2467.

9. Nussbaum G, Ben-Adi S, Genzler T, Sela M, Rosen G: **Involvement of Toll-Like Receptors 2 and 4 in the Innate Immune Response to *Treponema denticola* and Its Outer Sheath Components**. *Infect Immun* 2009, **77**(9):3939-3947.

10. Chan ECS, McLaughlin R: **Taxonomy and virulence of oral spirochetes**. *Oral Microbiol Immun* 2000, **15**(1):1-9.

11. Sela MN: **Role of *Treponema denticola* in periodontal diseases**. *Crit Rev Oral Biol M* 2001, **12**(5):399-413.

12. Batista da Silva AP, Lee W, Bajenova E, McCulloch CA, Ellen RP: **The major outer sheath protein of *Treponema denticola* inhibits the binding step of collagen phagocytosis in fibroblasts**. *Cellular microbiology* 2004, **6**(5):485-498.

13. Edwards AM, Jenkinson HF, Woodward MJ, Dymock D: **Binding properties and adhesion-mediating regions of the major sheath protein of *Treponema denticola* ATCC 35405**. *Infect Immun* 2005, **73**(5):2891-2898.

14. Fenno JC, Tamura M, Hannam PM, Wong GWK, Chan RA, McBride BC: **Identification of a *Treponema denticola* OppA homologue that binds host proteins present in the subgingival environment**. *Infect Immun* 2000, **68**(4):1884-1892.

15. Lee SH, Kim KK, Choi BK: **Upregulation of intercellular adhesion molecule 1 and proinflammatory cytokines by the major surface proteins of *Treponema maltophilum* and *Treponema lecithinolyticum*, the phylogenetic group IV oral spirochetes associated with periodontitis and endodontic infections**. *Infect Immun* 2005, **73**(1):268-276.

16. Mathers DA, Leung WK, Fenno JC, Hong Y, McBride BC: **The major surface protein complex of *Treponema denticola* depolarizes and induces ion channels in HeLa cell membranes**. *Infect Immun* 1996, **64**(8):2904-2910.

17. Wang Q, Ko KS, Kapus A, McCulloch CAG, Ellen RP: **A spirochete surface protein uncouples store-operated calcium channels in fibroblasts - A novel cytotoxic mechanism**. *J Biol Chem* 2001, **276**(25):23056-23064.

18. Cameron CE, Lukehart SA, Castro C, Molini B, Godornes C, Van Voorhis WC: **Opsonic potential, protective capacity, and sequence conservation of the *Treponema pallidum* subspecies *pallidum* Tp92**. *J Infect Dis* 2000, **181**(4):1401-1413.

19. Van Voorhis WC, Barrett LK, Lukehart SA, Schmidt B, Schriefer M, Cameron CE: **Serodiagnosis of syphilis: Antibodies to recombinant Tp0453, Tp92, and Gpd proteins are sensitive and specific indicators of infection by *Treponema pallidum***. *J Clin Microbiol* 2003, **41**(8):3668-3674.

20. Reumann S, Davila-Aponte J, Keegstra K: **The evolutionary origin of the protein-translocating channel of chloroplastic envelope membranes: Identification of a cyanobacterial homolog**. *P Natl Acad Sci USA* 1999, **96**(2):784-789.

21. Voulhoux R, Bos MP, Geurtsen J, Mols M, Tommassen J: **Role of a highly conserved bacterial protein in outer membrane protein assembly**. *Science* 2003, **299**(5604):262-265.

22. Genevrois S, Steeghs L, Roholl P, Letesson JJ, van der Ley P: **The Omp85 protein of *Neisseria meningitidis* is required for lipid export to the outer membrane**. *Embo J* 2003, **22**(8):1780-1789.

23. Thomas KL, Leduc I, Olsen B, Thomas CE, Cameron DW, Elkins C: **Cloning, overexpression, purification, and immunobiology of an 85-kilodalton outer membrane protein from *Haemophilus ducreyi***. *Infect Immun* 2001, **69**(7):4438-4446.

24. Adler B, Bulach D, Chung J, Doughty S, Hunt M, Rajakumar K, Serrano M, van Zanden A, Zhang YM, Ruffolo C: **Candidate vaccine antigens and genes in *Pasteurella multocida***. *J Biotechnol* 1999, **73**(2-3):83-90.

25. Loosmore SM, Yang YP, Coleman DC, Shortreed JM, England DM, Klein MH: **Outer membrane protein D15 is conserved among *Haemophilus influenzae* species and may represent a universal protective antigen against invasive disease**. *Infect Immun* 1997, **65**(9):3701-3707.

26. Horwood NJ, Elliott J, Martin TJ, Gillespie MT: **Osteotropic agents regulate the expression of osteoclast differentiation factor and osteoprotegerin in osteoblastic stromal cells**. *Endocrinology* 1998, **139**(11):4743-4746.

27. Jimi E, Nakamura I, Duong LT, Ikebe T, Takahashi N, Rodan GA, Suda T: **Interleukin 1 induces multinucleation and bone-resorbing activity of osteoclasts in the absence of osteoblasts/stromal cells**. *Experimental cell research* 1999, **247**(1):84-93.

28. Socransky SS, Haffajee AD, Smith C, Duff GW: **Microbiological parameters associated with IL-1 gene polymorphisms in periodontitis patients**. *J Clin Periodontol* 2000, **27**(11):810-818.

29. Bodet C, Chandad F, Grenier D: **Inflammatory responses of a macrophage/epithelial cell co-culture model to mono and mixed infections with *Porphyromonas gingivalis*, *Treponema denticola*, and *Tannerella forsythia***. *Microbes Infect* 2006, **8**(1):27-35.

30. Ferreira Jr SB, Trombone APF, Repeke CE, Cardoso CR, Martins Jr W, Santos CF, Trevilatto PC, Ávila-Campos MJ, Campanelli AP, Silva JS: **An interleukin-1β (IL-1β) single-nucleotide polymorphism at position 3954 and red complex**

periodontopathogens independently and additively modulate the levels of IL-1β in diseased periodontal tissues. *Infect Immun* 2008, **76**(8):3725-3734.

31. Goutoudi P, Diza E, Arvanitidou M: **Effect of periodontal therapy on crevicular fluid interleukin-1β and interleukin-10 levels in chronic periodontitis**. *Journal of dentistry* 2004, **32**(7):511-520.

32. Schroder K, Tschopp J: **The inflammasomes**. *Cell* 2010, **140**(6):821-832.

33. Benko S, Philpott DJ, Girardin SE: **The microbial and danger signals that activate Nod-like receptors**. *Cytokine* 2008, **43**(3):368-373.

34. Maedler K, Sergeev P, Ris F, Oberholzer J, Joller-Jemelka HI, Spinas GA, Kaiser N, Halban PA, Donath MY: **Glucose-induced beta cell production of IL-1β contributes to glucotoxicity in human pancreatic islets**. *J Clin Invest* 2002, **110**(6):851-860.

35. Mariathasan S, Weiss DS, Newton K, McBride J, O'Rourke K, Roose-Girma M, Lee WP, Weinrauch Y, Monack DM, Dixit VM: **Cryopyrin activates the inflammasome in response to toxins and ATP**. *Nature* 2006, **440**(7081):228-232.

36. Marina-Garcia N, Franchi L, Kim YG, Miller D, McDonald C, Boons GJ, Nunez G: **Pannexin-1-mediated intracellular delivery of muramyl dipeptide induces caspase-1 activation via cryopyrin/NLRP3 independently of Nod2**. *J Immunol* 2008, **180**(6):4050-4057.

37. Martinon F, Mayor A, Tschopp J: **The Inflammasomes: Guardians of the Body**. *Annu Rev Immunol* 2009, **27**:229-265.

38. Martinon F, Pétrilli V, Mayor A, Tardivel A, Tschopp J: **Gout-associated uric acid crystals activate the NALP3 inflammasome**. *Nature* 2006, **440**(7081):237-241.

39. Yamasaki K, Muto J, Taylor KR, Cogen AL, Audish D, Bertin J, Grant EP, Coyle AJ, Misaghi A, Hoffman HM, Richard LG: **NLRP3/Cryopyrin Is Necessary for Interleukin-1β (IL-1β) Release in Response to Hyaluronan, an Endogenous Trigger of Inflammation in Response to Injury**. *J Biol Chem* 2009, **284**(19):12762-12771.

40. Franchi L, Eigenbrod T, Munoz-Planillo R, Nunez G: **The inflammasome: a caspase-1-activation platform that regulates immune responses and disease pathogenesis**. *Nat Immunol* 2009, **10**(3):241-247.

41. Arnaout MA, Mahalingam B, Xiong JP: **Integrin structure, allostery, and bidirectional signaling**. *Annu Rev Cell Dev Bi* 2005, **21**:381-410.

42. Wyss C, Choi BK, Schupbach P, Guggenheim B, Gobel UB: ***Treponema maltophilum* sp. nov., a small oral spirochete isolated from human periodontal lesions**. *International journal of systematic bacteriology* 1996, **46**(3):745-752.

43. Choi BK, Jung JH, Suh HY, Yoo YJ, Cho KS, Chai JK, Kim CK: **Activation of matrix metalloproteinase-2 by a novel oral spirochetal species *Treponema lecithinolyticum***. *J Periodontol* 2001, **72**(11):1594-1600.

44. Han SH, Kim JH, Martin M, Michalek SM, Nahm MH: **Pneumococcal lipoteichoic acid (LTA) is not as potent as staphylococcal LTA in stimulating Toll-like receptor 2**. *Infect Immun* 2003, **71**(10):5541-5548.

45. Jun HK, Lee HR, Lee SH, Choi BK: **Mapping of the proinflammatory domains of MspTL of *Treponema lecithinolyticum***. *Microbiology* 2007, **153**(Pt 8):2386-2392.

46. Magalhaes PO, Lopes AM, Mazzola PG, Rangel-Yagui C, Penna TCV, Pessoa A: **Methods of endotoxin removal from biological preparations: a review**. *J Pharm Pharm Sci* 2007, **10**(3):388-404.

47. Rosen G, Naor R, Kutner S, Sela MN: **Characterization of Fibrinolytic-Activities of *Treponema denticola***. *Infect Immun* 1994, **62**(5):1749-1754.

48. Skare JT, Shang ES, Foley DM, Blanco DR, Champion CI, Mirzabekov T, Sokolov Y, Kagan BL, Miller JN, Lovett MA: **Virulent-Strain Associated Outer-Membrane Proteins of *Borrelia-Burgdorferi***. *J Clin Invest* 1995, **96**(5):2380-2392.

49. Ji S, Hyun J, Park E, Lee BL, Kim KK, Choi Y: **Susceptibility of various oral bacteria to antimicrobial peptides and to phagocytosis by neutrophils**. *Journal of periodontal research* 2007, **42**(5):410-419.

50. Livak KJ, Schmittgen TD: **Analysis of relative gene expression data using real-time quantitative PCR and the 2-Delta/Delta CT method**. *methods* 2001, **25**(4):402-408.

51. Hamada K, Takuwa N, Yokoyama K, Takuwa Y: **Stretch activates jun N-terminal kinase/stress-activated protein kinase in vascular smooth muscle cells through mechanisms involving autocrine ATP stimulation of purinoceptors**. *J Biol Chem* 1998, **273**(11):6334-6340.

52. Thornberry NA, Lazebnik Y: **Caspases: Enemies within**. *Science* 1998, **281**(5381):1312-1316.

53. Kleinnijenhuis J, Joosten LAB, van de Veerdonk FL, Savage N, van Crevel R, Kullberg BJ, van der Ven A, Ottenhoff THM, Dinarello CA, van der Meer JWM: **Transcriptional and inflammasome-mediated pathways for the induction of IL-1β production by *Mycobacterium tuberculosis***. *European journal of immunology* 2009, **39**(7):1914-1922.

54. Netea MG, Nold-Petry CA, Nold MF, Joosten LAB, Opitz B, van der Meer JHM, van de Veerdonk FL, Ferwerda G, Heinhuis B, Devesa I: **Differential**

requirement for the activation of the inflammasome for processing and release of IL-1β in monocytes and macrophages. *Blood* 2009, **113**(10):2324-2335.

55. Fiser A, Sali A: **MODELLER: Generation and refinement of homology-based protein structure models**. *Method Enzymol* 2003, **374**:461-+.

56. Dostert C, Pétrilli V, Van Bruggen R, Steele C, Mossman BT, Tschopp J: **Innate immune activation through Nalp3 inflammasome sensing of asbestos and silica**. *Science's STKE* 2008, **320**(5876):674.

57. Franchi L, Kanneganti TD, Dubyak GR, Nunez G: **Differential requirement of P2X7 receptor and intracellular K^+ for caspase-1 activation induced by intracellular and extracellular bacteria**. *J Biol Chem* 2007, **282**(26):18810-18818.

58. Yilmaz O, Sater AA, Yao LY, Koutouzis T, Pettengill M, Ojcius DM: **ATP-dependent activation of an inflammasome in primary gingival epithelial cells infected by *Porphyromonas gingivalis***. *Cellular microbiology* 2010, **12**(2):188-198.

59. Petrilli V, Papin S, Dostert C, Mayor A, Martinon F, Tschopp J: **Activation of the NALP3 inflammasome is triggered by low intracellular potassium concentration**. *Cell Death & Differentiation* 2007, **14**(9):1583-1589.

60. Lamkanfi M, Mueller JL, Vitari AC, Misaghi S, Fedorova A, Deshayes K, Lee WP, Hoffman HM, Dixit VM: **Glyburide inhibits the Cryopyrin/Nalp3 inflammasome**. *The Journal of cell biology* 2009, **187**(1):61-70.

61. Miao EA, Leaf IA, Treuting PM, Mao DP, Dors M, Sarkar A, Warren SE, Wewers MD, Aderem A: **Caspase-1-induced pyroptosis is an innate immune effector**

mechanism against intracellular bacteria. *Nat Immunol* 2010, **11**(12):1136-U1194.

62. Bellis SL: **Variant glycosylation: an underappreciated regulatory mechanism for beta1 integrins**. *Biochimica et biophysica acta* 2004, **1663**(1-2):52-60.

63. Isaji T, Sato Y, Zhao Y, Miyoshi E, Wada Y, Taniguchi N, Gu J: **N-glycosylation of the β-propeller domain of the integrin α5 subunit is essential for α5β1 heterodimerization, expression on the cell surface, and its biological function**. *J Biol Chem* 2006, **281**(44):33258-33267.

64. Bauernfeind FG, Horvath G, Stutz A, Alnemri ES, MacDonald K, Speert D, Fernandes-Alnemri T, Wu J, Monks BG, Fitzgerald KA: **Cutting edge: NF-κB activating pattern recognition and cytokine receptors license NLRP3 inflammasome activation by regulating NLRP3 expression**. *The Journal of Immunology* 2009, **183**(2):787-791.

65. Seshadri G, Myers GSA, Tettelin H, Eisen JA, Heidelberg JF, Dodson RJ, Davidsen TM, DeBoy RT, Fouts DE, Haft DH, Selengut J, Ren Q, Brinkac LM, Madupu R, Kolonay J, Durkin SA, Daugherty SC, Shetty J, Shavartsbeyn A, Gebregeorgis E, Geer K, Tsegaye G, Malek J, Ayodeji B, Shatsman S, McLeod MP, Smajs D, Howell JK, Pal S, Amin A, Vashisth P, Mcneill TZ, Xiang Q, Sodergren E, Baca E, Weinstock GM, Norris SJ, Fraser CM, Paulsen IT: **Comparison of the genome *Treponema denticola* with of the oral pathogen other spirochete genomes**. *P Natl Acad Sci USA* 2004, **101**(15):5646-5651.

66. Ellen RP: **Adhesion of oral spirochaetes to host cells and its cytopathogenic consequences**: Cambridge: Cambridge University Press; 2002.

67. Hashimoto M, Ogawa S, Asai Y, Takai Y, Ogawa T: **Binding of *Porphyromonas gingivalis* fimbriae to *Treponema denticola* dentilisin**. *FEMS microbiology letters* 2003, **226**(2):267-271.

68. Ikegami A, Honma K, Sharma A, Kuramitsu HK: **Multiple functions of the leucine-rich repeat protein LrrA of *Treponema denticola***. *Infect Immun* 2004, **72**(8):4619-4627.

69. Graves DT, Cochran D: **The contribution of interleukin-1 and tumor necrosis factor to periodontal tissue destruction**. *J Periodontol* 2003, **74**(3):391-401.

70. Haynes DR, Atkins GJ, Loric M, Crotti T, Geary SM, Findlay DM: **Bidirectional signaling between stromal and hemopoietic cells regulates interleukin-1 expression during human osteoclast formation**. *Bone* 1999, **25**(3):269-278.

71. Wei S, Kitaura H, Zhou P, Ross FP, Teitelbaum SL: **IL-1 mediates TNF-induced osteoclastogenesis**. *J Clin Invest* 2005, **115**(2):282-290.

72. Nukaga J, Kobayashi M, Shinki T, Song H, Takada T, Takiguchi T, Kamijo R, Hasegawa K: **Regulatory effects of interleukin-1β and prostaglandin E_2 on expression of receptor activator of nuclear factor-kappaB ligand in human periodontal ligament cells**. *J Periodontol* 2004, **75**(2):249-259.

73. Palmqvist P, Persson E, Conaway HH, Lerner UH: **IL-6, leukemia inhibitory factor, and oncostatin M stimulate bone resorption and regulate the expression of receptor activator of NF-kappa B ligand, osteoprotegerin, and receptor activator of NF-kappa B in mouse calvariae**. *J Immunol* 2002, **169**(6):3353-3362.

74. Choi BK, Moon SY, Cha JH, Kim KW, Yoo YJ: **Prostaglandin E_2 is a main mediator in receptor activator of nuclear factor-kappa B ligand-dependent**

osteoclastogenesis induced by *Porphyromonas gingivalis*, *Treponema denticola*, and *Treponema socranskii*. *J Periodontol* 2005, **76**(5):813-820.

75. Liu XH, Kirschenbaum A, Yao S, Levine AC: **Interactive effect of interleukin-6 and prostaglandin E_2 on osteoclastogenesis via the OPG/RANKL/RANK system**. *Annals of the New York Academy of Sciences* 2006, **1068**:225-233.

76. Yucel-Lindberg T, Nilsson S, Modeer T: **Signal transduction pathways involved in the synergistic stimulation of prostaglandin production by interleukin-1β and tumor necrosis factor α in human gingival fibroblasts**. *J Dent Res* 1999, **78**(1):61-68.

77. Engsig MT, Chen QJ, Vu TH, Pedersen AC, Therkidsen B, Lund LR, Henriksen K, Lenhard T, Foged NT, Werb Z, Delaisse JM: **Matrix metalloproteinase 9 and vascular endothelial growth factor are essential for osteoclast recruitment into developing long bones**. *J Cell Biol* 2000, **151**(4):879-889.

78. Baqui AA, Meiller TF, Chon JJ, Turng BF, Falkler WA, Jr.: **Granulocyte-macrophage colony-stimulating factor amplification of interleukin-1beta and tumor necrosis factor α production in THP-1 human monocytic cells stimulated with lipopolysaccharide of oral microorganisms**. *Clinical and diagnostic laboratory immunology* 1998, **5**(3):341-347.

79. Choi BK, Lee HJ, Kang JH, Jeong GJ, Min CK, Yoo YJ: **Induction of osteoclastogenesis and matrix metalloproteinase expression by the lipooligosaccharide of *Treponema denticola***. *Infect Immun* 2003, **71**(1):226-233.

80. Grenier D, Grignon L: **Response of human macrophage-like cells to stimulation by *Fusobacterium nucleatum* ssp *nucleatum* lipopolysaccharide**. *Oral Microbiol Immun* 2006, **21**(3):190-196.

81. Nakamura T, Nitta H, Ishikawa I: **Effect of low dose *Actinobacillus actinomycetemcomitans* lipopolysaccharide pretreatment on cytokine production by human whole blood**. *Journal of periodontal research* 2004, **39**(2):129-135.

82. Wang PL, Ohura K, Fujii T, Oido-Mori M, Kowashi Y, Kikuchi M, Suetsugu Y, Tanaka J: **DNA microarray analysis of human gingival fibroblasts from healthy and inflammatory gingival tissues**. *Biochem Bioph Res Co* 2003, **305**(4):970-973.

83. Zhong Y, Slade GD, Beck JD, Offenbacher S: **Gingival crevicular fluid interleukin-1β, prostaglandin E_2 and periodontal status in a community population**. *J Clin Periodontol* 2007, **34**(4):285-293.

84. Asakawa R, Komatsuzawa H, Kawai T, Yamada S, Goncalves RB, Izumi S, Fujiwara T, Nakano Y, Suzuki N, Uchida Y, Ouhara K, Shiba H, Taubman MA,Kurihara H, Sugal M: **Outer membrane protein 100, a versatile virulence factor of *Actinobacillus actinomycetemcomitans***. *Mol Microbiol* 2003, **50**(4):1125-1139.

85. Hiramine H, Watanabe K, Hamada N, Umemoto T: ***Porphyromonas gingivalis* 67-kDa fimbriae induced cytokine production and osteoclast differentiation utilizing TLR2**. *FEMS microbiology letters* 2003, **229**(1):49-55.

86. Ouhara K, Komatsuzawa H, Shiba H, Uchida Y, Kawai T, Sayama K, Hashimoto K, Taubman MA, Kurihara H, Sugai M: ***Actinobacillus actinomycetemcomitans* outer membrane protein 100 triggers innate immunity and production of β-defensin and the 18-kDa cationic antimicrobial protein through the fibronectin-integrin pathway in human gingival epithelial cells**. *Infect Immun* 2006, **74**(9):5211-5220.

87. Agerer F, Lux S, Michel A, Rohde M, Ohlsen K, Hauck CR: **Cellular invasion by *Staphylococcus aureus* reveals a functional link between focal adhesion kinase and cortactin in integrin-mediated internalisation**. *J Cell Sci* 2005, **118**(10):2189-2200.

88. Ozeri V, Rosenshine I, Ben-Ze'Ev A, Bokoch GM, Jou TS, Hanski E: **De novo formation of focal complex-like structures in host cells by invading Streptococci**. *Mol Microbiol* 2001, **41**(3):561-573.

89. Plancon L, Du Merle L, Le Friec S, Gounon P, Jouve M, Guignot J, Servin A, Le Bouguenec C: **Recognition of the cellular β1-chain integrin by the bacterial AfaD invasin is implicated in the internalization of afa-expressing pathogenic *Escherichia coli* strains**. *Cellular microbiology* 2003, **5**(10):681-693.

90. Kwok T, Zabler D, Urman S, Rohde M, Hartig R, Wessler S, Misselwitz R, Berger J, Sewald N, Konig W, Bachert S: ***Helicobacter* exploits integrin for type IV secretion and kinase activation**. *Nature* 2007, **449**(7164):862-U864.

91. Jiménez-Soto LF, Kutter S, Sewald X, Ertl C, Weiss E, Kapp U, Rohde M, Pirch T, Jung K, Retta SF: ***Helicobacter pylori* type IV secretion apparatus exploits β1 integrin in a novel RGD-independent manner**. *PLoS pathogens* 2009, **5**(12):e1000684.

92. Cho BA, Cho NH, Seong SY, Choi MS, Kim IS: **Intracellular Invasion by *Orientia tsutsugamushi* Is Mediated by Integrin Signaling and Actin Cytoskeleton Rearrangements**. *Infect Immun* 2010, **78**(5):1915-1923.

93. Tsuda K, Furuta N, Inaba H, Kawai S, Hanada K, Yoshimori T, Amano A: **Functional analysis of α5β1 integrin and lipid rafts in invasion of epithelial cells by *Porphyromonas gingivalis* using fluorescent beads coated with bacterial membrane vesicles**. *Cell structure and function* 2008, **33**(1):123-132.

94. Kato T, Kawai S, Nakano K, Inaba H, Kuboniwa M, Nakagawa I, Tsuda K, Omori H, Ooshima T, Yoshimori T, Amano A: **Virulence of *Porphyromonas gingivalis* is altered by substitution of fimbria gene with different genotype**. *Cellular microbiology* 2007, **9**(3):753-765.

95. Buensuceso C, de Virgilio M, Shattil SJ: **Detection of Integrin αIIbβ3 Clustering in Living Cells**. *J Biol Chem* 2003, **278**(17):15217-15224.

96. Orlando RA, Cheresh DA: **Arginine-glycine-aspartic acid binding leading to molecular stabilization between integrin αvβ3 and its ligand**. *J Biol Chem* 1991, **266**(29):19543.

97. Agostini L, Martinon F, Burns K, McDermott MF, Hawkins PN, Tschopp J: **NALP3 forms an IL-1β-processing inflammasome with increased activity in Muckle-Wells autoinflammatory disorder**. *Immunity* 2004, **20**(3):319-325.

98. Dowds TA, Masumoto J, Zhu L, Inohara N, Nunez G: **Cryopyrin-induced interleukin 1β secretion in monocytic cells: enhanced activity of disease-associated mutants and requirement for ASC**. *J Biol Chem* 2004, **279**(21):21924-21928.

99. Hoffman HM, Rosengren S, Boyle DL, Cho JY, Nayar J, Mueller JL, Anderson JP, Wanderer AA, Firestein GS: **Prevention of cold-associated acute inflammation in familial cold autoinflammatory syndrome by interleukin-1 receptor antagonist**. *Lancet* 2004, **364**(9447):1779-1785.

100. Dinarello CA: **Blocking IL-1 in systemic inflammation**. *J Exp Med* 2005, **201**(9):1355-1359.

101. Liu CM, Hou LT, Wong MY, Rossomando EF: **Relationships between clinical parameters, interleukin 1β and histopathologic findings of gingival tissue in periodontitis patients**. *Cytokine* 1996, **8**(2):161-167.

102. Jun HK, Kang YM, Lee HR, Lee SH, Choi BK: **Highly conserved surface proteins of and potent inducers of proinflammatory oral spirochetes as adhesins and osteoclastogenic factors**. *Infect Immun* 2008, **76**(6):2428-2438.

103. Orozco A, Gemmell E, Bickel M, Seymour G: **Interleukin-1β, interleukin-12 and interleukin-18 levels in gingival fluid and serum of patients with gingivitis and periodontitis**. *Oral Microbiol Immun* 2006, **21**(4):256-260.

104. Kornman KS, di Giovine FS: **Genetic variations in cytokine expression: a risk factor for severity of adult periodontitis**. *Annals of periodontology* 1998, **3**(1):327-338.

105. Diehl SR, Wang YF, Brooks CN, Burmeister JA, Califano JV, Wang S, Schenkein HA: **Linkage disequilibrium of interleukin-1 genetic polymorphisms with early-onset periodontitis**. *J Periodontol* 1999, **70**(4):418-430.

106. Bostanci N, Emingil G, Saygan B, Turkoglu O, Atilla G, Curtis M, Belibasakis G: **Expression and regulation of the NALP3 inflammasome complex in periodontal diseases**. *Clinical & Experimental Immunology* 2009, **157**(3):415-422.

107. Toma C, Higa N, Koizumi Y, Nakasone N, Ogura Y, McCoy AJ, Franchi L, Uematsu S, Sagara J, Taniguchi S: **Pathogenic Vibrio activate NLRP3 inflammasome via cytotoxins and TLR/nucleotide-binding oligomerization domain-mediated NF-κB signaling**. *The Journal of Immunology* 2010, **184**(9):5287.

108. Roman J, Ritzenthaler JD, Fenton MJ, Roser S, Schuyler W: **Transcriptional regulation of the human interleukin 1beta gene by fibronectin: role of protein kinase C and activator protein 1 (AP-1)**. *Cytokine* 2000, **12**(11):1581-1596.

109. Chen XM, Wang JZ, Fu B, Yu LF: **RGD-containing peptides trigger apoptosis in glomerular mesangial cells of adult human kidneys**. *Biochem Bioph Res Co* 1997, **234**(3):594-599.

110. Kanneganti TD, Lamkanfi M, Kim YG, Chen G, Park JH, Franchi L, Vandenabeele P, Nunez G: **Pannexin-1-mediated recognition of bacterial molecules activates the cryopyrin inflammasome independent of Toll-like receptor signaling**. *Immunity* 2007, **26**(4):433-443.

111. Hirakawa M, Oike M, Watanabe M, Karashima Y, Ito Y: **Pivotal role of integrin α5β1 in hypotonic stress-induced responses of human endothelium.** *FASEB J.* 2006, **20**(12);1992-1999.

112. Solini A, Chiozzi P, Morelli A, Adinolfi E, Rizzo R, Baricordi OR, Di Virgilio F: **Enhanced P2X7 activity in human fibroblasts from diabetic patients: a possible pathogenetic mechanism for vascular damage in diabetes**. *Arteriosclerosis, thrombosis, and vascular biology* 2004, **24**(7):1240-1245.

113. Kahlenberg JM, Dubyak GR: **Mechanisms of caspase-1 activation by P2X7 receptor-mediated K^+ release**. *American journal of physiology Cell physiology* 2004, **286**(5):C1100-1108.

114. Pelegrin P, Surprenant A: **Pannexin-1 mediates large pore formation and interleukin-1β release by the ATP-gated P2X7 receptor**. *The EMBO journal* 2006, **25**(21):5071-5082.

115. Halle A, Hornung V, Petzold GC, Stewart CR, Monks BG, Reinheckel T, Fitzgerald KA, Latz E, Moore KJ, Golenbock DT: **The NALP3 inflammasome is involved in the innate immune response to amyloid-β**. *Nat Immunol* 2008, **9**(8):857-865.

116. Hornung V, Bauernfeind F, Halle A, Samstad EO, Kono H, Rock KL, Fitzgerald KA, Latz E: **Silica crystals and aluminum salts activate the NALP3 inflammasome through phagosomal destabilization**. *Nat Immunol* 2008, **9**(8):847-856.

117. Cruz CM, Rinna A, Forman HJ, Ventura ALM, Persechini PM, Ojcius DM: **ATP activates a reactive oxygen species-dependent oxidative stress response and secretion of proinflammatory cytokines in macrophages**. *J Biol Chem* 2007, **282**(5):2871-2879.

118. Tschopp J, Schroder K: **NLRP3 inflammasome activation: The convergence of multiple signalling pathways on ROS production?** *Nature reviews Immunology* 2010, **10**(3):210-215.

.

국문초록

치주염과 관련된 구강나선균의 공통 표면단백질의 병독력과 NLRP3 인플라마좀 활성

전 혜 경

서울대학교 치의학대학원

치의학과 면역 및 분자미생물 전공

(지도교수 최 봉 규)

목적

모든 구강나선균은 광범위한 다양성을 가진 *Treponema*종으로 구성되어 있고 치주 병원성과 관련이 깊다. 다양한 종 또는 계통형의 *Treponema*가 한 환자와 단일 치주낭에서 자주 발견되고 구강나선균의 존재는 질환의 중증도와 높은 관련성을 나타낸다. 구강나선균의 몇 몇 외막단백질은 면역조절자로 중요하며 이는 분자적 병인기전 연구로 증명된 바 있다. Tp92는 *T. pallidum*의

표면단백질로서 옵소닌 작용과 매독에 대한 방어적 면역반응을 유도한다고 알려졌고 그람음성 세균에도 비슷한 기능을 가진 유사단백질이 있다. IL-1β는 염증성 및 골흡수적인 특성을 가진 치주염의 면역병원성과 연관이 있고, 이는 치주조직의 파괴를 야기한다. IL-1β는 선천면역을 구성하는 세포내 센서인 인플라마좀 복합체 형성으로 생성된 활성형 caspase-1이 활성화시킨다. 이 연구에서, 치주염과 관련된 4가지 주요한 구강나선균 (*T. denticola*, *T. lecithinolyticum*, *T. maltophilum*, *T. socranskii* subsp. *socranskii*)에 존재하는 Tp92 유사단백질을 찾고 이들의 병인적 특성을 규명하였다.

실험 방법

Tp92 유사단백질을 *Esherichia coli*에서 발현시키고 재조합단백질을 정제하였다. Tp92 유사단백질의 부착능을 보기 위하여 편평세포 암종인 KB 세포에 FITC를 붙인 Tp92 유사단백질 또는 carboxyfluorescein diacetate succinimidyl ester (CFSE)를 붙인 세균과 반응시켰다. Tp92 유사단백질들의 교차반응은 *T. denticola*의 Td92에 대한 항혈청으로 확인하였다. Tp92 유사단백질의 생리활성능 측정을 위하여 인간 단핵세포와 인간 치주인대 세포에 반응시킨 후 염증 및 조직 파괴와 관련된 다양한 인자들을 분석하였다.

T. denticola Td92에 의한 IL-1β 활성의 분자적 기전을 찾기 위하여 Td92를 KCl, oxATP, K^+ channel 억제자가 있거나 없는 상태에서 대식세포로 분화시킨 세포에 자극시켰다. 이 세포에서 caspase-1 활성, proIL-1β, IL-1β의 분비를 확인하였다. Td92에 의해 유도된 caspase-1 활성과 연관된 인플라마좀 구성분을 찾기 위하여 NLRP3, ASC, NLRC4에 대한 siRNA를 사용하여 확인하였다. Td92에

의한 인플라마좀 활성에서 Td92의 세포내 유입이 필수적인 요인인지 확인하기 위하여 단백질 유입시약이나 cytochalasin D를 사용하였다. 인플라마좀 활성과 관련된 Td92의 세포내 수용체를 친화성 리간드 결합법으로 찾았다. 수용체와 결합한 Td92가 proIL-1β 발현을 유도할 때 어떤 신호전달를 통하여 이루어지는지를 확인하기 위하여 여러가지 억제제 또는 중성화 항체를 처리하여 MAPK 경로 활성과 NF-κB 핵내이동 보았다.

결과

구강나선균의 Tp92 유사단백질은 신호 펩타이드 (20-31아미노산기)와 88-92-kDa의 분자량을 가진다. 이 단백질에 대한 유전자를 *E. coli*에서 재조합 형태로 발현시키고 정제하였다. Tp92 유사단백질은 KB세포에 부착하였고 Td92에 의해 *T. denticola*의 세포 부착이 억제 되었다. *T. lecithinolyticum*, *T. maltophilum*, *T. socranskii* subsp. *socranskii*, 각각의 Tp92 유사단백질를 *T. denticola* Td92에 대한 항혈청(IgG)과 반응시켰을 때 교차반응을 나타냈다. Tp92 유사단백질은 사람 단핵구와 인간 치주인대세포를 자극하여 IL-1β, IL-6, IL-8, TNF-α, COX-2, PGE_2, MMP-9 등과 같은 염증 및 파골세포 형성 관련 인자들을 유도하였다.

대식세포를 *T. denticola* Td92로 자극하였을 때 ATP 방출과 K^+이 유출되었고 그 결과로써 caspase-1 활성, proIL-1β 발현, IL-1β 분비가 유도되었다. Td92의 caspase-1 활성은 NLRP3 또는 ASC의 결핍에 의해 크게 줄었지만 NLRC4의 결핍은 Td92의 caspase-1활성에 영향을 주지 않았다. Td92의 세포내 빠른 유입은 Td92의 caspase-1 활성을 감소시켰으며 Td92의 유입 억제는 caspase-1과 proIL-1β

발현에 영향을 주지 않았다. 인테그린 α5β1이 *T. denticola* Td92에 대한 세포내 수용체로서 NLRP3 인플라마좀을 활성화시키는데 중요한 역할을 하였다. Td92는 인테그린 α5β1과 fibronectin에 모두 부착하였고 Td92에 의해 유도된 NLRP3 인플라마좀 활성은 fibronectin과 관계없이 인테그린 α5β1과 직접 결합함으로써 매개되었다. Td92와 인테그린 α5β1의 결합은 NF-κB에 활성을 통하여 proIL-1β 발현, NLRP3 발현, caspase-1 활성을 유도하였다.

결론

Td92와 인테그린 α5β1의 직접적 상호작용이 NLRP3 인플라마즘 활성과 proIL-1β를 합성함으로써 과도한 IL-1β 분비를 야기할 수 있다. 그러므로 인테그린 α5β1은 Td92에 의한 NLRP3 인플라마좀 활성과 IL-1β 전사를 위한 중요한 세포막의 수용체로 여겨지며, Td92와 인테그린 α5β1간의 상호작용에 대한 이해는 치주염 치료를 위한 새로운 치료제 발전에 기여할 것이다.

주요어: 구강나선균, Tp92 유사단백질, 염증, NLRP3 인플라마좀, 인테그린 α5β1, 치주질환

학 번: 2004-22655